

國立交通大學

電機資訊學院 電子與光電學程

碩士論文

主動矩陣式有機發光二極體驅動電路使用時間比例灰階
技術之研究

Time Ratio Grayscale Driving Circuits for Active Matrix Organic Light
Emitting Diodes

研究生：曾銘松

指導教授：黃 威 教授

中華民國九十四年八月

主動矩陣式有機發光二極體驅動電路使用時間比例灰階
技術之研究

Time Ratio Grayscale Driving Circuits for Active Matrix Organic Light
Emitting Diodes

研究生：曾銘松

Student : Min-Sung Tseng

指導教授：黃 威

Advisor : Wei Huang



Submitted to Degree Program of Electrical Engineering Computer Science
College of Electrical Engineering and Computer Science
National Chiao Tung University
in Partial Fulfillment of the Requirements
for the Degree of Master of Science
in
Electronics and Electro-Optical Engineering

August 2005

Hsinchu, Taiwan, Republic of China

中華民國九十四年八月

主動矩陣式有機發光二極體驅動電路使用時間比例灰階技術之研究

學生：曾銘松

指導教授：黃 威

國立交通大學電機資訊學院 電子與光電學程（研究所）碩士班

摘 要

本論文提出一個改善發光效率之設計應用於主動有機發光二極體驅動電路。而這個被驅動的畫素是以兩個電晶體及一個電容所組成的架構。藉由增加發光時間及減少定址時間來提升傳統的時間比例灰階驅動方式之發光效率。兩種可行方案被提出。取樣的移位暫存器採用倍速串列輸入將減少定址時間。振幅調變編碼的使用將減少子圖框的數目進而增加發光時間。結合上述兩種方案的驅動方式能夠提升 24% 的發光。較高的發光特性，將使得每個畫素面積減少，較小的畫素使得較高解析度的顯示器能夠被製造。此外將驅動電路整合在面板上是最終目標，面板上常使用的多晶矽薄膜電晶體有臨界電壓及遷移率變異的問題，而這些變異使得類比線路設計不易實現於面板上。而這個改良的時間比例灰階驅動方式也是使用數位驅動方式，在驅動電路部分它不需類比電路，他使得驅動電路完全整合於面板上將成為可能。為了正確影像顯示，另外提出掃描訊號阻絕，以防止兩個相鄰的掃描線切換時所造成的顯示資訊錯誤寫入。

這個主動矩陣式有機發光二極體驅動電路是用 0.6 微米 18V CMOS 製程來模擬。由於點亮時間的限制，此一驅動電路適合應用於 QVGA 或低於此解析度。

Time Ratio Grayscale Driving Circuits for Active Matrix Organic Light Emitting Diodes

student : Min-Sung Tseng

Advisors : Dr. Wei Huang

Degree Program of Electrical Engineering Computer Science
National Chiao Tung University

ABSTRACT

Using improved luminance efficiency for the driving circuit of Active Matrix Organic Light Emitting Diodes (AMOLED) is presented in this thesis. The driven pixel is based on the structure with two transistors and one capacitor. We propose to enhance the luminance efficiency of conventional time ratio grayscale by increased lighting time and decreased addressing time. Two practical approaches to enhance luminance will be proposed. For decreased addressing time, shift register of sampling adopt double rate serial-in. For increased lighting time, amplitude modulation coding will reduce the number of sub-frame, and increase the lighting time. The combined method could enhance 24% luminance. The higher luminance allows a small pixel. Small pixel will allow high resolution displays to be created. Moreover, the final goal is that driver circuits are integrated on the display panel. TFT by poly-silicon is always adopted. For poly-silicon thin film transistor (TFT), both mobility and threshold-voltage vary randomly across the plate. The former two variables would lead to analog circuit is hard to implement on panel. The improved time ratio grayscale also adopts the digital driving. There is no analog design in driver by this method. It is possible that the driving circuit is fully implemented to System on Panel (SOP). Another proposed scan signal gating for correct image display prevent from error-programming when adjacent scan line are toggling.

A prototype of this AMOLED driver is simulated by 0.6 um 18V CMOS technology. Because lighting time is limited, it is suitable for the Quarter Video Graphic Array (QVGA) or below the resolution.

Acknowledgements

The thesis is successfully. First, I would like to thank my advisor, Prof. Wei Hwang. He has given me a lot of guidance for three years, and his encouragement, concern, and instruction make me grow up greatly. It is also make me unforgettable. That is my honor that I could be the Prof. Wei Hwang's student.

I would also like to thank all of my laboratory friends. Among them are Wagon Chang, CS Hua, Lawrence Wu, Jerry Young and Chynny Chen, they give their enthusiasm to help me. By their assistance, my school life is more smoothly.

My colleagues, Howard Tsai, Heng Wang, Wisdom Shan, Anderson Tsai, Spring Ye, and Alex Hwang, have been a valuable source of moral support. I would like to thank all of them for their toleration during my years at NCTU.

My wife Te-Yin Liao, she is the most important source of inspiration and happiness when I am tired and depressed. I also appreciate my family, they have always been a tremendous source of encouragement and support.



CONTENTS

Chapter 1: Introduction	1
1.1 Keep Your Eye on The Future	1
1.2 History	2
1.3 Performance and Application	4
1.4 Scope of This Work.....	6
Chapter 2: Related Techniques and Characterization for OLED	7
2.1 LED and OLED.....	7
2.2 PLED and OLED	8
2.3 Light Emission Structure	9
2.4 Emission Properties	10
2.5 Color Present	10
2.5.1 Patterned Lateral RGB Emitters	11
2.5.2 Color Change Media	12
2.5.3 Color Filter	12
2.5.4 Color Stacked OLED	13
2.6 Electric Illumination Characterization	14
2.7 Matrix Addressing.....	15
2.7.1 Passive Matrix	16
2.7.1.1 Pixel Structure	16
2.7.1.2 Pixel Addressing	16
2.7.1.3 Pixel Concern	17
2.7.2. Active Matrix Addressing	19
2.7.2.1 Pixel Structure	19
2.7.2.2 Pixel Addressing	20
2.7.2.3 Pixel Concern	21
2.7.2.3.1 Constant Current or Source Follower.....	21
2.7.2.3.2 Driving Device Choice.....	22
2.7.2.3.3 IR-Drop.....	22
2.8 Top-Emission and Bottom-Emission.....	23

Chapter 3: AMOLED Review for Driving Design	25
3.1 Category.....	25
3.2 Transistor Technologies	26
3.2.1 Poly Silicon	26
3.2.2 Amorphous Silicon	26
3.2.3 Organic Transistor	27
3.2.4 Crystalline Silicon	27
3.3 Analog Driving	28
3.3.1 Voltage Programming Pixel.....	29
3.3.1.1 Voltage Programmed with 4T2C Pixel Structure	29
3.3.1.2 Voltage Programmed with 5T1C Pixel Structure	30
3.3.2 Current Programming Pixel	32
3.3.2.1 Current Programmed with Current-Copy Pixel	32
3.3.2.2 Current Programmed with Current-Mirror Pixel	33
3.4 Digital Driving.....	34
3.4.1 Area Ratio Grayscale	34
3.4.2 Time Ratio Grayscale.....	35
Chapter 4: AMOLED Driver Design.....	36
4.1 Active Matrix Driving.....	26
4.2 Image Display.....	40
4.3 Data Driver	42
4.3.1 Architecture	43
4.3.2 Serial to Parallel Circuit with Double Rate Serial-in	44
4.3.2.1 Image Mirror	46
4.3.3 Improved Time Ratio Grayscale with Amplitude Modulation.....	47
4.3.4 Decoder and Analog Switch	50
4.3.5 Simulation Result and Summary	52
4.4 Scan Driver	55
4.4.1 Architecture	55
4.4.2 Sequential Scan with Image Handstand	56
4.4.2.1 Non-overlap with Scan Signal Gating	58
4.4.3 Cathode Electrical Switch for IR Drop Issue	60
4.4.4 Simulation Result and Summary	62

4.5	Voltage Regulator.....	63
4.5.1	Block Diagram of Voltage Regulator	65
4.5.2	Voltage Reference	66
4.5.2.1	Zero Temperature Coefficient	67
4.5.2.2	Architecture	70
4.5.2.3	Simulation Result and Summary	72
4.5.3	Pass Device Concern.....	73
4.5.4	Frequency Response of Voltage Regulator	75
4.5.5	Voltage Regulator with OTA Structure.....	77
4.5.6	Simulation Result and Summary	79
Chapter 5: Conclusions and Future Work.....		81
5.1	Conclusions	81
5.2	Future Work.....	82
References.....		83



TABLE CAPTIONS

Table 1-1 Every kind of compare of display characteristic---2

Table 2-1 Power dissipation in PMOLED displays with increasing size and resolution.---18

Table 3-1 Comparison of the saturation currents of a-Si:H and poly-Si TFTs---27

Table 4-1 Amplitude modulation coding---48

Table 4-2 Sub-frame value vs. physical output ---48

Table 4-3 Decoding relationship---51

Table 4-4 Comparison of pass element devices---75



FIGURE CAPTIONS

- Fig. 1-1 FOLED by UDC---3
- Fig. 1-2 Predict for OLED---5
- Fig. 2-1 A typical LED---7
- Fig. 2-2 A typical structure of an OLED device---9
- Fig. 2-3 One pixel by lateral RGB Emitter---11
- Fig. 2-4 One pixel by color change media---12
- Fig. 2-5 One pixel by color filter---13
- Fig. 2-6 Three pixels by color-stacked---13
- Fig. 2-7 A typical brightness and voltage data relation for different color OLED---14
- Fig. 2-8 A typical brightness and current data relation for different color OLED---15
- Fig. 2-9 Structure of a simple matrix-type display---16
- Fig. 2-10 Multiplexing principle for a matrix-type array of organic LEDs---17
- Fig. 2-11 Principle of active matrix addressing of an OLED display---19
- Fig. 2-12 Circuit diagram of an active matrix OLED---21
- Fig. 2-13 Constant current pixel---22
- Fig. 2-14 Source follower pixel---22
- Fig. 2-15 IR-drop perspective---23
- Fig. 2-16 A variant pixel with additional TFT---23
- Fig. 2-17 Bottom and top emission structure---24
- Fig. 3-1 Relation of operation frequency and field effect mobility for different technology--28
- Fig. 3-2 Conventional voltage programming pixel with threshold compensation---29
- Fig. 3-3 Timing diagram for 4T2C operation---30
- Fig. 3-4 Novel voltage programming pixel with threshold compensation---31
- Fig. 3-5 Timing diagram for 5T1C operation---31
- Fig. 3-6 Current programmed with current-copy pixel---32
- Fig. 3-7 Current programmed with current mirror pixel---33
- Fig. 3-8 Sub-pixel arrangement in monochrome display using area-ratio technique---34
- Fig. 3-9 A schema for time ratio gray-scale---35
- Fig. 4-1 A schema for AMOLED driving---38
- Fig. 4-2 Current source non-uniformity---38
- Fig. 4-3 Scan lines timing diagram---39
- Fig. 4-4 Image display---41
- Fig. 4-5 Timing diagram for sub-frame---41
- Fig. 4-6 Block diagram of data driver---43

Fig. 4-7 Non-overlap clock generator---	44
Fig. 4-8 Non-overlap clock for serial-in register---	45
Fig. 4-9 Addressing time dissipation---	45
Fig. 4-10 Image mirror with shift register control---	46
Fig. 4-11 Save signal sequential for sampling latch---	47
Fig. 4-12 Composition of each frame by proposition---	50
Fig. 4-13 Output stage for data driver---	51
Fig. 4-14 Output of data driver---	52
Fig. 4-15 Lighting percentage in frame for convention driving---	53
Fig. 4-16 Compared lighting percentage ---	54
Fig. 4-17 Block diagram of scan driver---	55
Fig. 4-18 Image handstand with shift register control---	56
Fig. 4-19 Signal sequential for scan driver---	57
Fig. 4-20 Adjacent scan line overlapping---	58
Fig. 4-21 Scan signal gating---	59
Fig. 4-22 Cathode electrical switch---	60
Fig. 4-23 I-R drop prevention---	61
Fig. 4-24 Output of scan driver---	62
Fig. 4-25 Voltage-current curve for poly-silicon pixel ---	63
Fig. 4-26 Block diagram of linear regulators---	65
Fig. 4-27 Linear regulator structures with PMOS---	66
Fig. 4-28 Conceptual block diagram of bandgap---	67
Fig. 4-29 Generation of PTAT voltage---	68
Fig. 4-30 Bandgap structure---	70
Fig. 4-31 Bandgap with start-up circuit---	71
Fig. 4-32 Simulation for start-up circuit in bandgap---	72
Fig. 4-33 Variation of the zero-TC---	72
Fig. 4-34 Pass devices topologies---	74
Fig. 4-35 Block diagram of linear regulator---	76
Fig. 4-36 Frequency response of linear regulator under two different loads---	77
Fig. 4-37 Linear regulator with OTA structure---	78
Fig. 4-38 Simulated bode plot for loop response---	79
Fig. 4-39 Output variation under a full load current change---	80

Chapter1

Introduction

1.1 Keep Your Eye on The Future

Along with the technological advance, the mode of the person and the external world communication changes constantly. The daily life thing of today is through speech and graphics to take the data and communicate with the external world-- for example television, computer network, personal digital assistant, and the third generation cell phone system etc..

The display of the graphics and image depends on the display so that the display becomes the product that the modern people must get in touch with everyday. At the earlier period, the cathode ray tube is the representative of the display. However, the cathode ray tube has the huge problem in physical volume, his turns the disadvantage in the thin type and reducing weight. To get thin and flexible displays that roll up like paper, the researchers are already developing a number of innovative display approaches. These new displays include liquid crystal display, vacuum fluorescence display, organic light emitting display, plasma display etc..

Although the current liquid crystal display occupies the market of the above even display in 80%, the color, visual angle, and thickness etc. still can't reach the perfect level. This makes other display techniques still contain existent space. Every kind of compare of display characteristic is on showing at table 1-1 [1-1]. In next generation, OLEDs will be a super star after LCDs. The most important difference between LCDs and OLEDs is that the OLEDs are emissive displays, which means that they generate their own light. LCDs are passive displays, and simply transmit or block an external light source to form an image. The light source for LCDs is typically either ambient light reflected by a metallic layer behind the display, or by a backlight system. Emissive displays don't need ambient light to be viewable, and don't require a backlight. This eliminates the cost, space, weight and power consumption of a backlighting system, and offers an image with much higher contrast. For example, OLED technology can be used to great benefit for both direct view and micro-display applications. In both cases, OLEDs offer higher efficiency and lower weight than competing liquid crystal displays, since they don't require backlights or reflective light sources. These are very important attributes for head-mounted and portable products. In addition, emissive OLED

displays offer a much wider viewing angle of 160 degrees.

	CRT	LCD	PDP	VFD	OLED
thin	×	○	△	△	◎
driving voltage	×	◎	△	○	◎
bright	◎	○	○	◎	◎
color	◎	○	○	○	○
response time	◎	△	◎	○	◎
view angle	◎	△	◎	◎	◎
manufacture cost	◎	◎	×	△	○

◎ : excellent ○ : good △ : fair × : bad

Table 1-1 Every kind of compare of display characteristic

Although large OLED panel prototypes have been shown at engineering shows, only a few products have shipped so far, and only in devices using much smaller displays, such as cell phones and car audio receiver. Nevertheless, OLEDs are attracting much attention [1-2][1-3]. There are some excellent characteristics in OLED such as fast response time, thin, high brightness, active emissive, wide viewing angle, wide operation temperature and flexible display. In this case, OLED have attracted great attention. Several famous companies are working on such next-generation displays, including Kodak which is the originator of the technology, IBM, Cambridge Display Technology, Philips, Pioneer and Sony.

1.2 History

In 1963, Pope et al. reported electroluminescence in single crystals of anthracene. Practical applications did not result from this early work because of the large driving voltages and the poor charge injection into the single crystals.

The problem of the large driving voltage was eliminated by the use of thin-film deposition techniques — Langmuir–Blodgett film deposition and vacuum sublimation of amorphous thin films of anthracene. The efficiency of these devices was still very poor before Tang and Van Slyke [1-4] could fabricate low-voltage (10 V), bright organic light-emitting devices from thin organic films of 8-hydroxyquinoline aluminum (Alq3).

This breakthrough was followed shortly afterward with the demonstration by Burroughes et al. [1-5] of electroluminescence in conjugated polymer films based on p-polyphenylenevinylene (PPV). At the same time, polymeric semiconductors that could be cast as thin films were developed. Scientists at the Xerox Research Center of Canada are developing semiconducting organic polymers that show promise for enabling the printing of electronic patterns on plastic substrates. Such materials could be alternatives to silicon transistors and lead to surprising applications, like a television screen rendered on a poster. Imagine monitors made of single sheets of flexible plastic.

In the last decade, we have seen a multidisciplinary thrust in designing stable high-performance organic and polymeric materials for flat panel display and plastic electronics applications and a concurrent effort in understanding the electronic and optical transport properties of such materials. The US Defense Advanced Research Project Agency (DARPA) is trying to speed development of FOLEDs (Flexible Organic Light Emitting Displays). In fact, a contract had been awarded to Universal Display Corporation to create flexible substrates that range from transparent plastic to opaque metal foils. One of several prototypes based on FOLED technology that is due to ship in two to three years is a flexible as shown in Fig. 1-1. FOLEDs sit on pliable surfaces such as thin plastic strips or metal foils, and can be laminated onto a wall, instrument panel, or piece of clothing, or bent or rolled, allowing retractable designs, like a window shade.



Fig. 1-1 FOLED by UDC

Transparent Organic Light Emitting Device (TOLED) is also developing, could be used as a display on windshields and cockpit windows. The combination of flexibility and transparency raises new possibilities for displays. Another prototype is a razor-thin Samsung cell phone that has a 2.2-inch display created with phosphorescent OLED (PHOLED) technology.

1.3 Performance and Application

OLED (Organic Light Emitting Display) panels use organic materials to produce light. When thin layers of this material are sandwiched between appropriate anode and cathode layers, a small voltage (typically 2 - 10 volts) applied across the material will cause it to emit light in a process called electroluminescence. This combination of anode materials, cathode materials and light emitting organic materials forms the OLED.

They can operate uniformly at very low levels as several nits ($1 \text{ nit} = \text{cd/m}^2$) for night time operation. They also operate well at very high brightness level as over 100,000 nits. However, OLEDs are usually specified to operate at more moderate level because operating lifetime is inversely proportional to brightness. At 100 nits, operating lifetimes of 5000-10000 hours are commonly reported [1-6][1-7][1-8]. Although the performance are adequate for some products, new materials are under development for increasing brightness and long lifetimes in more demanding applications.

In general, OLEDs are organized in a matrix structure of Rows and Columns with each pixel electrically connected between one Row lead and one Column lead. For applications that require low information content display the relatively simpler Passive Matrix (PM) addressing [1-9][1-10][1-11] scheme can be used. A passive matrix OLED (PMOLED) array consists of two sets of electrically isolated leads (Rows and Columns) arranged in orthogonal with an OLED at each intersection. An electronic switch is employed to address each of these rows.

Although the PMOLED panel structure has advantage of simplicity, the time available to drive each pixel decreases as the number of rows increases, driving up the peak brightness levels necessary to achieve adequate average brightness levels and causing the row line current to rise. Huge current cause large voltage drops in the row lines, and push the OLED operation to higher voltages where it is less power efficient. Since light emission from OLEDs

does not show any remanence, when an average each line has to excited with a peak luminance of $N \times L_m$, N being the number of lines in the display. The light output from the OLED is proportional to the current that passes through it. Clearly, the currents required for higher resolutions, such as SXGA or UXGA, cannot be supported in passive matrix architecture without significant improvements in OLED efficiency. Due to all these limitations, Active Matrix (AM) addressing [1-12] [1-13] is necessary for high information content large area FPDs, and is the need to manage heat or power dissipation, display power efficiency is an important metric in portable system design.

Active matrix and passive matrix screens are two fundamental types of OLED display assembly. Each type lends itself to different applications. Driving the OLEDs with an active matrix leads to lower voltage operation, low peak pixel current, and a display with much greater efficiency and brightness. The role of the active matrix is to provide a constant current throughout the entire frame time, eliminating the high currents encountered in the passive matrix approach. iSuppli / Stanford Resources, an electronic-display-market research firm, sees a bright long-term future for the OLED approach and predicts the revenue generated globally by the technology will rise from \$112 million in 2002 to \$2.3 billion in 2008 , as shown in Fig. 1-2 shows. The predicts that OLED displays, particularly those using active-matrix technology, will become more popular during the next four years and generate an increasing amount of revenue.

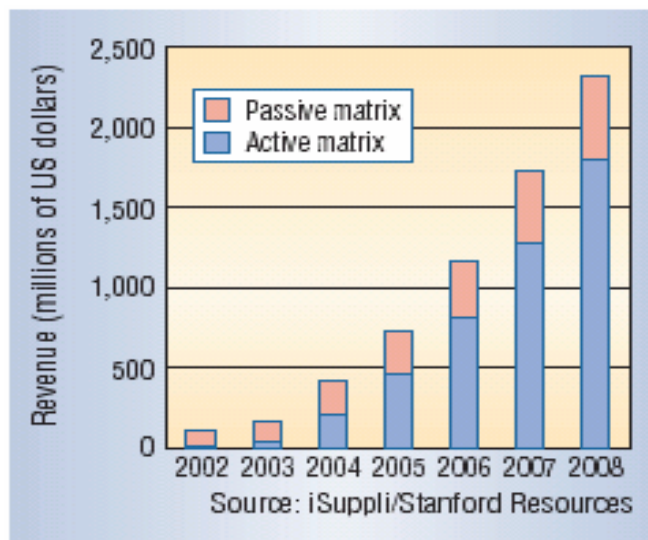


Fig. 1-2 Predict for OLED

1.4 Scope of This Work

Many famous companies have been actively developing OLED displays as a future display technology. Active matrix OLED technology opens up the route to high resolution and large color displays, which will be difficult to realize using passive matrix technology.

In this thesis, we propose to enhance the luminance efficiency of conventional time ratio grayscale by increased lighting time and decreased addressing time. Two practical approaches to enhance luminance will be proposed. For decreased addressing time, shift register of sampling adopt double rate serial-in. For increased lighting time, amplitude modulation coding will reduce the number of sub-frame, and increase the lighting time. The combined method is able to enhance the luminance. Besides, the main features of the AMOLED driver include selectable shift register for image mirror, selectable shift register for image handstand, scan signal gating for non-overlap scan, cathode electrical switch for I-R drop issue and voltage regulator which provide a lower voltage from a higher input voltage for different luminance and digital core .

In chapter 2, related technique and characterization for OLED are presented. In chapter 3, we take an AMOLED review for driving design. In chapter 4, design of AMOLED driver is described. Implementation details and the main simulation result are also given. Finally, conclusion and future work are given in chapter 5.

Chapter2

Related Techniques and Characterization for OLED

2.1 LED and OLED

Because they generate their own light, light-emitting diodes (LED) have long been considered the way to a better display. Conventional LED displays have been used successfully in giant screens usually seen in outdoor advertising, but these cannot be easily adapted to the small, high-resolution screens found in notebook computers. However, the OLED is an LED of a totally different kind - based on carbon-based molecules instead of inorganic semiconductors.

LED's are special diodes that emit light when connected in a circuit. They are frequently used as "pilot" lights in electronic appliances to indicate whether the circuit is closed or not. A clear (or often colored) epoxy case enclosed the heart of an LED, the semi-conductor chip. The two wires extending below the LED epoxy enclosure, or the bulb indicate how the LED should be connected into a circuit. It is depend on each different material to send out the different wavelength light. Fig. 2-1 shows the typical LED. The product depends on the light wavelength and the factor that eye feel, can be divided into the infrared rays LED and the visible light LED. The material of the usage has decided the wavelength that the LED release light, and the material that suits to make the high brightness LED includes the AlGaAs, AlGaInP and the GaInN etc..

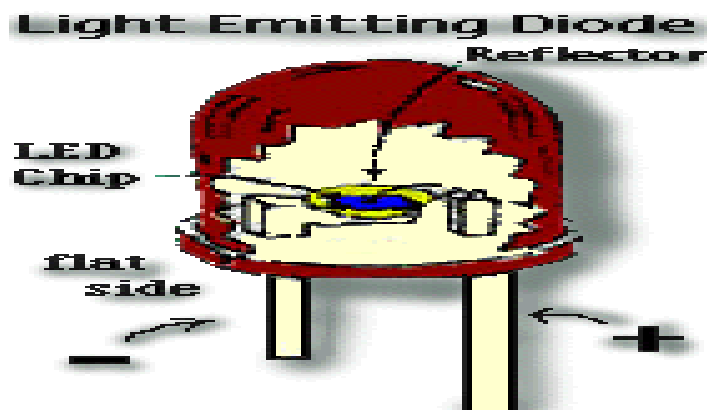


Fig. 2-1 A typical LED

The organic light emitting diode calls Organic Electroluminescence (OEL) also. The principle of luminescence is alike to light emitting diode (LED), make use of the material characteristic equally. When electron and hole come close at emission layer, they capture one another and form a neutral, excited state. This form is called exciton. The exciton then decays and emits a photon. The OLED and LED are similar in many respect, but still have some different in basic structures. The most main discrepancy is the transmission of the charge. The OLED is not a mode that uses the band transmission, but it carry on the transmission of the charge by jump. This also make it the low rate of mobility, the impedance of OLED is higher than the impedance of LED. Besides organic light emitting diode can use various different base (substrates) materials in the low temperature (<150°C.) manufacturing. The defect of the organic light emitting diode lies in its life and operation temperature ranges.

2.2 PLED and OLED

According to the organic thin film material that OLED use, the organic light emitting diode can be divided to small molecule OLED and macromolecule OLED that is polymer-based. In the late 1970s, Eastman Kodak Company scientist Dr. Ching Tang discovered that sending an electrical current through a carbon compound caused these materials to glow. Dr. Tang and Steven Van Slyke continued research in this vein. In 1987, they reported OLED materials that became the foundation for OLED displays produced today. In 1990, Richard Friend at Cambridge University demonstrated the first polymer-based OLED using conjugated poly pr PPY.

In general, small-molecule devices are fabricated using vacuum deposition [2-1] and PLED are built using spin-coating or ink-jet printing [2-2][2-3]. In addition to in the material of differently, the small molecule OLED and PLED also is different in and component characteristics. Small molecule OLED outpace PLED with respect to efficiencies and lifetimes. Over 40 lm/W for sm-OLED by green phosphorescent and 20 lm/W for green PLED have been reported [2-4].

Over the past decade, great resources have been invested to develop better materials, new device structures, and processing technology for both systems. Today, it is still in technology development cycle, and both technologies hold great promise. In 1997, a glass-base 256x64 pixel display for an automotive radio consol was developed by Pioneer Electronic Corporation. Recently, Motorola introduced a cellular phone with eye-catching OLED display from Pioneer.

Many companies are focused on introducing monochrome, multi-color PMOLED display. Rapid progress is also being made to develop full-color AMOLED for higher-information display, e.g., internet-compatible cell phones, digital cameras and GPS.

2.3 Light Emission Structure

Fig. 2.2 shows the typical structure of an OLED device. OLED is a monolithic, thin film, semi-conductive device that emits light when voltage is applied to it. In its most basic form, an OLED consists of a series of organic thin films that are sandwiched between two thin-film conductors. On a glass substrate, the anode is an Indium Tin Oxide (ITO) layer, the hole-injection, hole-transport emissive and the electron transport layers are organic thin films which are optimized for each color. When voltage is applied, one layer becomes negatively charged relative to another transparent layer. As energy passes from the negatively charged (cathode) layer to the other (anode) layer, it stimulates organic material between the two, which emits light visible through an outermost layer of glass.

A wide variety of colors can be made by employing the specific organic materials. Doping or enhancing organic material helps control the brightness and color of light [2-5]. To maximize the device performance, the cathode is usually a reflective thin film of a low work function metal to maximize the device performance, another electrode which is anode use a high work function material. The overall thickness of the device is less than 2000 Å .

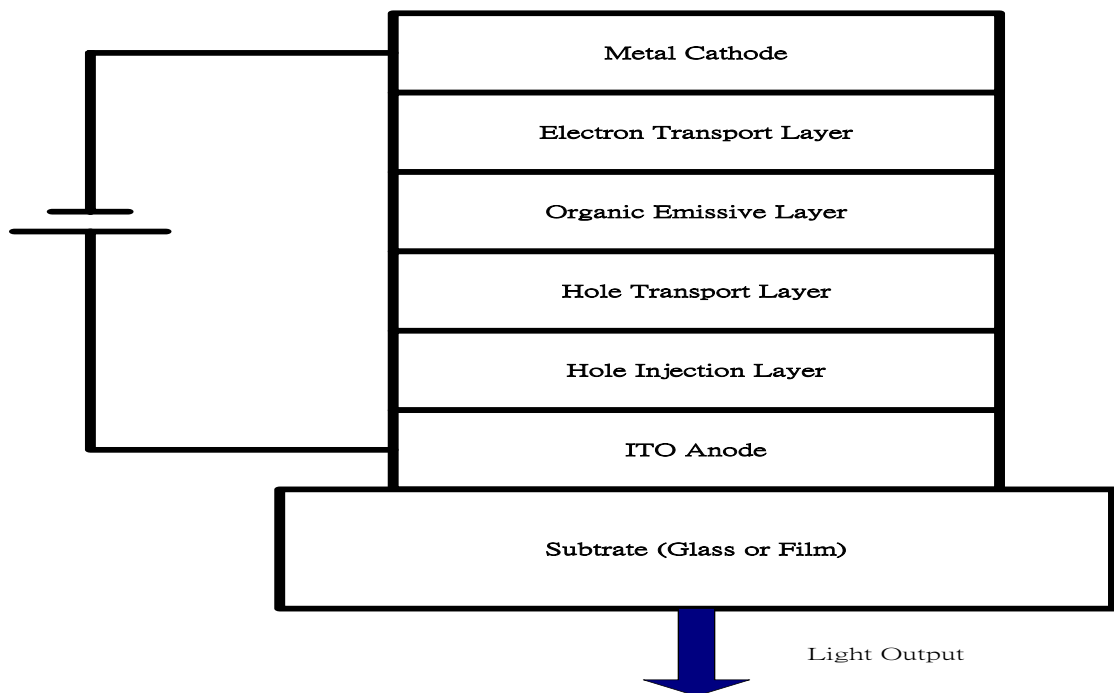


Fig. 2-2 A typical structure of an OLED device

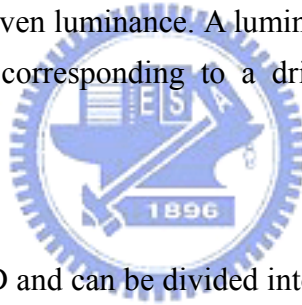
2.4 Emission Properties

The structure of a conventional OLED is shown in Fig. 2-2. Electrons and holes are correspondingly injected from the cathode and anode, and migrate through the electron and hole transport layers. Electroluminescence is generated by radiative recombination of these carriers near the interface between the two transport layers.

The relation between the drive current density J and instantaneous luminance in the direction of substrate normal $L(0)$ if an OLED is given by [2-4] [2-6]

$$J = \frac{C_n C_E \pi L(0)}{C_v \eta} \dots\dots\dots (2-1)$$

Where η is the quantum efficient. The constants C_n , C_E and C_v depend on the refractive index or the emission spectrum of the material. For an OLED using Alq_3 as the emissive material, $C_n=1.1$, $C_v=427 \text{ lm/W}$, and $C_E=0.44\text{V}^{-1}$. Equation (2-1) gives the drive current density required to achieve a given luminance. A luminance of 100cd/m^2 is usually considered sufficient for video displays, corresponding to a drive current density of 3.6mA/cm^2 for $\eta=1\%$.



2.5 Color Present

The color presents in OLED and can be divided into monochromatic, partial color and full color. Because the OLED has the characteristic of the self-moving optics and high brilliance, the display method of the monochromatic display and partial color still does not lack its usage situation. Current, green technology of organic light emitting diode in small molecule is the most mature, the blue and red optics have also started commercializing.

For high-information content display, the full color is an essential condition on the application of the display. Applications aiming at a full-color OLED display are making steady progress. Red, green and blue are necessary in each full color pixel. Up to present, several schemes exist for generating full color on the display of OLED. Prototypes have been demonstrated or reported by several research organizations, and each of them took a different approach to the fabrication. For example, the first approach employs patterned lateral RGB emitters, as shown in Fig. 2-3 [2-7]. This method has a good possibility of high luminous efficiency although patterning of organic layers is difficult. The second one utilizes blue OLEDs as a light source with fluorescent color arrays as color-changing media (CCM) to obtain RGB colors, as shown in Fig 2-4 [2-8]. This method does not require organic layer

patterning, but its low color change efficiency especially for red color is undesirable. The third approach uses white OLEDs with color filter array, as shown in Fig. 2-5 [2-9] [2-10]. This method has no need to pattern organic materials and is able to adopt the color filter technique used in LCD panel. But the efficiency of emitting light has a significant drop by passing through the color filters. Furthermore, there are other methods such as stacked RGB emitters. A stacked OLED was built at Princeton University with separate red, green and blue sub-pixels in a vertical, coaxial emitting geometry. Single pixels can be tunable to red, green, blue and white, as shown in Fig. 2-6 [2-11].

2.5.1 Patterned Lateral RGB Emitters

The simplest is to place red, green and blue(R, G and B) sub-pixels side by side and address them separately. Red, blue and green materials can be arranged in triads for each pixel through techniques such as precision shadow masking. This method blocks areas of the substrate surface for exact deposition and registration without gaps or overlap in color areas. Organic light emitting diode technology uses substances that emit red, green, blue or white light. Without any other source of illumination, OLED materials present bright, clear video and images that are easy to see at almost any angle.

To make use of the precise metal mask and CCD images position, red, green and blue by the order deposition constitute a pixel. Because the precise metal mask makes use of the super and thin lamella of metal, mask in the mechanical strength after taking shape will be under the influence of certain restrict, also cause an issue for position accuracy. OLEDs display development incline to the big size, over 10 inches, so will cause very big challenges, including the manufacture for the precise mask in big size and position technique.

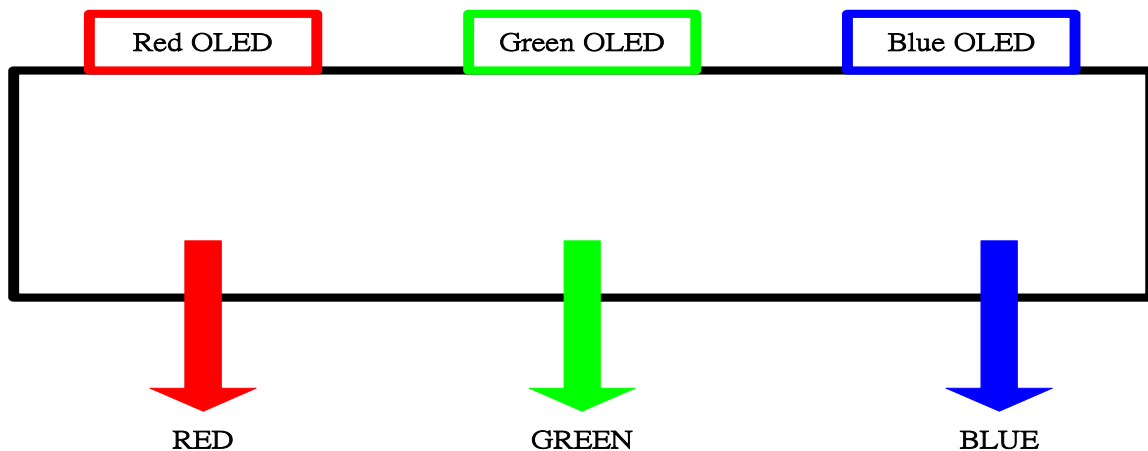


Fig. 2-3 One pixel by lateral RGB Emitter

2.5.2 Color Change Media

Single blue-emitting OLED may serve as a pump of R and G fluorescent color-changing media (CCM), which efficiently absorb blue light and reemit the energy as green or red light. This method does not require organic layer patterning. Its advantage is not to need the precise alignment to the technique, only needing the deposition for blue glow OLED component. A full-color organic display with 10 in. diagonal size was reported. This display was based on blue OLEDs with color-changing media. A potential problem to overcome in such displays is that “color bleeding” as light waveguided in the substrate can result in unintentional pumping of photoluminescence in adjacent pixels [2-6][2-12].

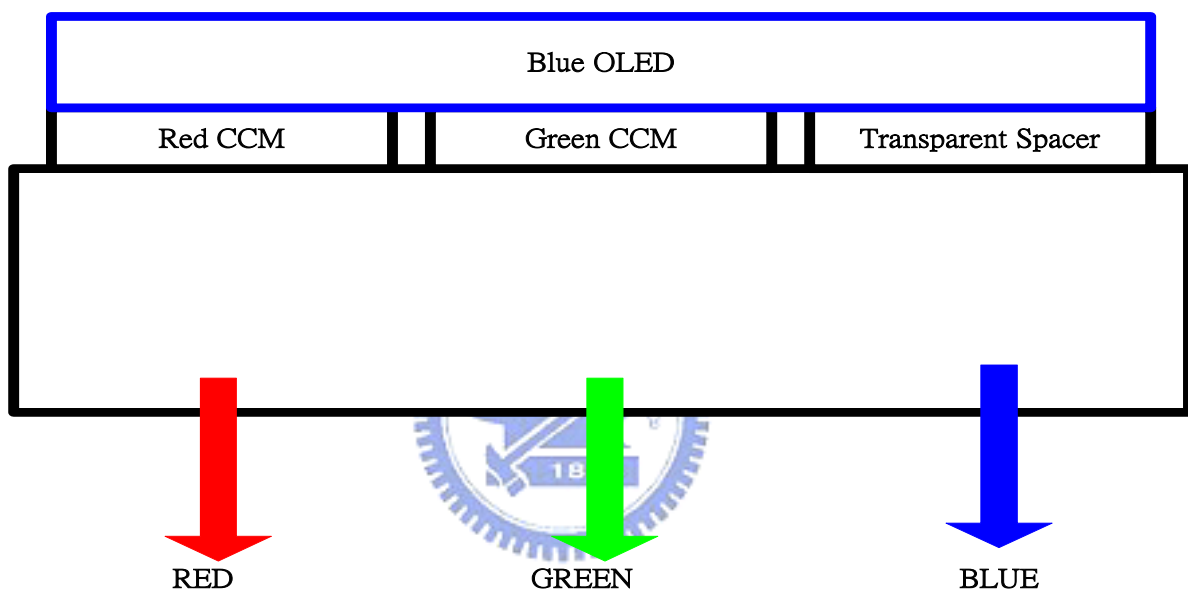


Fig. 2-4 One pixel by color change media

2.5.3 Color Filter

The way is to use a single white-emitting organic LED and filter. The light pass through R, G, and B media or dielectric. Full-color effects also can be produced using a white emitting layer. A color filter array made through photolithographic techniques is inserted between the anode and substrate layers to produce red, blue and green effects. The combination of a white electroluminescent material and a color filter does not require precise alignment as rigorous as pixelized OLED displays. Nevertheless, the principal drawback of this approach is that much of the white OLED output must be removed by the filter to obtain the required primary colors. For example, up to 90% of the optical power from the white OLED is filtered in order to obtain a sufficiently saturated red pixel, with the result that the OLED must be driven up to ten times brighter than the required R-G-B pixel brightness.

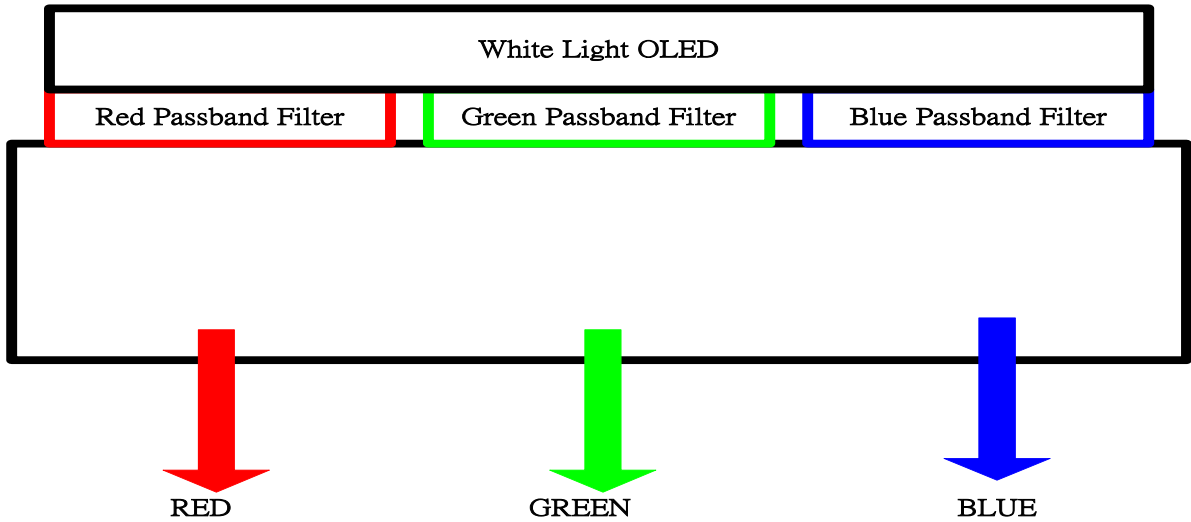


Fig. 2-5 One pixel by color filter

2.5.4 Color Stacked OLED

Current research on OLEDs is focusing on the integration of OLEDs into full-color, flat panel displays. The recent success in surface-emitting OLEDs has led to a new kind of integrated full-color pixel: the stacked OLED. In this technique, the layers that emit different colors are stacked on top of each other along with the required electrode to independently address each layer. The advantages of this approach in processing are that the patterning step and process control requirements are now essentially the same as for a monochrome display. Assuming that the patterning and addressing issue could be satisfactorily resolved, stacked OLEDs will triple resolution offered by the conventionally patterned RGB sub-pixels[2-12][2-13].

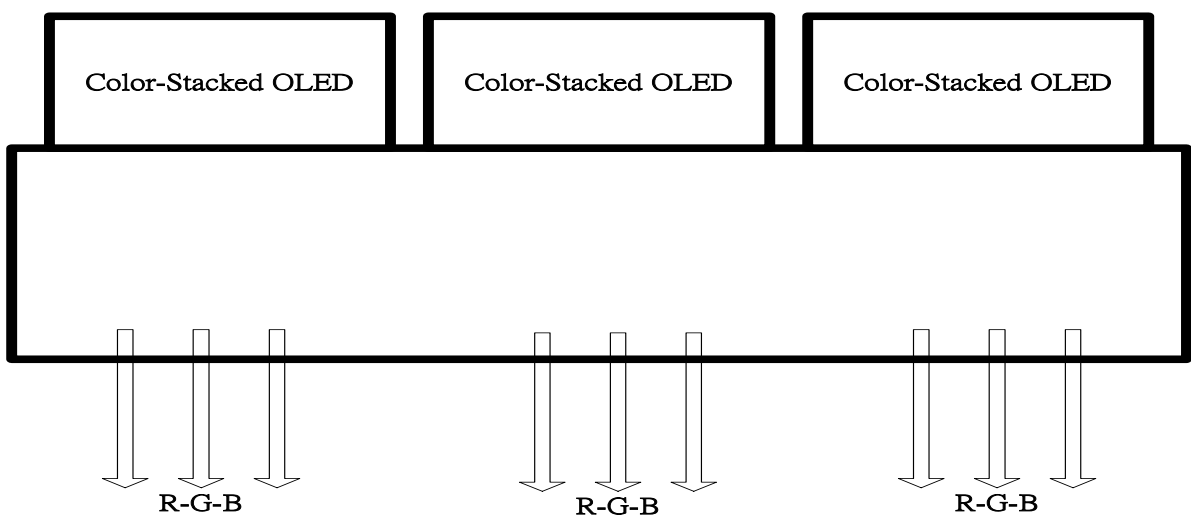


Fig. 2-6 Three pixels by color-stacked

2.6 Electric Illumination Characterization

Two drive methods are used in active-matrix OLED display: voltage driving and current driving. Voltage driving works by applying image signals to pixels as voltage data, which are converted to current data by pixel drive transistors. Converted current data flow to pixel OLED devices, which then emit light. Current driving works by applying image signals to pixels as current data, which are retained by pixel capacitors. Retained current data flows from pixel drive transistors to the OLED devices, which then emit light.

The voltage driving method applies voltage data to the source signal lines of the OLED display. Applied voltage data are converted to current data by pixel drive transistors and applied to OLED devices. Because current data converted by drive transistors have a nonlinear relationship to voltage data, the OLED device luminance has a nonlinear relationship to voltage data, as shown in Fig. 2-7. Current driving applies current data to the source signal line of the OLED display. Current data and OLED device luminance have a linear relationship, as shown in Fig. 2-8. Because OLED devices of RGB differ from on the current-luminance characteristics and the voltage-luminance characteristics, a adjustment circuit for brightness is necessary.

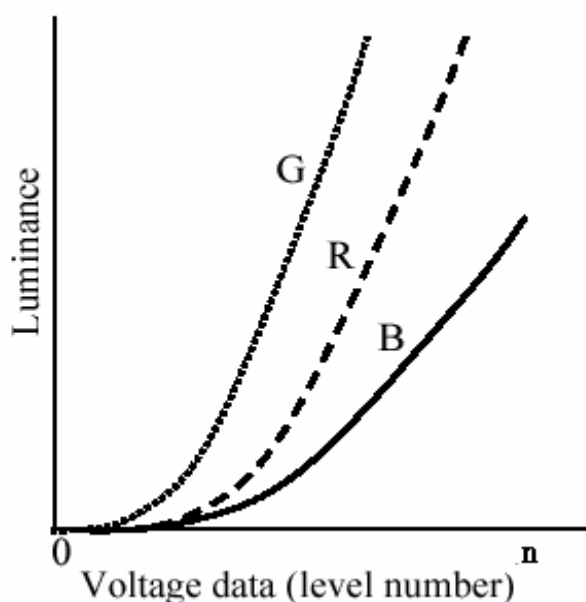


Fig. 2-7 A typical brightness and voltage data relation for different color OLED

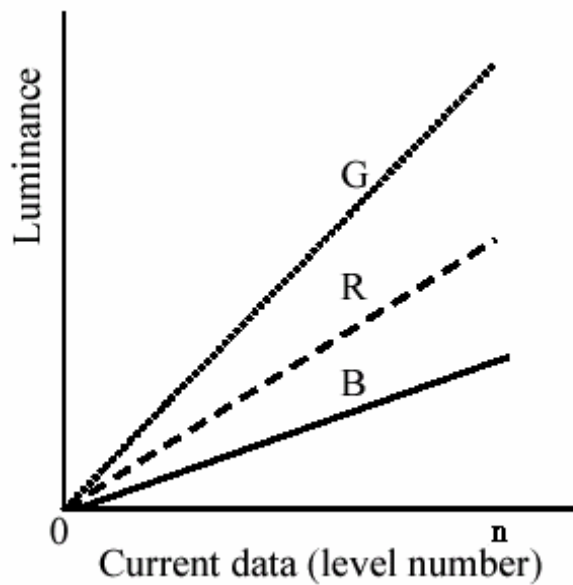


Fig. 2-8 A typical brightness and current data relation for different color OLED

2.7 Matrix Addressing

A display is an array of independently controllable pixels, the number of which depends on its dimension and resolution required by a particular application. Very large pixel counts are encountered in high-information content displays. For example, an NTSC standard TV screen requires 1.5×10^5 pixels. The addressing of a large number of pixels in an array is an important issue in the display technology. Among the five addressing schemes used in electronic displays[2-14], direct addressing and matrix addressing are suitable for OLED-based systems. The direct addressing scheme, where each pixel is connected to an individual driver, can only be used for discrete indicators and simple alphanumeric displays with few characters. In this case, complex character patterns be realized using shadow masks. By comparison, inorganic LED alphanumeric displays are expensive to fabricate because of the many individual diodes required to make up a single character, each with its own contacts and leads. In a matrix addressed display, pixel are organized in rows (scan line) and columns (data line), and each pixel is electrically connected between one row lead, and one column lead. The addressing schemes where active electronic components are added to pixels are called active matrix (AM) addressing; while those without extra active components in the pixels are termed passive matrix (PM) addressing.

2.7.1 *Passive matrix*

2.7.1.1 Pixel Structure

As shown in Fig 2-9, passive matrix (PM) OLED displays stack layers in a linear pattern, much like a grid, with “columns” of organic and cathode materials superimposed on “rows” of anode material. Each intersection or pixel contains all three substances. External circuitry controls electrical current passing through the anode “rows” and cathode “columns,” stimulating the organic layer within each pixel. As pixels turn on and off in sequence, pictures form on the screen.

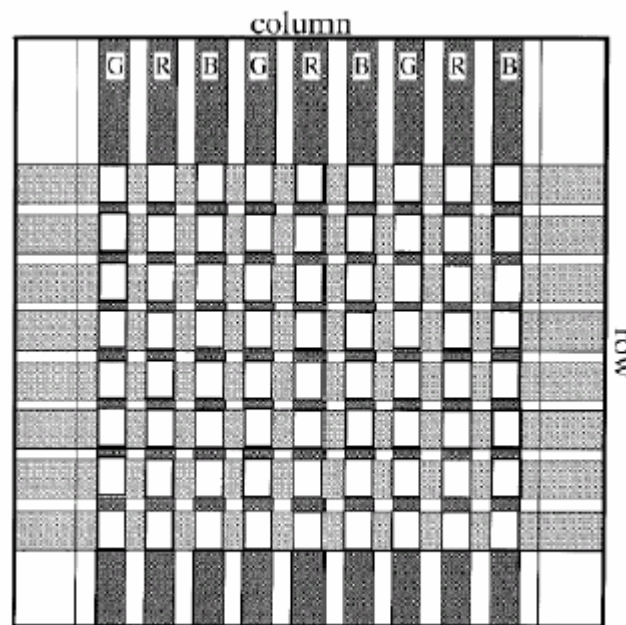


Fig. 2-9 Structure of a simple matrix-type display

2.7.1.2 Pixel Addressing

To address a matrix-type array of OLEDs is to perform a passive multiplexing. This mode of operation is well adapted since the electroluminescence phenomenon is fast (intrinsic response time in the 10^{-9} s range) and the current voltage characteristics of OLEDs are non-linear (diode-like). To achieve gray scales, the column drivers must be current sources since the pixel luminance is proportional to the drive current. There are two types of driving method [2-15] to implement gray scale . PAM (pulse amplitude modulation) and PWM (pulse width modulation) driving methods are well known. In increasing of the full color grayscale level and panel resolution, It is hard to exact current control. Therefore, the developed data driver IC is made by PWM method which has constant current source. The method of the

driving PM OLED is different from that of the LCD (liquid crystal display).

In this addressing mode, the matrix-type display is scanned line by line over the frame time. An electronic switch is employed to address each of the rows sequentially. When a line is selected, each pixel in the line is fed with a constant current pulse whole time duration is adapted to the desired level of brightness (pulse width modulation technique). Fig.2-10 schematically shows this principle of operation.

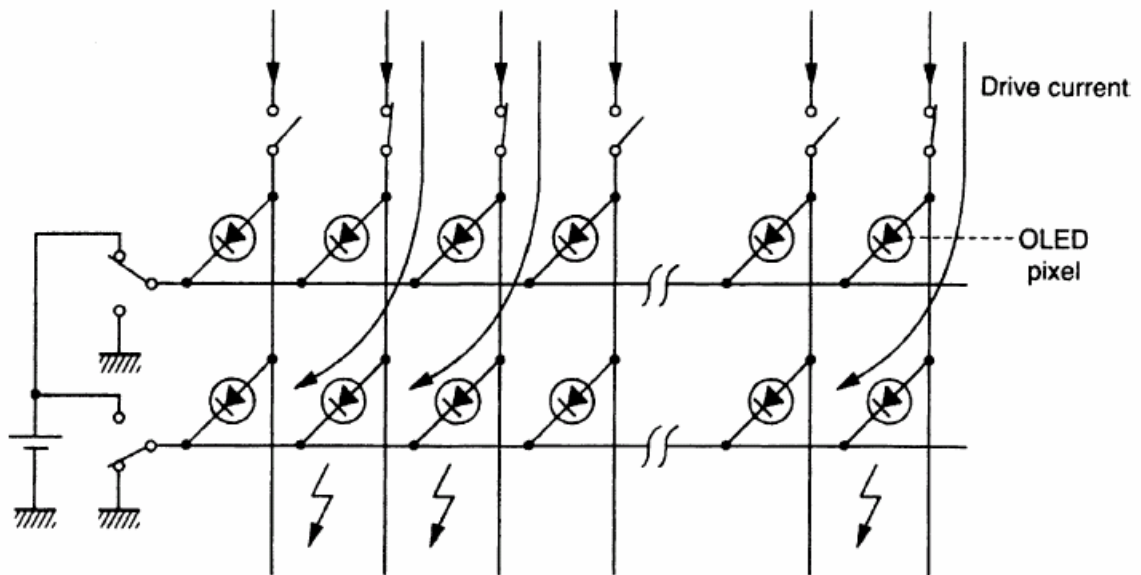


Fig. 2-10 Multiplexing principle for a matrix-type array of organic LEDs

2.7.1.3 Pixel Concern

To achieve an average display luminance of L_d , the pixel must be driven to an instantaneous luminance of $L(0)$ [2-4] [2-6]

$$L(0) = \frac{M L_d}{r_a d} \dots\dots\dots (2-2)$$

where M is number of rows of a display, d is the duty cycle of a pulsed current addressing the pixels and r_a is the aperture ratio of the display. The aperture ratio $r_a = \frac{W_r W_c}{(W_r + D_r)(W_c + D_c)}$, where W_r , W_c are the row-line width and column-line width respectively, and D_r , D_c are the gap width between the row lines and between the column lines in a PMOLED display respectively.

The instantaneous luminance requirement may limit the number of rows in a display. For a mean luminance 100 cd/m^2 , an instantaneous luminance up to 10^5 cd/m^2 limits the display row number to 500 for $d = 50\%$, $r_a = 100\%$. For a VGA display, this instantaneous luminance translated to a peak current about 1A on the row lines. These huge currents cause large voltage drops in the row lines and push the OLED operation to higher voltage, and then lowers the power efficiency. Table 2-1 [2-16] shows the power dissipation increases dramatically in PMOLED displays with increasing size and resolution. This simulation shows that when increasing the display area by a factor of 4(2 times larger diagonal), the total power dissipation increases by a factor of 10. It seems a bigger passive matrix display becomes impractical, and it will be necessary to move to an active matrix technology. Therefore, PM OLED displays' function and configuration are well-suited for text and icon displays in dashboard and audio equipment. Comparable to semiconductors in design, PM OLED displays are easily, cost-effectively manufactured with today's production techniques.

Resolution Col./row/size	$P_{\text{light}}(\text{mW})$	$P_{\text{cap}}(\text{mW})$	$P_{\text{res}}(\text{mW})$	$P_{\text{total}}(\text{mW})$	Efficacy(lm/W)
80/60 1.2"	15	10	1	26	5.3
160/120 2.4"	80	110	10	200	2.8
320/240 5"	400	1300	300	2000	1.1
640/480 10"	2000	18000	8000	28000	0.3

Assumptions: 300um x 300um pixels, efficiency 15Cd/A (typical for green emitting OLEDs), average brightness over frame period 100 cd/m^2 .

Light Production: $P_{\text{light}} = I_{\text{OLED}} \times V_{\text{OLED}}$

Capacitive losses: $P_{\text{cap}} = C \times V^2 \times \text{freq.}$

Resistive losses: $P_{\text{res}} = I^2 \times R$

Table 2-1 Power dissipation in PMOLED displays with increasing size and resolution.

2.7.2 Active Matrix Addressing

2.7.2.1 Pixel Structure

Active matrix (AM) OLED displays stack cathode, organic, and anode layers on top of another layer – or substrate – that contains circuitry. The pixels are defined by the deposition of the organic material in a continuous, discrete “dot” pattern. Each pixel is activated directly: A corresponding circuit delivers voltage to the cathode and anode materials, stimulating the middle organic layer.

AMOLED can be driven in a manner similar to the active matrix TFT-LCD. A conventional pixel is as shown in Fig. 2-11 [2-17]. The pixel structure of the voltage programmed driving scheme contains one switching transistor (TFT M1), one driving transistor (TFT M2) and one storage capacitor (C_s). In this circuit, TFT M2 is a PFET device connected in a common source arrangement, and plays the role of a current source to supply constant current to the OLED. The V_{gs} of the driving transistor for a specific output current will be programmed in the capacitor through the switching transistor (TFT M1). However, such voltage programmed pixel structure encounters the non-uniformity problem.

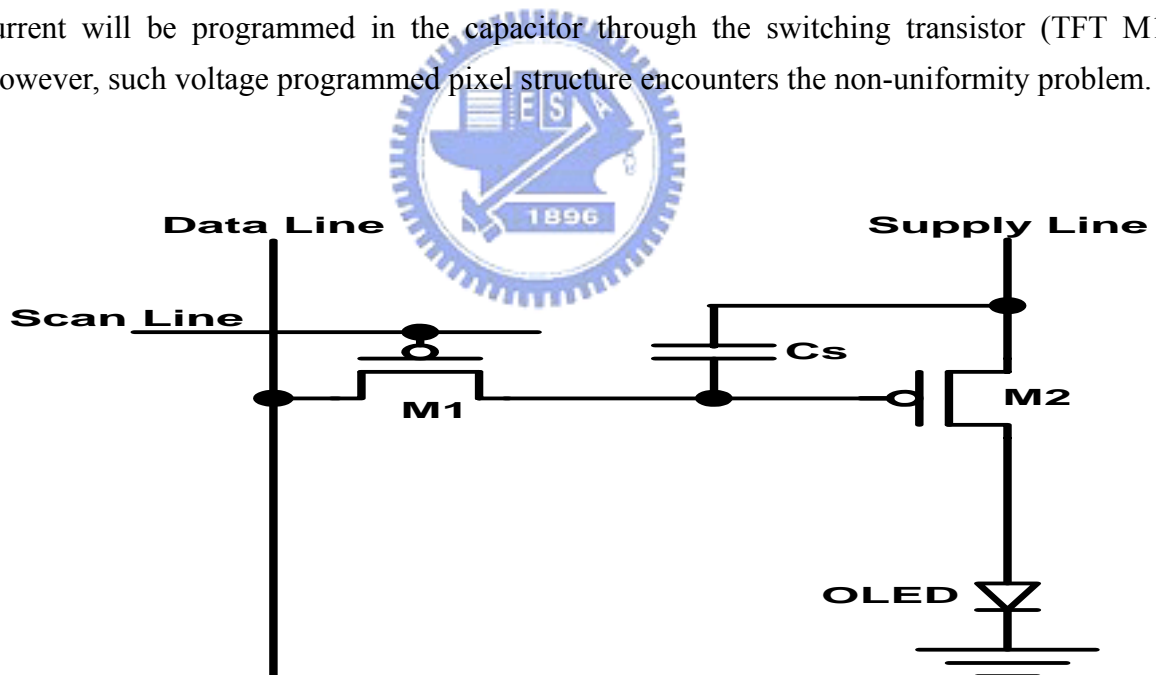


Fig. 2-11 Principle of active matrix addressing of an OLED display..

The saturation current of a TFT is usually approximated using the following equation(2-3), where W is the channel width, L is the channel length, Cox is the capacitance per unit area of the gate dielectric layer, V_{th} is the threshold voltage, and U is the field-effect mobility:

$$I_d = \frac{W}{2L} U_p C_{ox} (V_{gs} - V_{th})^2 \dots \dots \dots (2-3)$$

From the asymptotic square equation for transistor current, it is obvious that the threshold voltage and mobility variation will result in great variation of the output driving current, and the non-uniformity in grey scales will be induced. Variations in threshold voltage and mobility depending upon implementation may add to luminance variations. With p-Si., initial variations are higher due to grain size and boundary variations[2-18]. With a-Si, time related electrical stress can give large threshold voltage variations[2-19] [2-20]. These luminance variations are tolerable if they occur gradually across a display, because the eye is insensitive to such variation. However, if they occur randomly from pixel to pixel, the eye can readily detect these variations.

2.7.2.2 Pixel Addressing

Fig. 2-12 show the active matrix addressed OLED(AMOLED). Each pixel in AMOLED has a driving transistor in series with the OLED which supplies a constant current throughout the frame time. As shown in Fig. 2-11, the scan line of the display are sequentially scanned over the frame time. When a line is selected, all the M1 transistors in this line are switched-on and the voltage data are transferred on the gates of the M2 transistors. These data voltages are maintained on the gates of M2 transistors as M1 transistors are switched-off, when the next line is selected. A storage capacitor can be added to compensate the leakage current of M1 transistors. In this addressing mode, the current is supplied to the organic LED during the whole frame time. The necessary current levels are much smaller , but cause the setting times to be much longer. For a 300um x 100um pixel at typical luminance levels of 100 cd/m², the transistor current is only a few micro-amps [2-21] [2-22] [2-23]. As for a typical pixel capacitance of 5 pF, it takes about 8us for a 3uA current to charge 5 pF though 5 volts.

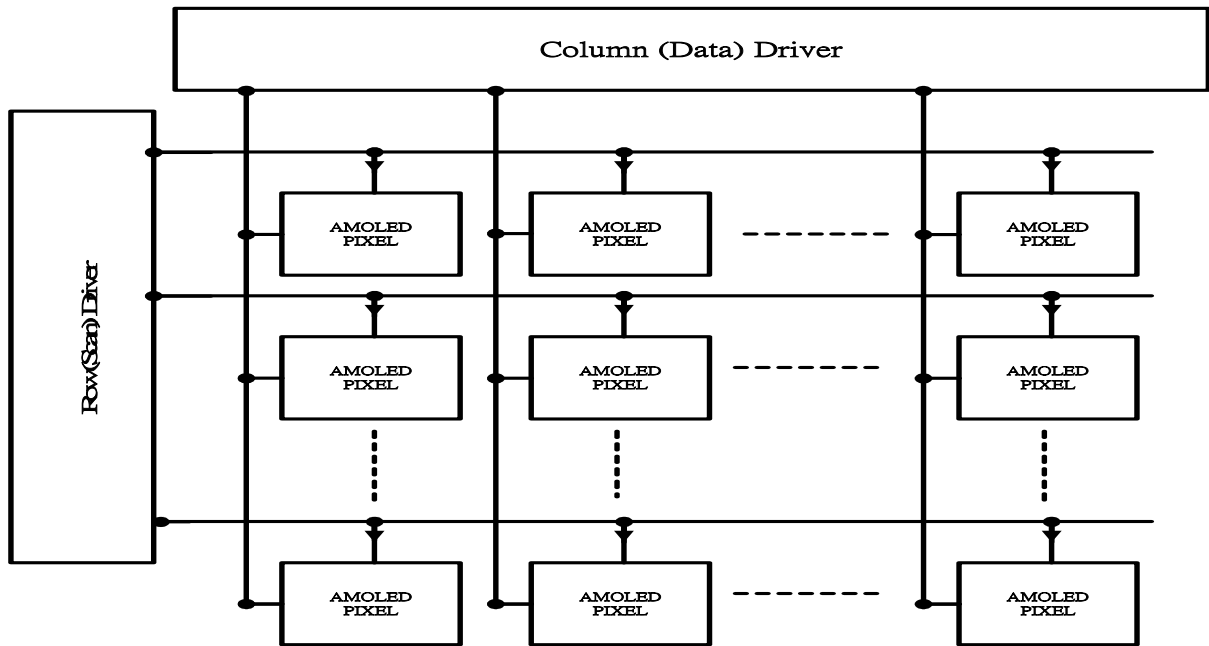


Fig. 2-12 Circuit diagram of an active matrix OLED

2.7.2.3 Pixel Concern

2.7.2.3.1 Constant Current or Source Follower

In order to continuously supply the current to the AMOLED pixel while the other scan lines are addressed. At least two TFTs are required for one pixel. The equivalent pixel circuit for this approach based on the n-channel TFT is shown in Fig. 2-13 and Fig. 2-14 [2-20]. Fig. 2-13 and 2-14 are the constant current arrangement the source follower arrangement, respectively. Due to the constant current circuit can eliminate the slight threshold voltage (V_{th}) shift of OLED and maintain the same output current level, it is preferred. That is the brightness remains even if a slight V_{th} shift of OLED is existent. Since OLEDs are extremely sensitive to moistures, wet process like photolithography is usually forbidden after the deposition of the organic layers. Therefore, the pixel circuits for AMOLED needs to be defined before the deposition of the organic layers. This limitation makes it very difficult to achieve the configuration as shown in Fig. 2-13, where the interconnection between the cathode of the OLED and the drain electrode of TFT M2 needs to be established. This implies that the constant current configuration for the n-channel TFT is difficult to realize for the two TFT circuit. For Source follower in Fig. 2-14, the drawback of this circuit is that the current depends upon the OLED voltage. The OLED voltage may vary from pixel to pixel and increase slowly with usage, $\sim 0.1\text{-}1\text{mV/hour}$, providing additional sources of non-uniformity.

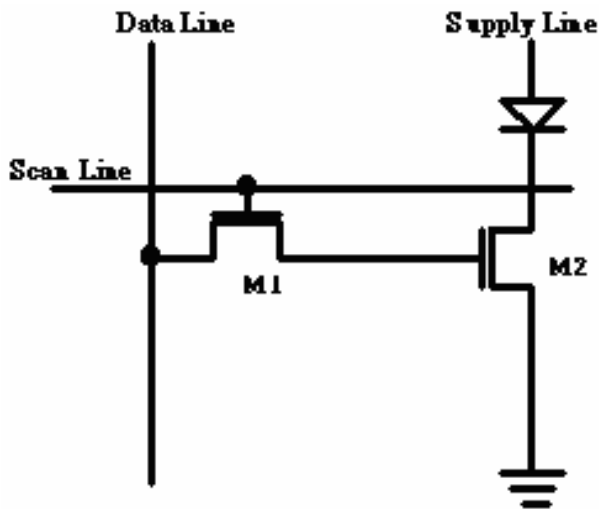


Fig. 2-13 Constant current pixel

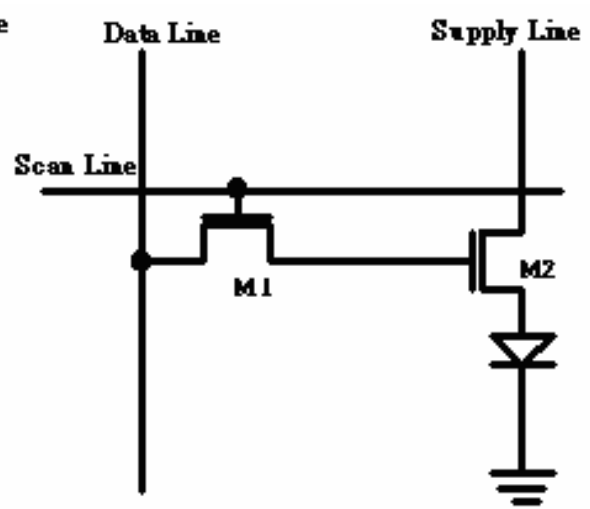


Fig. 2-14 Source follower pixel

2.7.2.3.2 Driving Device Choice

To solve the above pixel issue, NFET in Fig. 2-14 is replaced by PFET. A current source with storage capacitor (Cs) is shown in Fig. 2-11. The OLED voltage dependence on current is eliminated with the circuit. The data voltage is written onto the data storage capacitor Cs when the TFT M1 gate line is brought to negative level. TFT M2 is a PFET device connected in a common source arrangement. TFT M2 play the role of a current source to supply constant current to the OLED. The current is proportional to $(V_{dd}-V_{data}-V_{th})^2$ for $V_{th} > V_{oled}-V_{data}$ where V_{th} is the TFT threshold voltage.

2.7.2.3.3 IR-drop

OLED makes a direct current pass and emit light from the organic compound of the fluorescence excited by supplying electric field. The current is proportion to the data voltage which is written onto the data storage capacitor Cs. The period for the written data voltage is called addressing time. Since OLED is a current driver element, there is an IR drop issue on supply line along scan line direction while a turned on OLED is during addressing time, as shown in Fig. 2-15 [2-23]. A bad affect exist. That is, the pixel closed to supply line will be programmed an exact data voltage, but the far pixel will be programmed a wrong data voltage. The variation of gate-source leads to the divergent color. A variant of this circuit as shown in Fig. 2-16 uses an additional TFT to block any current flowing into the EL element while the scan line is addressed. The purpose is to reduce signal error due to resistance of the supply line.

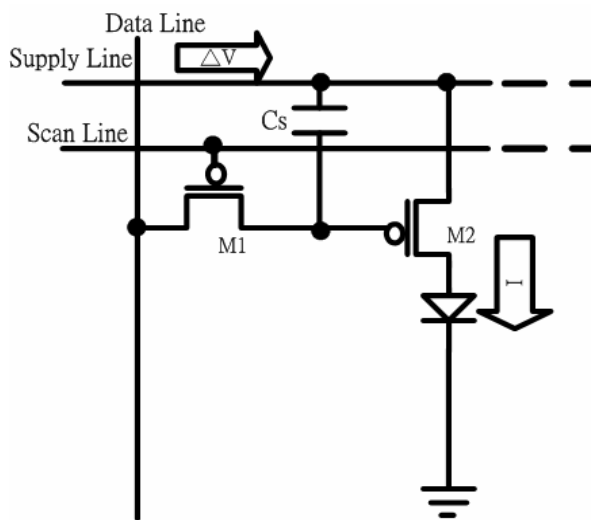


Fig. 2-15 IR-drop perspective

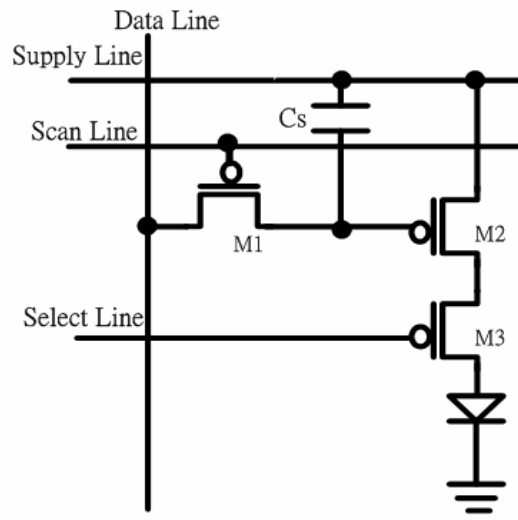


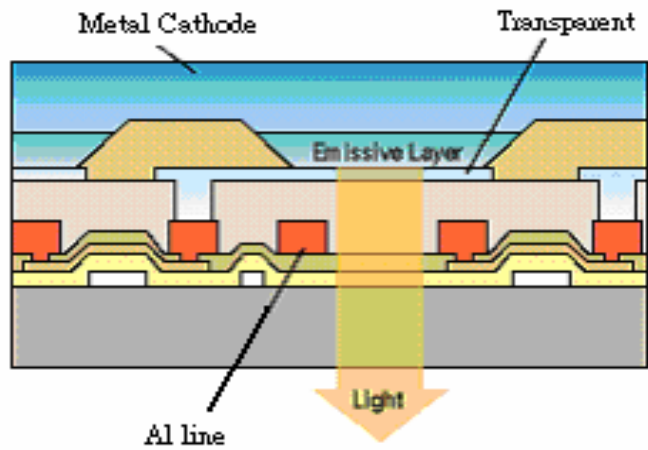
Fig. 2-16 A variant pixel with additional TFT

2.8 Top-Emission and Bottom-Emission

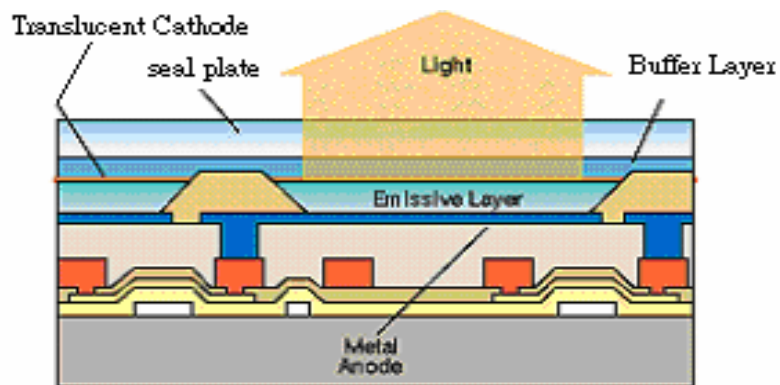
With the creation of a 13-in. color active-matrix organic electroluminescent (OEL) display, Sony (Tokyo, Japan) has demonstrated its proprietary top emission adaptive current (TAC) drive technology [2-24], which allows the fabrication of high-quality displays measuring over 10 in. The 800 x 600-pixel OEL display is presented as the largest of its type, presaging the use of OEL technology in a wider variety of applications beyond portable and compact devices.

Traditional polysilicon TFT drive systems often induce nonuniformity of luminance between the individual pixels, which makes it difficult to create a large-scale OLED display. TAC technology expands on the two-transistor driver circuit by using four transistors, of which two are paired to offset pixel variation for uniform luminance over the entire screen. A detail description for circuit is introduced in next chapter.

In addition, unlike the bottom-emission structure of traditional OLED displays where light is partly blocked by the TFT structure as shown in Fig. 2-17(a), the top-emission structure as shown in Fig. 2-17(b) emits light through the opposite side of the display matrix without any interference. In addition to increasing luminance, the pixels may be fabricated smaller to achieve higher resolutions.



(a) Bottom Emission Structure



(b) Top Emission Structure

Fig. 2-17 Bottom and top emission structure

Chapter3

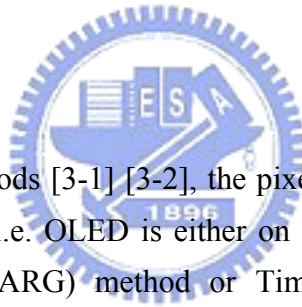
AMOLED Review for Driving Design

3.1 Category

In AM addressing scheme, electronic switches are used with OLED for each pixel providing the means to retain the video information on a storage capacitor during the complete frame time. An additional active component, known as drive transistor is needed to provide the OLED with drive current at each pixel. The channel material of the TFTs can be Poly-silicon or amorphous-Silicon or even organic molecules. AM OLED pixels turn on and off more than three times faster than the speed of conventional motion picture film – making these displays ideal for fluid, full-motion video.

The AM addressing mechanisms are broadly categorized in two categories

- . Analog
- . Digital



In the Digital driving methods [3-1] [3-2], the pixel circuit drives OLED in digital mode using constant current source i.e. OLED is either on or off. Grayscales are generated using either Area ratio grayscale (ARG) method or Time ratio grayscale (TRG) method or combination of both. In Area ratio grayscale (ARG) generation method, the pixel circuit is repeated for every bit required. In Time ratio grayscale (TRG) generation method, pulse width modulated current source is used. In the analog methods [3-1][3-2], each OLED is driven by controlled current source of varying current depending upon the brightness required. The controlled current source can be programmed by using either a current source or a data voltage source and should provide desired current throughout the frame time corresponding to the gray- level.

we will present the general concept of the AMOLED technique. Transistor technologies including a-Si:H, poly-Si, crystalline Si, and organics will be reviewed with respect to application to AMOLED displays. Then we will introduce some traditional pixel structures and driving schemes.

3.2 Transistor Technologies

polysilicon and amorphous silicon(a-Si) are known as semiconductors of TFTs used in active matrix organic light emitting diode panels. However, only expensive polysilicon backplanes were used for OLED production, because of their greater electron mobility. But researchers have started creating OLED structures on cheaper amorphous silicon substrates. In fact, IDTech—a joint venture between Chi Mei Optoelectronics and IBM—has demonstrated a 20-inch full-color OLED panel on an amorphous silicon substrate. In next, transistor technologies including a-Si:H, poly-Si, crystalline Si, and organics will be reviewed with respect to application to AMOLED displays.

3.2.1 Poly Silicon

Polysilicon is recently the active matrix technology of choice for direct view AMOLED displays. This is due to the high drive currents and the long term stability of the devices compared to amorphous silicon transistors. The field effect mobility is around 50~400 cm²/Vs and the on-off ratio is about 10⁶ [3-3] [3-4]. It is suitable for pixel as well as driver integration on glass. Sanyo/Kodak demonstrated a stunning display at the SID'00 and Sony announced a new display at SID'01 Symposium. Thin film transistor technologies have large variations in output characteristics from device to device. These non-uniformities are due to the nature of the poly silicon material growth and the drift of the transistor characteristics during operation. These variations make it difficult to produce uniform current sources across many pixels. Since the pixel brightness is proportional to the current, any variation in the threshold voltage and mobility of the current drive transistor shows up as a variation in pixel brightness, creating a “salt and pepper” effect across the image. This effect is prevalent in poly silicon AMOLED displays. To avoid the objectionable effect, a lot of ideas are whether the driving method or the circuit attempts to correct for drive transistor variations.

3.2.2 Amorphous Silicon

Hydrogenated amorphous silicon (a-Si:H) TFT is of great interest because of the low cost and the large amorphous silicon manufacturing base[3-5]. Amorphous silicon deposition process tends to generate uniform initial threshold voltage, but the threshold voltage drift significantly over time. Besides, a-Si:H TFT has much smaller field mobility (<1cm²/Vsec) than poly-Si TFT (50~400 cm²/Vsec) [3-3] [3-6]. Therefore, the OLED driving current provided by an a-Si:H circuit will be much smaller than a polysilicon circuit. However, recent progress [3-3] [3-7] [3-8] in OLED efficiency make it possible to achieve a high brightness with much smaller current. For a typical OLED emission efficiency of 5.0 cd/A and a pixel

area of $2.0 \times 10^4 \text{ um}^2$, a current of $4.0 \times 10^{-7} \text{ A}$ is need to achieved a pixel brightness of 100 cd/m^2 . Table 3-1 shows the comparison of the saturation currents of a-Si:H and poly-Si TFTs.

item	material	a-Si:H TFT	Poly-Si TFT
Typical Mobility(cm^2/Vsec)		0.5	50
TFT W/L Ratio		10:01	10:01
Saturation Current(A)		2×10^{-6}	2×10^{-4}

Table 3-1 Comparison of the saturation currents of a-Si:H and poly-Si TFTs

3.2.3 Organic Transistor

A new technology just starting to enter the display area is organic thin-film transistors (OTFTs). The technology [3-9] uses organic films to make up the active regions of the transistor. Displays and circuits can be made on flexible plastic substrates, because the entire fabrication process takes place at temperatures $< 100^\circ\text{C}$. Using this process, analog and digital circuits can be built on plastic substrate. Mobility on the order of $1 \text{ cm}^2/\text{Vsec}$ has been achieved with low threshold voltages, providing a performance level comparable to amorphous silicon transistors. It is hoped that greater stability will be achieved through refinements in materials and processes, making for a more robust approach.

3.2.4 Crystalline Silicon

Another approach to produce uniform OLED pixels is to implement the active matrix in a crystalline silicon technology where the transistor variations are small enough to produce uniform displays without correction. The process of silicon is limited to wafers, so techniques are suitable for microdisplay application. For example, eMagin is pursuing small area displays on silicon that can be used in head-mounted systems. Besides, due to the nature of higher mobility, crystalline silicon can operate at higher frequency. As shown in Fig. 3-1, it is very easy to integrated scan and data driver on a AMOLED chip if the crystalline silicon is used. Parallel driving method is also applied to compensate the lower mobility for amorphous silicon and polysilicon, but it will induce higher hardware cost.

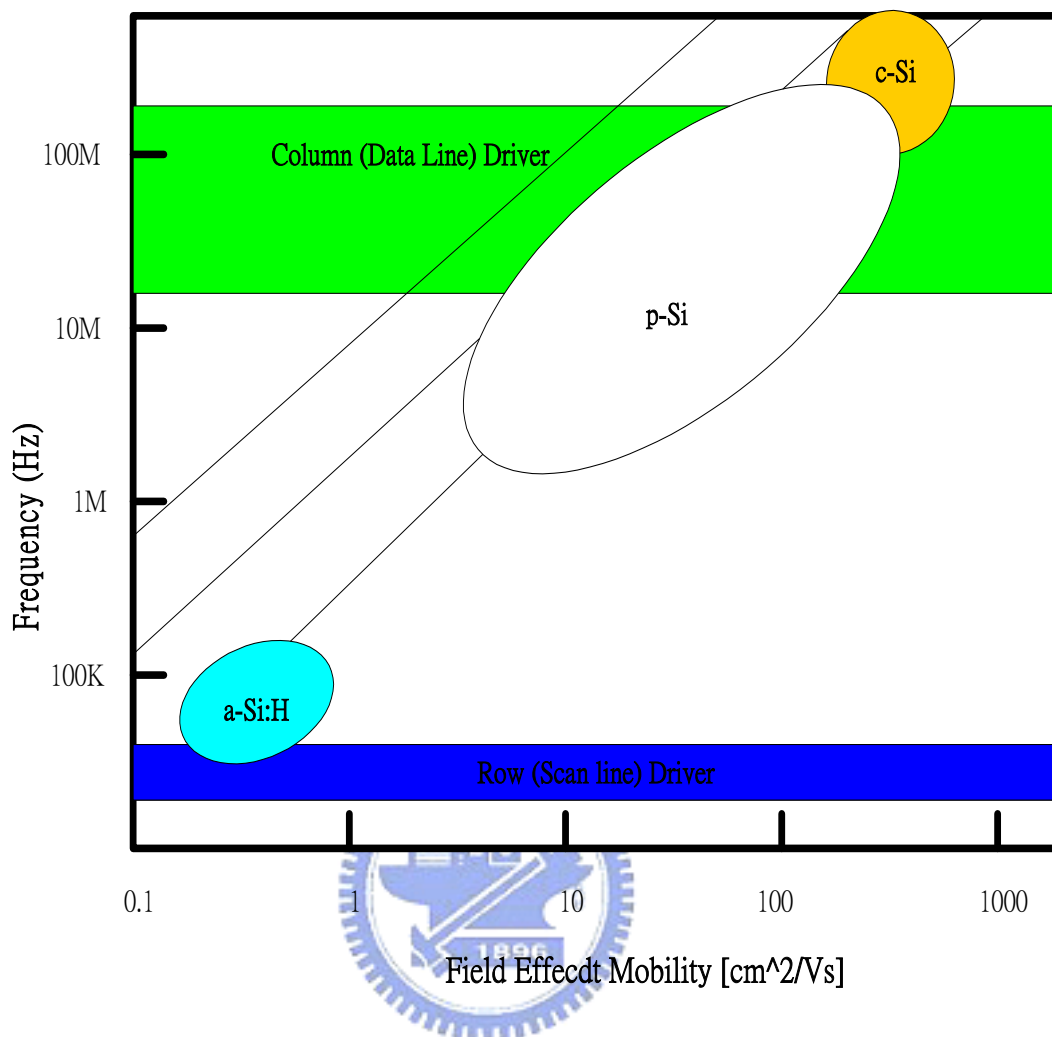


Fig. 3-1 Relation of operation frequency and field effect mobility for different technology

3.3 Analog Driving

Variations in threshold voltage and mobility depending upon implementation may add to luminance variations. Consequently, special pixel driver circuits are designed to overcome such difficulties in order to get the good image quality. An important distinction between different pixel circuits is whether the data being written to the pixel is current or voltage. Voltage driving works by applying image signals to pixels as voltage data, which are converted to current data by pixel drive transistors. Converted current data flow to pixel OLED devices, which then emit light. Current driving works by applying image signals to pixels as current data, which are retained by pixel capacitors. Retained current data flows from pixel drive transistors to the OLED devices, which then emit light. In next, the different circuits and driving methods are reviewed.

3.3.1 Voltage Programming Pixel

3.3.1.1 Voltage Programmed with 4T2C Pixel Structure

The problem of variation of TFT threshold voltages was first tackled by Dawson *et. al* in 1998, using a four-TFT configuration [3-10][3-11]. An improved AMOLED pixel was designed which eliminates the effect of the transistor threshold voltage variation. The schematic for this pixel is shown in Fig. 3-2. The advantage of the four-transistor pixel is that it uses an auto-zero cycle to reference the data against the transistor threshold voltage eliminating the effects of the transistor threshold voltage variation.

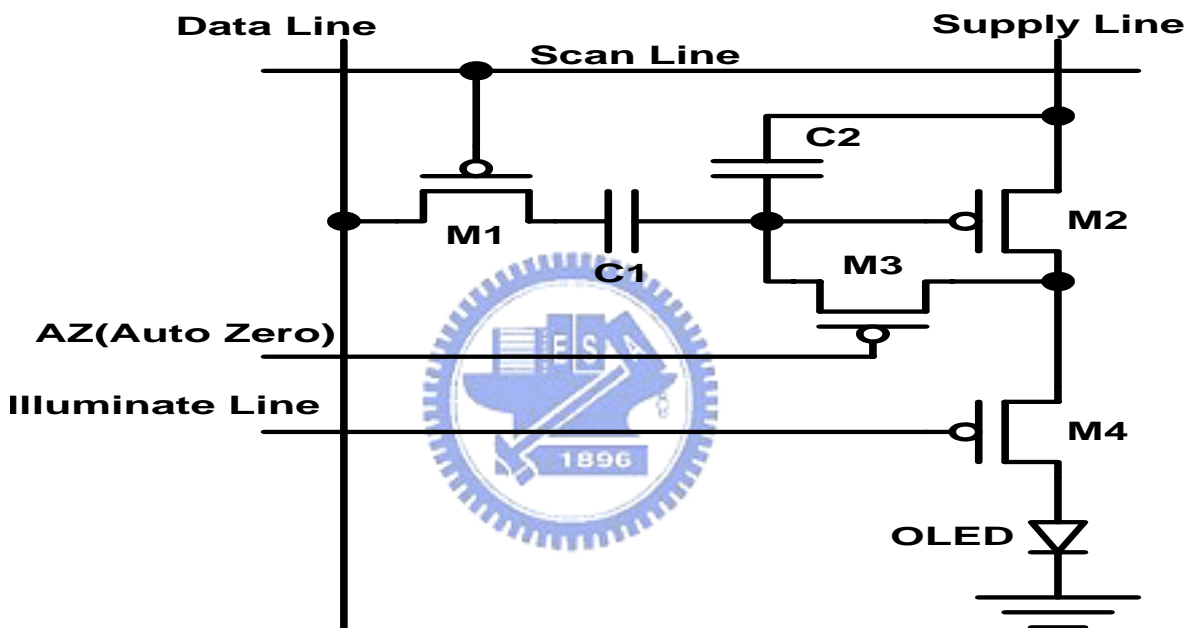


Fig. 3-2 Conventional voltage programming pixel with threshold compensation

The functionality of TFT M1 through TFT M4 is identical to that in the current data pixel circuit. However, the driving method is more complex in that TFT M2's threshold voltage must be established on the capacitors before writing data. With illuminate line low, the scan line is brought low with V_{sup} (Voltage on supply line) on the data line. Then, AZ is set low turning M3 on. A voltage across capacitor is developed that M2 forces to conduct. The illuminate line is brought high turning M4 off to isolate the circuit from the OLED. With M3 on, a voltage that is proportional to the threshold voltage of M2 is developed across both capacitors. The AZ input is brought high turning M3 off. The data voltage for luminance is presented on the data lines. A portion of data voltage is coupled onto the capacitor C2 by capacitor C1. The scan line is brought high followed by a low on the SW input turning M4 on. The OLED current is, to a first

order, proportional to the square of the C2's coupled data voltage. The step of the above operation is shown in Fig. 3.3.

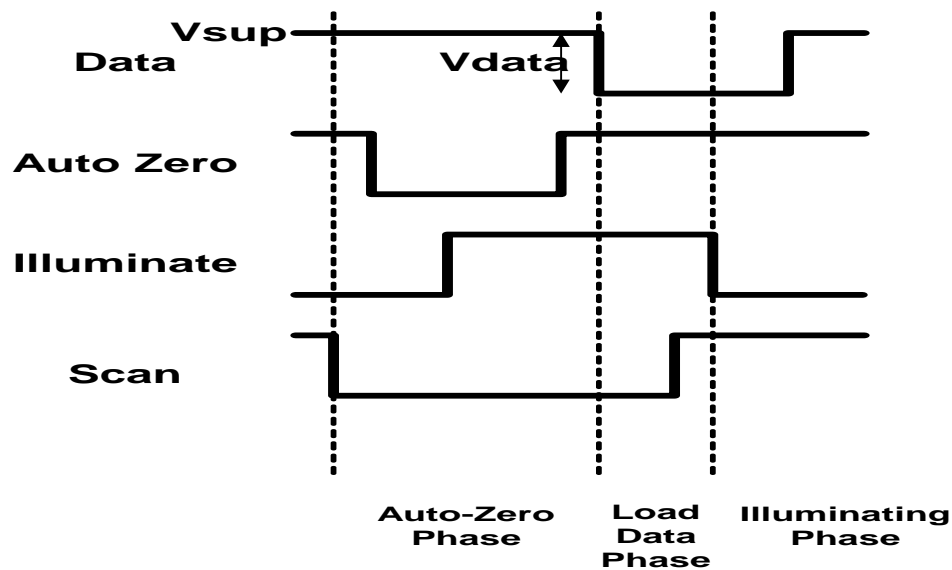


Fig. 3-3 Timing diagram for 4T2C operation

3.3.1.2 Voltage Programmed with 5T1C Pixel Structure

Fig. 3-2 shows the conventional pixel structure and timing diagram of that structure which can compensate threshold voltage variation and the degradation of supply voltage. But it needs 3 control lines and complex driving signals for data line and control line. Moreover the data line must be alternated to supply voltage level with every row (scan) line time to store a threshold voltage.

A novel pixel structure having 5TFTs, 1 capacitor and 1 control line is shown in Fig. 3-4 [3-12] with a timing diagram for operation. M2, M3, M4 and M5 are switching TFTs, and M1 is driving TFT, which supplies constant current to OLED for a frame time. V_{sus} produces a constant voltage which is lower than the programmed data to sustain the gate node voltage of M1 for a frame time. The gate node voltage of M1, the right side of C_{ST} , increases to ' $V_{DD}-V_{TH,M1}$ ' by diode connected M1 and the left side of C_{ST} is set to programmed data voltage during the current scan line time. After the row line time M4 and M5 are turned on and the potential of both side of C_{ST} decrease as a level of ' $V_{DATA}-V_{SUS}$ '. From that time OLED current flow by driving TFT M1, as follow equation (3-1).

$$\begin{aligned}
I_{OLED} &= \frac{\beta}{2} (|V_{GS,M1}| - |V_{TH,M1}|)^2 \\
&= \frac{\beta}{2} [V_{DD} - \{V_{DD} - |V_{TH,M1}| - (V_{DATA} - V_{SUS})\} - |V_{TH,M1}|]^2 \\
&= \frac{\beta}{2} (V_{DATA} - V_{SUS})^2 \dots\dots\dots (3-1)
\end{aligned}$$

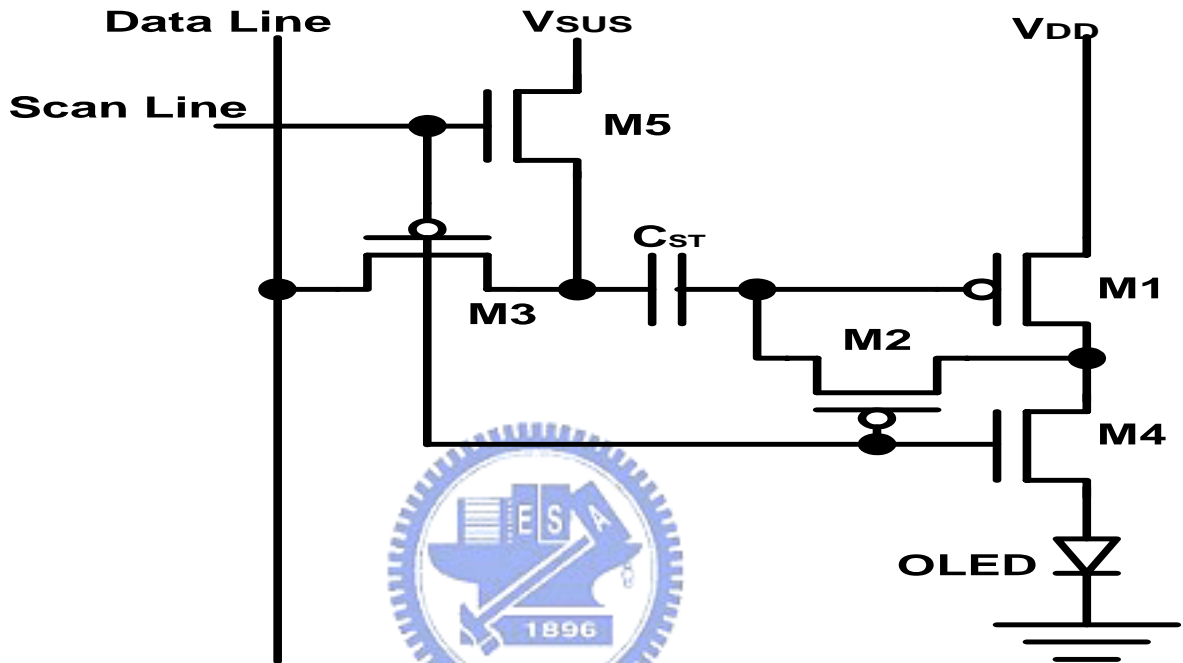


Fig. 3-4 Novel voltage programming pixel with threshold compensation

It has only one control line, scan line, for pixel operation and can use a whole row line time to program the data. The OLED current is controlled only by the V_{DATA} and V_{SUS} so that it has good immunity against the degradation of panel supply voltage. The step of the operation is shown in Fig. 3-5.

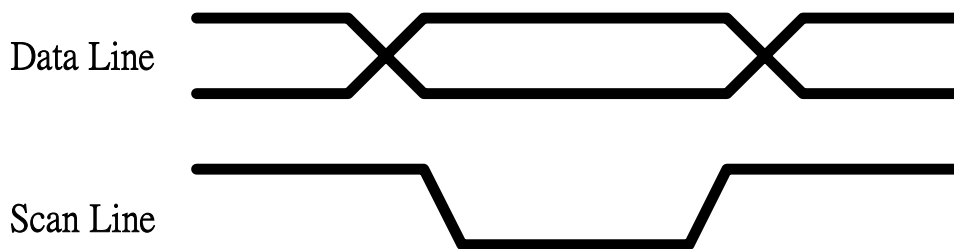


Fig. 3-5 Timing diagram for 5T1C operation

3.3.2 Current Programming Pixel

3.3.2.1 Current Programmed with Current-Copy Pixel

To avoid the non-uniformity problem induced by the variation of the threshold voltage and mobility of the TFTs, various pixel structures for current programmed driving scheme have been proposed [3-13] [3-14] [3-15]. Rather than the voltage signal to be programmed in the voltage programmed pixel structures, current signal on the data line is to be programmed into the pixel in these structures. In programming state, the scan line in Fig. 3-6 is activated, and the data line sinks for the specific TFT M2. This TFT is diode-connected by the supplementary switching TFT M3. Meanwhile, V_{gs} for the specific current through the TFT in saturation region is self-adjusted and stored in the storage capacitor (C_s). In the next state while the scan line is deactivated, often called the reproduction state, the configuration in the pixel is changed by the supplementary switching TFTs so that the stored V_{gs} on the driving TFT M2 will reproduce the current for the OLED. In this driving scheme, OLED current can be programmed and reproduced precisely, regardless the variation of the threshold voltage or mobility.

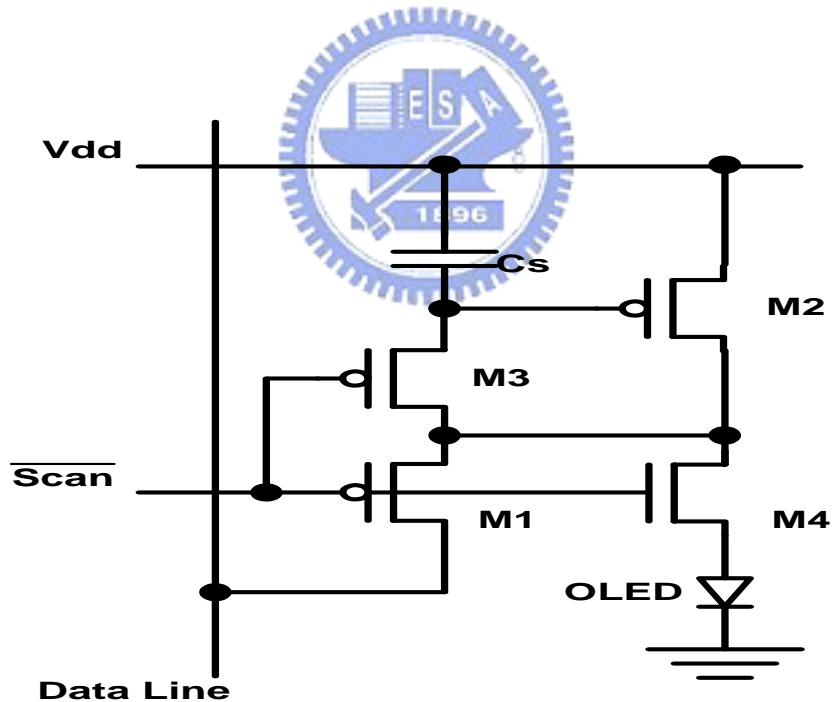


Fig. 3-6 Current programmed with current-copy pixel

3.3.2.2 Current Programmed with Current Mirror Pixel

However, though the foregoing current programmed pixel structures seem immune to the process variation at first glance, it takes a vary long time to charge the data line in the programming state due to the current needed is vary small (nA~uA). Even though the current programming method can be applied to achieve excellent image quality, its panel driving speed is too slow to implement high resolution displays.

Other current programmed circuits have been proposed, Fig. 3-7 show the scheme [3-16] proposed by Sony Corporation. To set the OLED current, the scan line input is brought low while pulling or sinking the data current out of the data line. TFT M1 and TFT M2 are turned on by the scan line. TFT M1 operates as a data switch allowing current to flow from the pixel circuit into the data line. TFT M2 functions as a switch changing operation of TFT M3 to that of a diode, which allows adjustment of the capacitor voltage for matching TFT M3's drain to source current to I_{data} . M4 drives the OLED based upon the capacitor voltage. The width of TFT M3 is large than the width of TFT M4. By this way, we can adjust the aspect ratio of the TFT M3, M4 to achieve the current mirror ratio needed. Thus, a larger current will change the data line during the programming state, and the current driving OLED is still small. This allows the data current to be larger in order to set the pixel current within a scan time for low luminance levels.

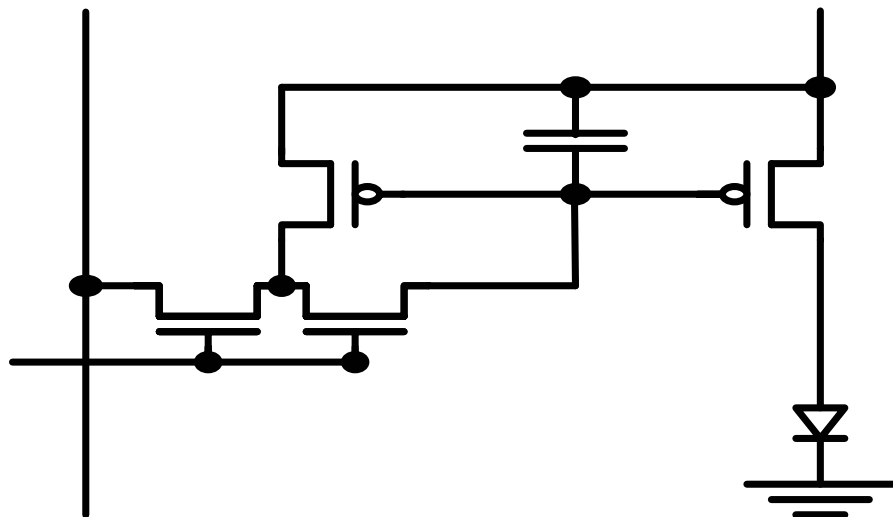


Fig. 3-7 Current programmed with current mirror pixel

3.4 Digital Driving

A full color display is more and more important in a life application. There are two types of driving method for Fig. 2-11. The analog driving and digital driving methods are well known. For analog driving, the intensity of each color is controlled by varying the amplitude of voltage applied to the sub-pixel during a picture frame.

The tendency, seems to be in favor of digital driving. For instance, Seiko-Epson use what they call area ration grey scale (ARG) in conjunction with time ration gray scale (TRG) [3-1][3-2]. In digital driving, each EL element is connected to a switch. The stored voltage range must exceed the worst-case threshold voltage to operate correctly. By pushing the driving transistor into its linear operating region, the pixel circuit operates in a digital mode, being fully on or off. The method can reduce the threshold voltage sensitivity of display image.

3.4.1 Area Ratio Grayscale

Fig. 3-8 show the ARG method, the number of grayscales is proportional to the total number of sub-pixels of equal size to connect to the supplied voltage. In this driving scheme, the idea is to divide an elementary pixel in sub-pixel and to have driving TFT in each sub-pixel working either in the 'on' or the 'off' state. In other words, no intermediate voltage values are used on the gate of the driving TFTs. For example, if the elementary pixel is divided into two sub-pixels, four grey levels (2^2) can be obtained. However, to use this gray-scale control method is not expected to attain high resolution, since the decrease of a pixel pitch may be difficult. In addition, it is hard to fabricate the TFT-OLEDs with large gray scale level because further increase of the number of sub-pixels may be difficult.

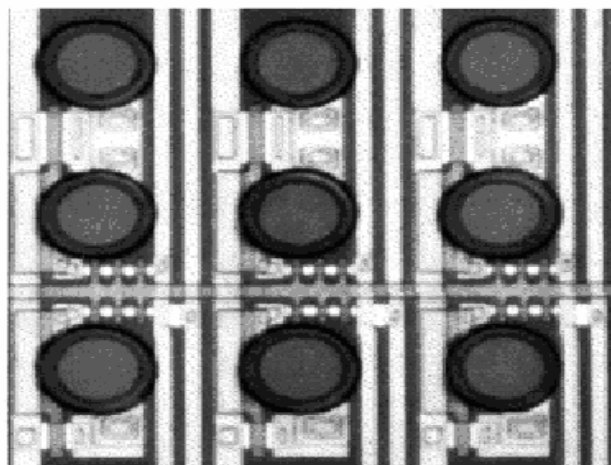


Fig. 3-8 Sub-pixel arrangement in monochrome display using area-ratio technique

3.4.2 Time Ratio Grayscale

This is implemented by dividing each picture frame into sub-frames with serial scan. During a sub-frame, all pixels are addressed – lit pixels are addressed by a specific voltage and then the display voltage is applied to the entire screen lighting those during the lighting time. As Fig. 3-9 [3-17][3-18], each sub-frame has a weighting ranging from 1 time unit to 32 time units for a typical six sub-frame arrangement. Time Unit depends on size and the number of pixels on the screen. This is a purely digital time-ratio control mechanism, which is a key advantage as it eliminates any unnecessary digital to analog conversions, making the OLED technology ideal for the all-digital age. The OLED is lighting for different amounts of time to obtain different brightness level, and then obtain the different gray scales.

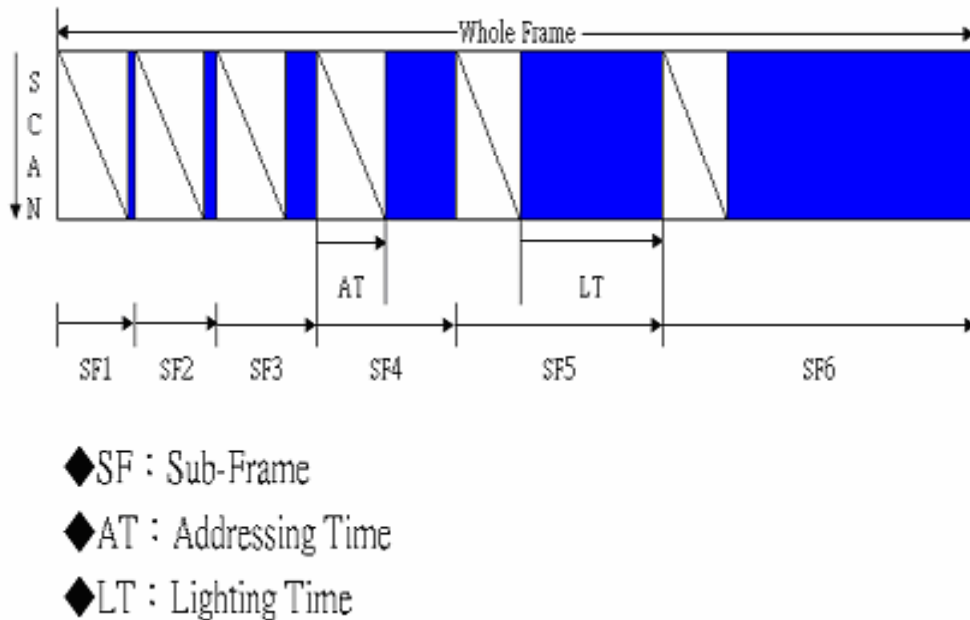


Fig. 3-9 A schema for time ratio gray-scale

Chapter4

Design of AMOLED Driver

4.1 Active Matrix Driving

Fig. 4-1 show the schema for the active matrix addressed OLED (AMOLED) , including TFT pixel array which are composed of organic light emitting diodes (OLED), scan driver, data drivers and regulator. Pixel could be any structure as shown in Chapter 2 and Chapter 3, the design of driver must be varied according to the pixel structure. If the pixel size and the best luminance are identical, then maximum aperture-ratio [4-1] is required. The aperture-ratio result from the number of TFT. The large TFT dimensions tend to limit the available pixel area for bottom emission. Therefore, to use the minimal number of TFT for AMOLED cell is a goal.

As shown in Fig. 2-11, it owns the least number of TFT in all pixel structure, and has a max. aperture-ratio comparing other pixel structure. The pixel structure by the voltage programmed driving scheme contains one switching transistor (TFT M1), one driving transistor (TFT M2) and one storage capacitor (Cs). In this circuit, TFT M2 is a PFET device connected in a common source arrangement, play the role of a current source to supply constant current to the OLED. The Vgs of the driving transistor for a specific output current will be programmed in the capacitor through the switching transistor (TFT M1). Unfortunately, this structure does not compensate the variation of Vt and mbility, the former two variables would lead to variation in illumination strength.

TFT is always made from both amorphous and ploy-silicon. Poly-silicon has much higher mobility, reducing the size of the drive TFT. The improving mobility of TFT is necessary to make high resolution and high performance AMOLED display which integrate driver circuits on the display panel. 100MHz shift register [4-2] was reported. Poly-silicon is required for system on panel (SOP). For poly-silicon display, both mobility and threshold-voltage vary randomly across the plate from pixel to pixel. As shown in Fig. 4-2 [4-3], this chart shows the theoretical display brightness non-uniformity for a display with threshold-voltage of 3V. From the chart, we know that variation in Vt are more serious than variation in mobility (U_p) for non-uniformity. Moreover, when lower brightness levels for the pixel is operating near the

driving transistor's threshold, any change in threshold results in large variations in brightness. Thus the driving by time ratio grayscale is adopted. Since the large voltage step is forced to pixel, it results in the reduction influence of variation of the characteristics of the driving transistor.

Based on the abovementioned concept on program pixel, it requires the cooperation of the data driver and scan driver to complete the programming for pixel. The number of data driver and scan driver depends on the AMOLED array. Data driver based on the data transmitted by the sequence controller, output the drive voltage corresponding to each data line. Scan driver based on the control signals transmitted by the sequence controller, choose the row. As the scan line is activated as shown in Fig. 4-3, display signal on the data line is to programmed into the pixel. When scan signal change from high to low, TFT M1 is turned on and voltage on data signal is stored in the gate of TFT M2 and storage capacitor (Cs). When the scan signal change back to high, TFT M1 is turned off but gate voltage of TFT M2 remains unchanged and drives the OLED until next time which the scan signal change to low.

At first, image display will be introduced in section 4.2. Based on the concept, we will know the operating principle of the display system. In section 4.3, data driver will be introduced and designed, and a new AMOLED display driving method which used both amplitude modulation and double rate serial-in to enhance luminance will be used. Next, scan driver will be introduced and designed, and several concerns for image quality will be implemented in scan driver. Finally, the regulator is discussed in section 4.5. It transfers high voltage to low voltage, and provide the different voltage level.

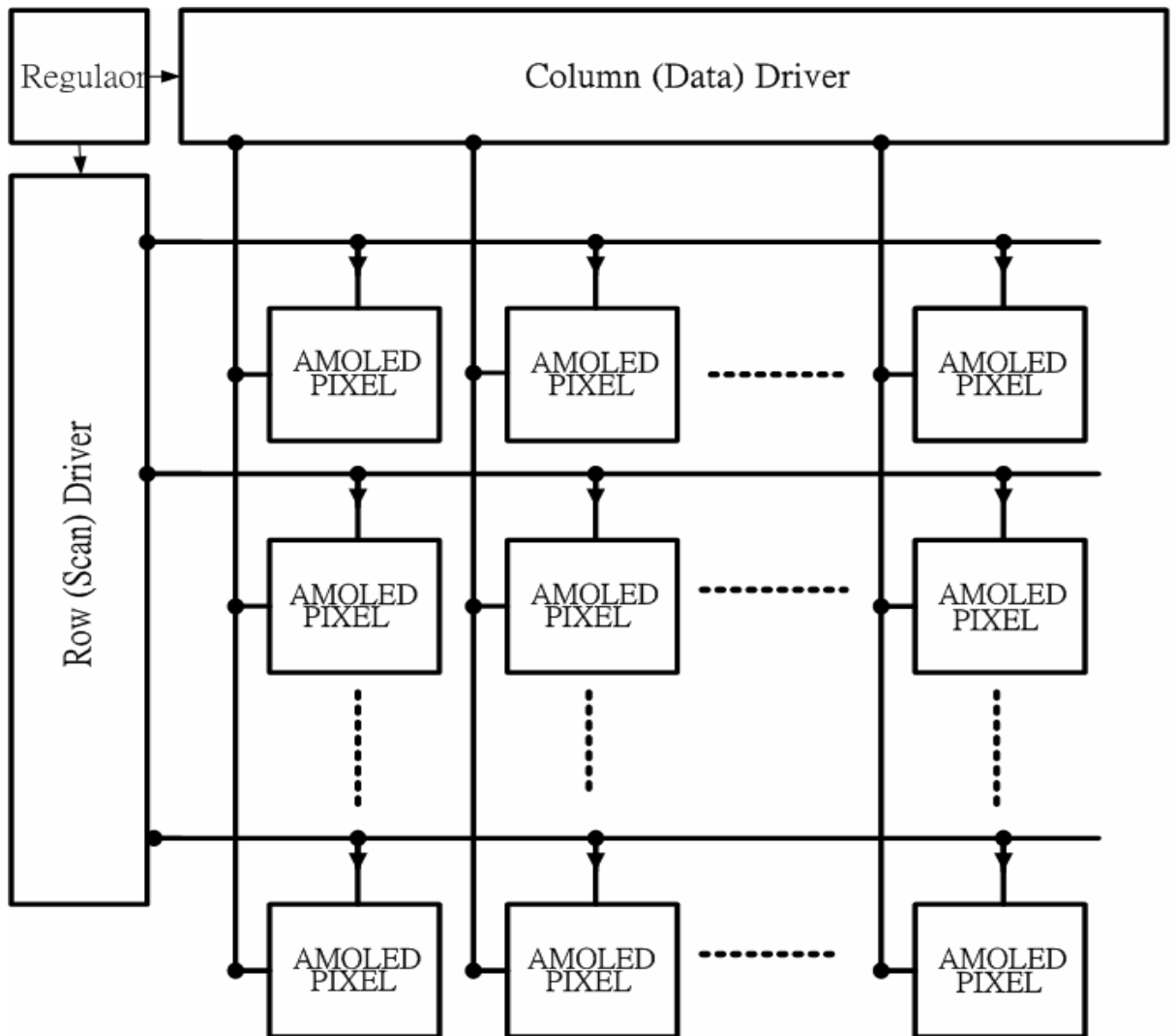


Fig. 4-1 A schema for AMOLED driving

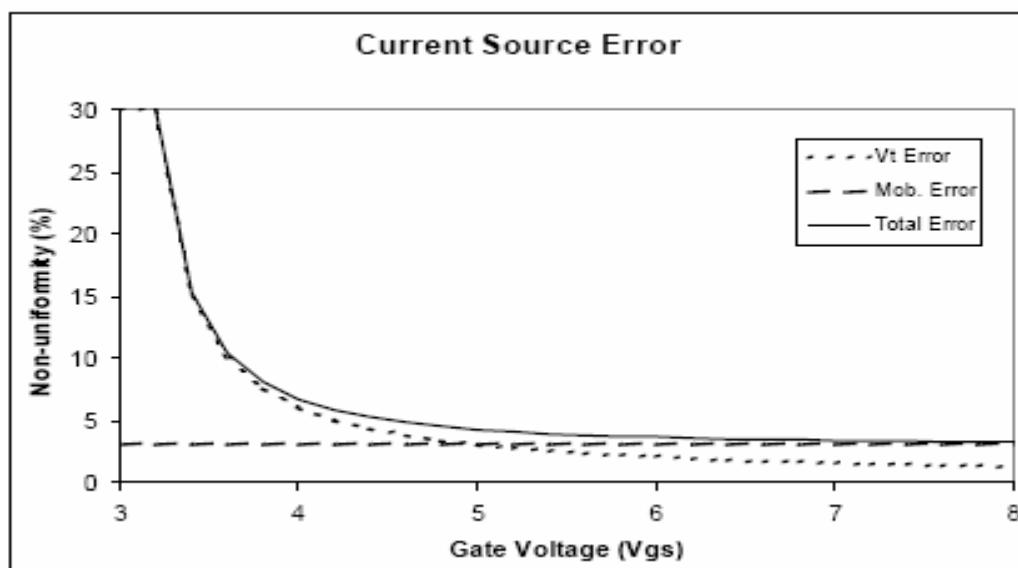


Fig. 4-2 Current source non-uniformity

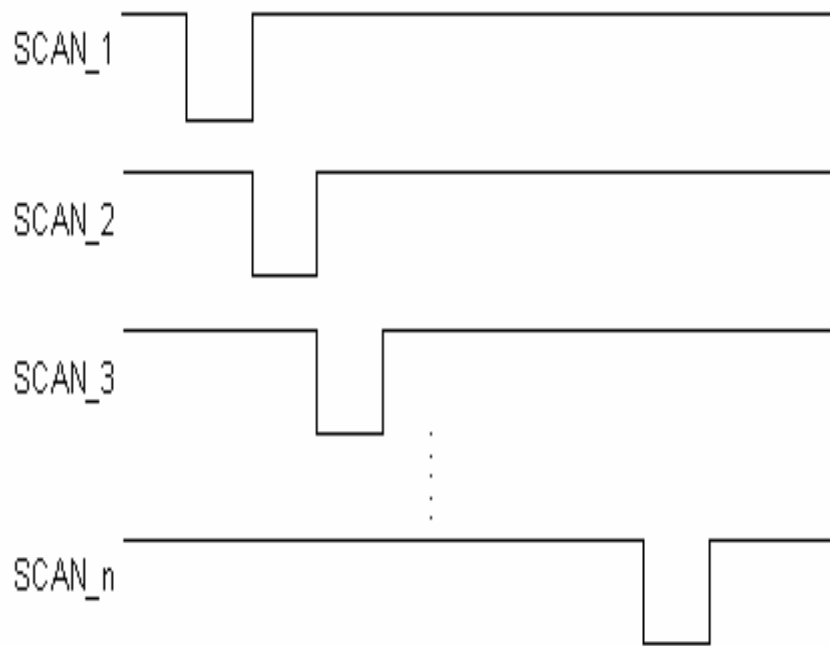


Fig. 4-3 Scan lines timing diagram



4.2 Image Display

The main parameters of the image display are as the following:

- (1) Resolution: Row×Column
- (2) Gray scale
- (3) Picture frame (Frame)

Fig. 4-4 is the relational graph of the display image, drive signals, and pixel. It is assumed that the display resolution has $m \times n$, and image is divided to $m \times n$ by scan line and data line. Each intersection of the scan line (row) and data line (column) is the location of a pixel. Thus one pixel is responsible for $1/(m \times n)$ of the image. The bit of pixel data refers to the gray scale included in each pixel; for example, 6 bits data means each pixel contains 64 gray scales.

Picture frame time is the time for presentation the image color of whole display. Time ratio grayscale is implemented by dividing each picture frame into sub-frames with serial scan. During a sub-frame, all pixels are addressed – lit pixels are addressed by a specific voltage and then the display voltage for 2T1C structure is applied to the entire screen lighting those during the lighting time. Each pixel should be addressed. That is, scan driver should scan from the first scan line to the last scan line. As shown in Fig. 3-9, each sub-frame has a weighting ranging from 1 time unit to 32 time units for a typical six sub-frame arrangement. Time unit depends on size and the number of pixels on the screen. The OLED is lighting for different amounts of time to obtain different brightness level, and then obtain the different gray level.

Fig. 4-5 is the control sequence chart for 8×16 driver with double rate serial-in. The total number of column contained in one horizontal line on the display. When the data driver receives the pixel data of one horizontal line, it converts the data into pixel drive signals, and receives the data of next horizontal line. Thus the cycle for each signal of horizontal synchronization picking up one entire scan line is the time for image data filling the data driver, as well as the time for the scan driver changing scan line.

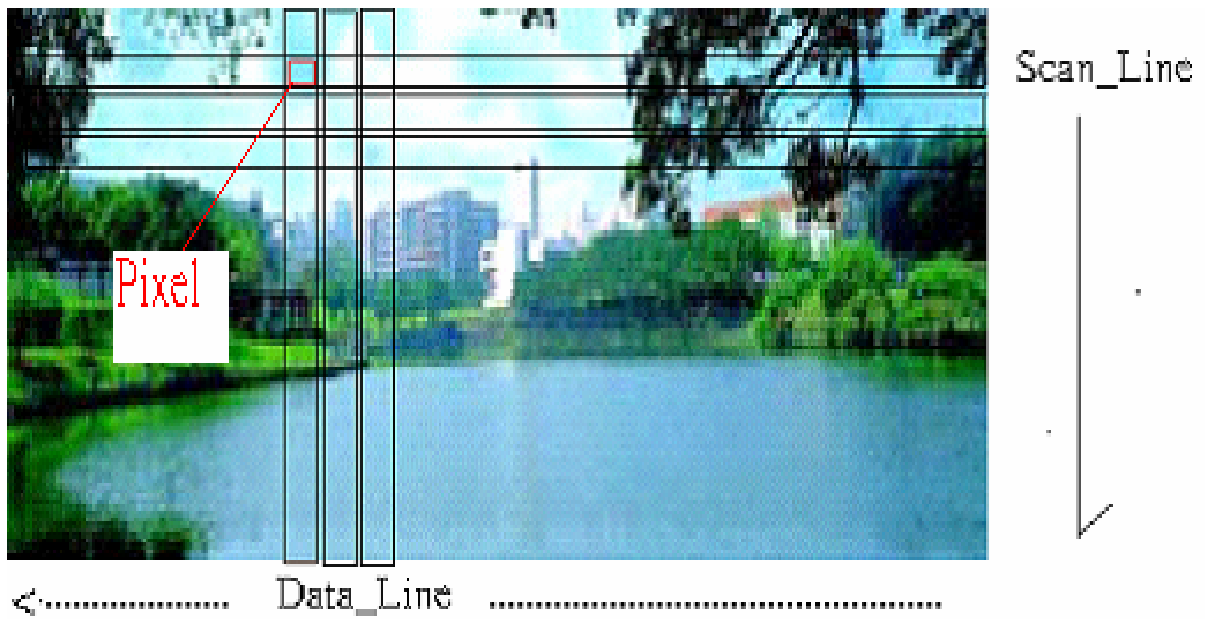


Fig. 4-4 Image display

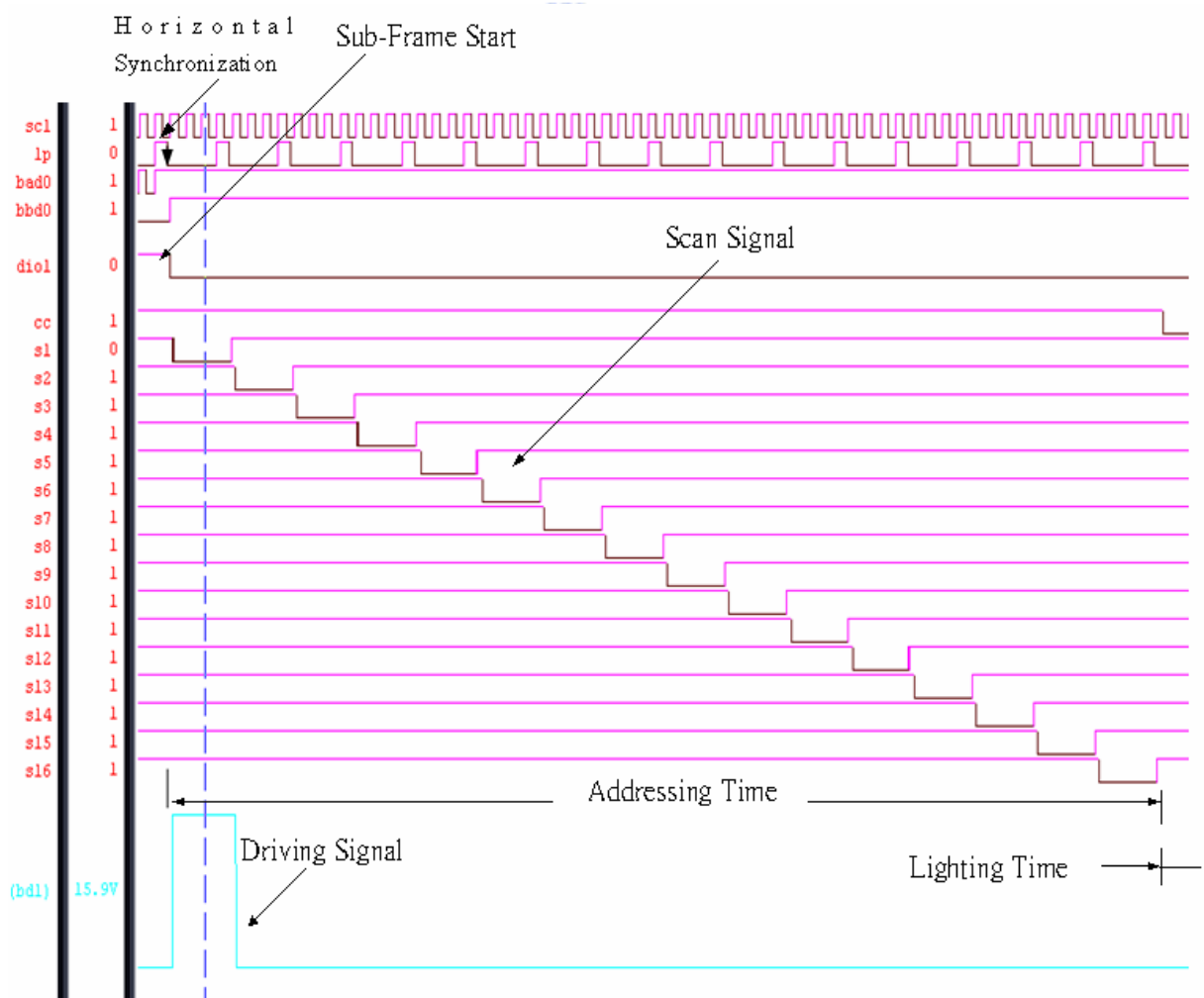


Fig. 4-5 Timing diagram for sub-frame

4.3 Data Driver

Base on the structure as shown in Fig. 2-11 and 6-bit grayscale by driving of conventional time ratio grayscale as shown in Fig. 3-9, using binary coding, each sub-frame has a weighting ranging from 1 time unit to 32 time units for a typical six sub-frame arrangement. Time unit depends on size and the number of pixels on the screen, and whole frame consist of six sub-frame and each sub-frame is divided into addressing time and lighting time. In the addressing time, a signal was added and stored in the gate electrode of the driving TFT of each pixel by scanning entire pixel. At this addressing period, the high voltage is applied to the cathode and is equal to the high voltage applied to the voltage in the supply line. Every OLED pixels are not emitting because the method will prevent from I-R drop issue under addressing time. About I-R drop issue, we will discuss it in the following section for scan driver. Shifting to a lighting time, low voltage is applied to the cathode. Then all of the pixels in which low voltage was given to the gate electrode of the driving TFT become bright. The OLED is lighting for different amounts of time to obtain different brightness level, and then obtain the different gray scales. The above description for conventional time-ratio grayscale indicates the following formula:

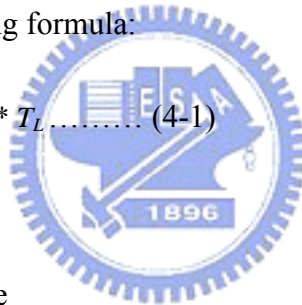
$$\text{Grayscale} = \sum_{i=1}^n S_i * [2^{i-1} / (2^n - 1)] * T_L \dots \dots \dots (4-1)$$

T_L : Total Lighting Time

S_i : Light factor for #i sub-frame

n: n bits for gray choice

i: #i sub-frame



The main issue with the conventional time ratio grayscale is that the data is loaded as digital data several times per frame. It is significantly to increases the data rate onto the display, and is difficult to drive the data onto the display fast enough. Moreover, each sub-frame is divided into addressing time and lighting time. Every OLED pixels are not emitting under addressing time of sub-frame. It will lead in the decreasing of luminance efficiency. Thus the design objectives are to shortening the addressing time to increasing the lighting time without increasing the system frequency and additional components in pixel [4-4] , and reducing the number of sub-frames to increase lighting time if gray level is the same or exceeding. A AMOLED display driving method which used both amplitude and double rate serial-in to enhance luminance. For improved time ratio grayscale with double rate serial-in , we propose

double rate serial-in for serial to parallel circuit. The addressing time is shorted to half time compared with conventional time ratio grayscale.

For improved time ratio grayscale with amplitude modulation, three OLED luminance levels which were controlled by driving TFT's gate voltages, V_{off} -luminance, V_{half} -luminance, V_{full} -luminance. Each frame, only use four sub-frame, obtain 3^4 gray levels, is superior to conventional time ratio grayscale. Few sub-frame will enhance the total lighting time, and each sub-frame has a weighting ranging from 2 time unit to 54 time units. By combining these two method, few sub-frame will enhance the total lighting time, and each sub-frame has a short addressing time.

4.3.1 Architecture of Data Driver

Data driver, based on the data transmitted by the sequence controller, outputs the drive voltage corresponding to each data line. Fig. 4-6 show a architecture of data driver with improved time ratio grayscale. The proposed driver including shift registers with double rate serial-in, sampling latch, hold latch, level shift and analog switch. Image mirror control with bi-directional shift register is also concern.

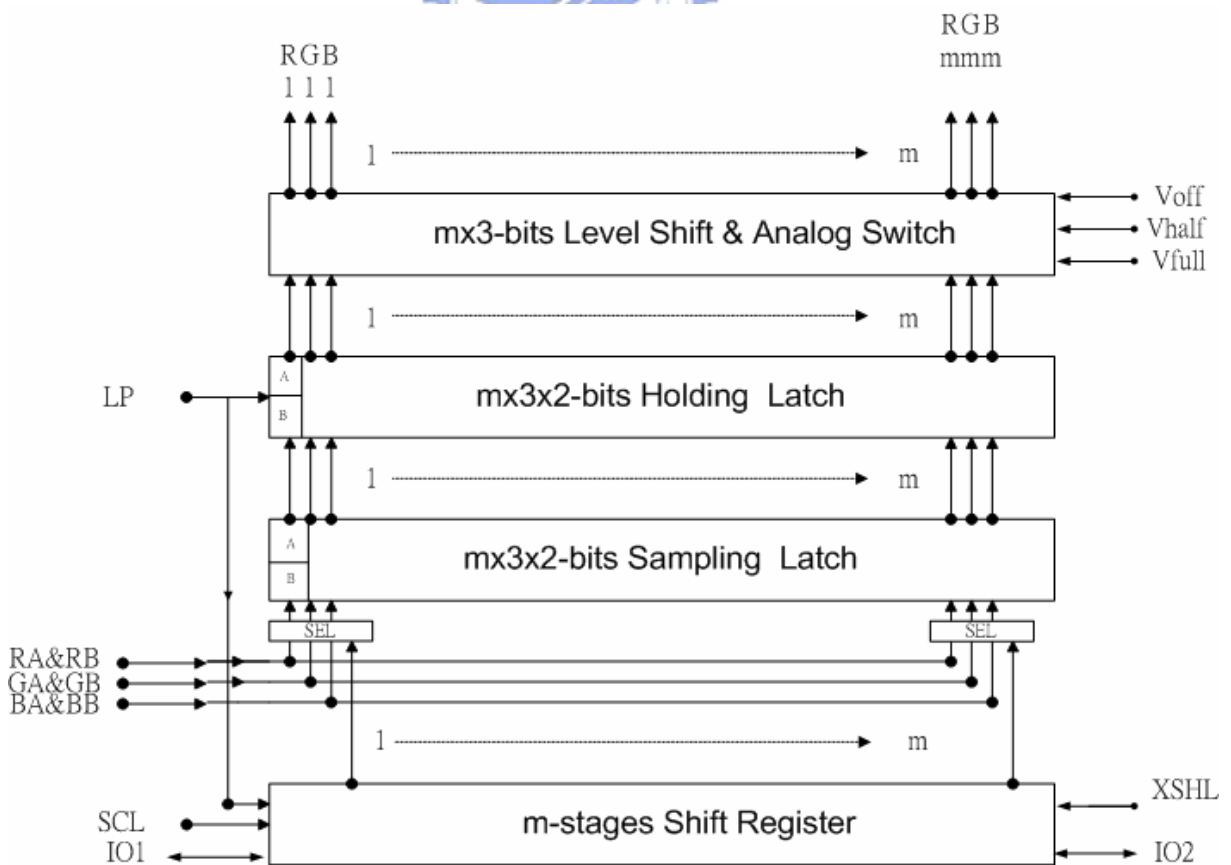


Fig. 4-6 Block diagram of data driver

4.3.2 Serial to Parallel Circuit with Double Rate Serial-in

As shown in Fig. 4-6, the serial to parallel circuit consists of shift registers, sampling latch stages and holding latch stages. Shift register convert the input horizontal signal to a series sampling signals sequentially. Then the sampling signals sample input R, G, B 2bit sub-frame data sequentially through the sampling latch stages. Holding latch stages convert the sampled series data to parallel data by an latch pulse signal.

The time to fill image data for holding latch in the data driver is the cycle for one entire horizontal line, as well as the time for the scan driver to change scan line. Because the period is during the addressing time, every OLED pixel is not emitting. To reduce the period, the lighting time will be enhanced.

At conventional time ratio grayscale, a serial-in with single clock is a usual skill in shift register. Each image data is latched to sampling latch accompanied by every clock, where it results in the longer data addressing time for data driver when there are the longer data streams. An improved time ratio grayscale will be introduced by double rate serial-in. Fig. 4-7 shows a non-overlap clock generator. Through this circuit, a clock input is split to two clocks. Fig. 4-8 shows the set of signals and timing. The non-overlap clock is the motive force in serial shift register while the image data is require for display. They are used to send the data respectively. A clock is responsible for odd register; another clock is responsible for even register.

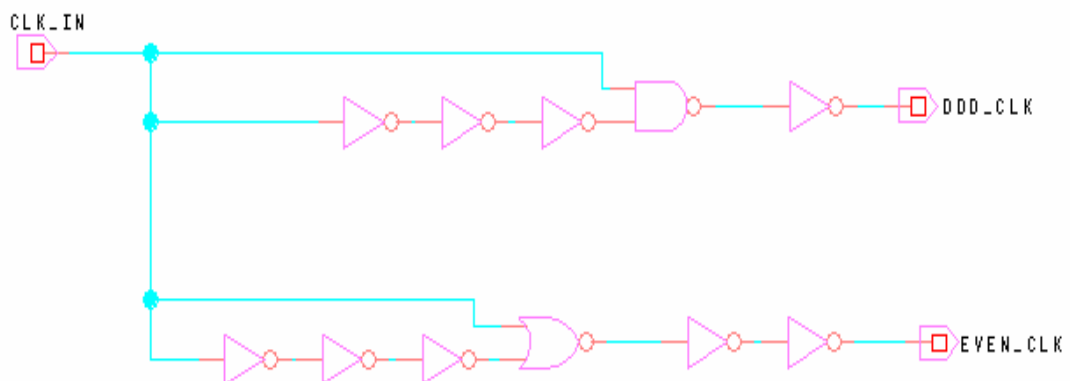


Fig. 4-7 Non-overlap clock generator

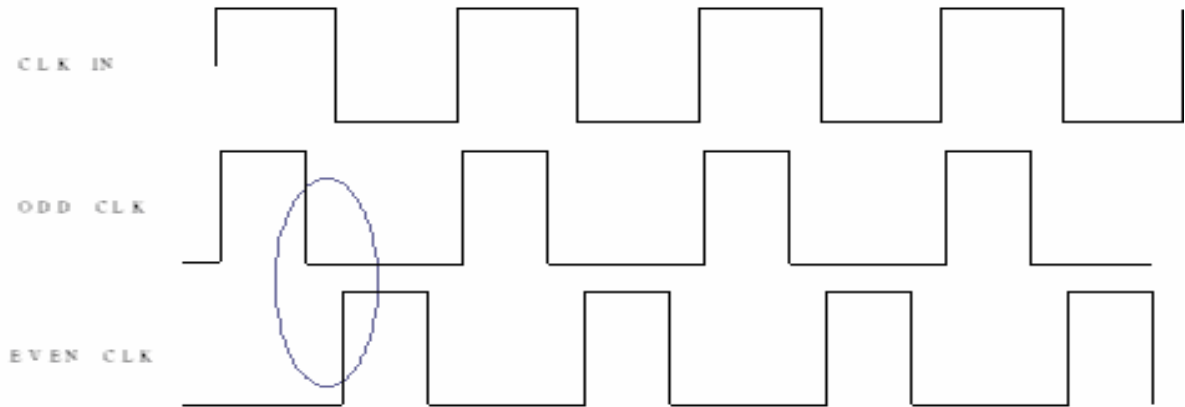


Fig. 4-8 Non-overlap clock for serial-in register

Under the same clock frequency (25MHz), four sub-frames, 60frames/sec and QCIF(Quarter Common Intermediate Format; 176×144), the improved time ratio grayscale with double rate serial-in can reduce addressing time compared with the conventional serial scan. By double rate serial-in, the addressing time is shorted to half time compared with conventional time ratio grayscale as shown Fig. 4-9. Every OLED pixel is not emitting under addressing time; therefore, the reduced addressing time will improve luminance efficiency. The same data stream can be transferred to the internal register of driver in same system clock, but the addressing time is decreased by double rate serial-in. That is, the lighting efficiency will be improved by the enhanced lighting time.

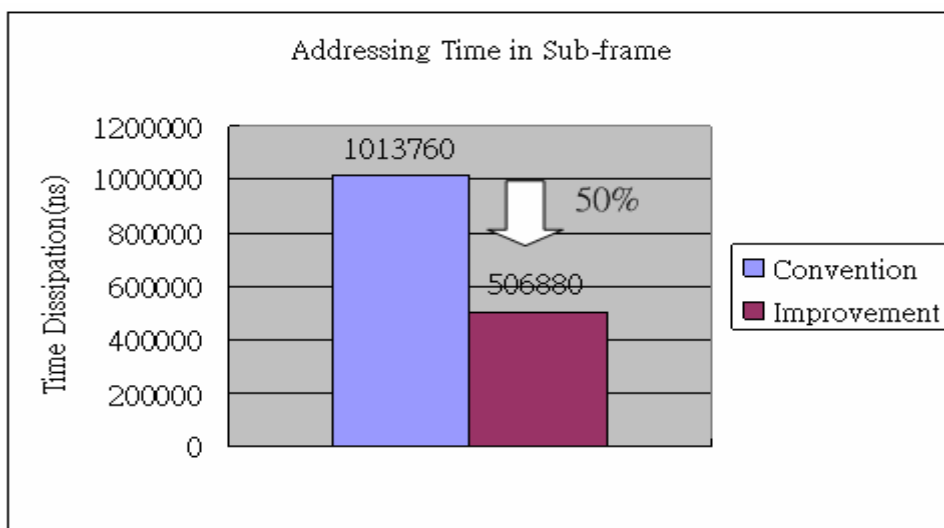


Fig. 4-9 Addressing time dissipation

4.3.2.1 Image Mirror

Input horizontal signal to a series sampling signals sequentially. Using shift register and comparator could complete the functions of sampling horizontal signal gradually. To achieve image mirror, the directional shift register should be designed. Fig. 4-10 shows the four stages of bi-directional shift register, while all other parts remain the same.

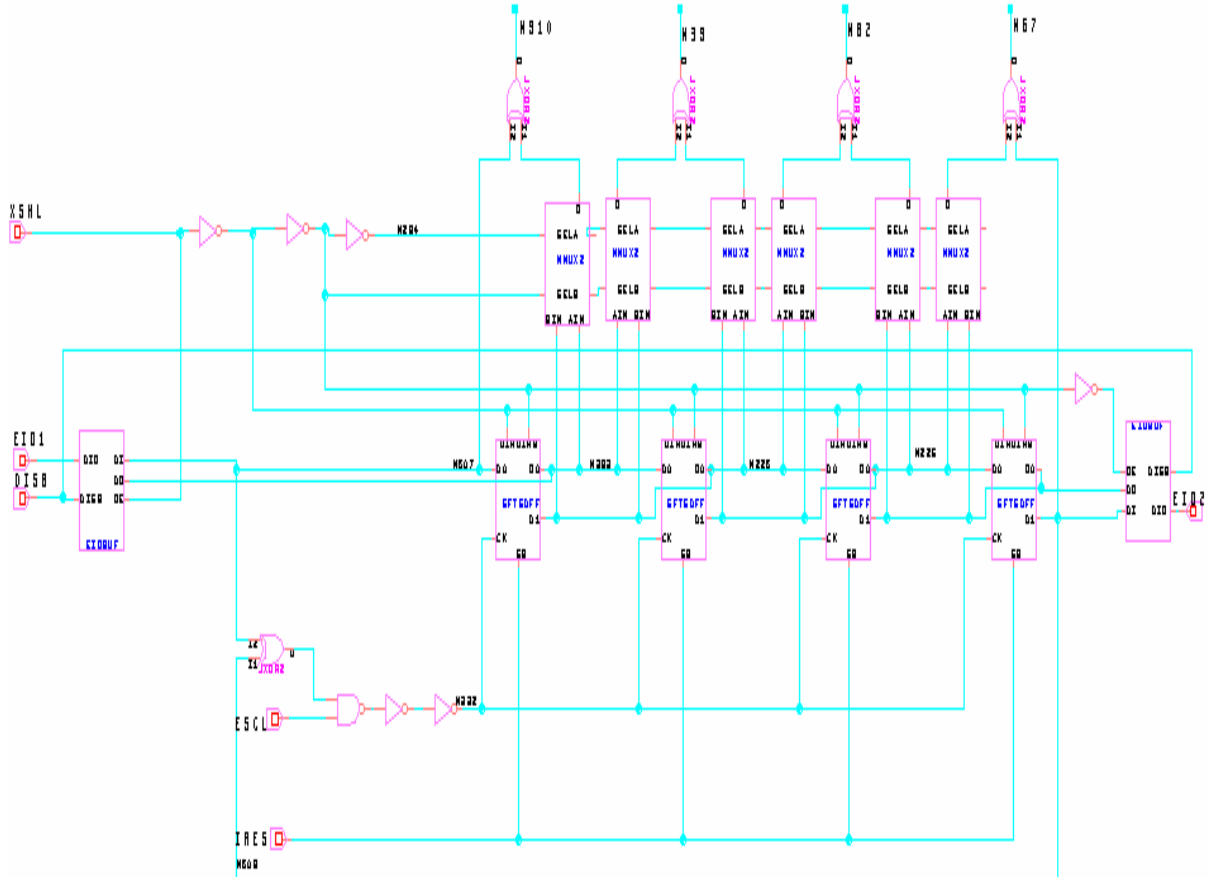
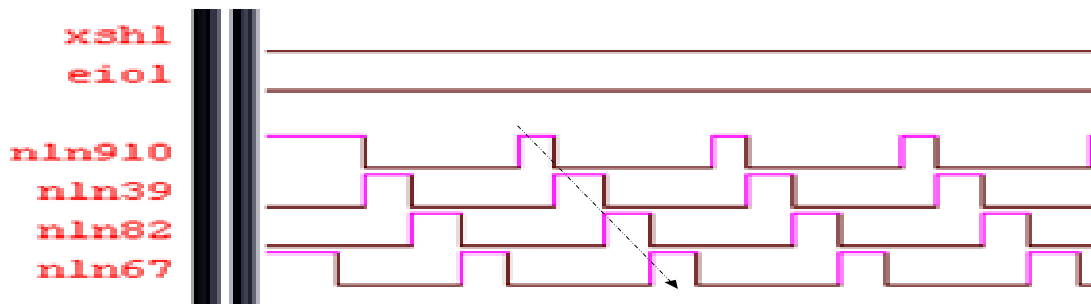
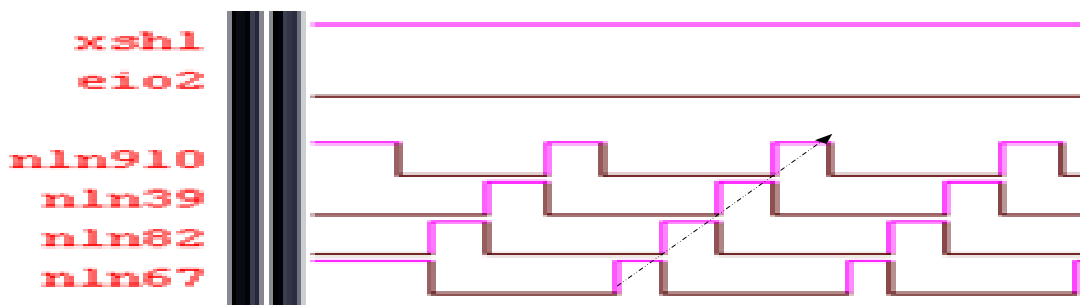


Fig. 4-10 Image mirror with shift register control

Fig. 4-11(a) shows the count for the following number, Fig. 4-11(b) shows the count for the previous number. Due to different counts are used, the sequence of saving horizontal signal into data driver may be opposite. The function for image mirror is able to achieve.



(a) Up count



(b) Down count

Fig. 4-11 Save signal sequential for sampling latch

4.3.3 Improved Time Ratio Grayscale with Amplitude Modulation

The previous section has introduced the method to shortening the addressing time to increasing the lighting time without increasing the system frequency and additional components in pixel, this section will discuss how to reduce the number of sub-frames to increase lighting time. This is, amplitude modulation coding is adopted. We will combine double rate serial-in and amplitude modulation [4-5] to get a better luminance.

Base on binary time coding, the conventional time ratio grayscale only uses Voff-luminance and Vfull-luminance. Take 6-bit grayscales for example, only 2^6 gray levels could be generated, and 6 sub-frames are required. Six sub-frames means 6 addressing time is required, and more addressing time can shorten the lighting time under the same frame rate.

Using amplitude modulation coding base on conventional time ratio grayscale could reduce the number of sub-frame, thus, increase the lighting time. The coding includes

Vhalf-luminance for coding, thus, three potentials are added for coding. If n is only 4, then there will be $3^4 = 81$ gray levels, and 4 sub-frames. Table 4-1 shows the coding of sub-frame combinations for 81 gray levels. Table 4-2 shows sub-frame value corresponding to actual Voff-luminance, Vhalf-luminance and Vfull-luminance.

Gray	Weight	SF1	SF2	SF3	SF4
0	0	0	0	0	0
1	0.5	0	0	0	0
2	1	0	0	0	0
3	0	0.5	0	0	0
4	0.5	0.5	0	0	0
5	1	0.5	0	0	0
6	0	1	0	0	0
7	0.5	1	0	0	0
8	1	1	0	0	0
9	0	0	0.5	0	0
10	0.5	0	0.5	0	0
11	1	0	0.5	0	0
12	0	0.5	0.5	0	0
13	0.5	0.5	0.5	0	0
14	1	0.5	0.5	0	0
15	0	1	0.5	0	0
16	0.5	1	0.5	0	0
17	1	1	0.5	0	0
18	0	0	1	0	0
19	0.5	0	1	0	0
20	1	0	1	0	0
21	0	0.5	1	0	0
22	0.5	0.5	1	0	0
23	1	0.5	1	0	0
24	0	1	1	0	0
25	0.5	1	1	0	0
26	1	1	1	0	0
27	0	0	0	0.5	0
28	0.5	0	0	0.5	0
29	1	0	0	0.5	0
30	0	0.5	0	0.5	0
31	0.5	0.5	0	0.5	0
32	1	0.5	0	0.5	0
33	0	1	0	0.5	0
34	0.5	1	0	0.5	0
35	1	1	0	0.5	0
36	0	0	0.5	0.5	0
37	0.5	0	0.5	0.5	0
38	1	0	0.5	0.5	0
39	0	0.5	0.5	0.5	0
40	0.5	0.5	0.5	0.5	0
41	1	0.5	0.5	0.5	0.5
42	0	1	0.5	0.5	0.5
43	0.5	1	0.5	0.5	0.5
44	1	1	0.5	0.5	0.5
45	0	0	1	0.5	0.5
46	0.5	0	1	0.5	0.5
47	1	0	1	0.5	0.5
48	0	0.5	1	0.5	0.5
49	0.5	0.5	1	0.5	0.5
50	1	0.5	1	0.5	0.5
51	0	1	1	0.5	0.5
52	0.5	1	1	0.5	0.5
53	1	1	1	0.5	0.5
54	0	0	0	1	0.5
55	0.5	0	0	1	0.5
56	1	0	0	1	0.5
57	0	0.5	0	1	0.5
58	0.5	0.5	0	1	0.5
59	1	0.5	0	1	0.5
60	0	1	0	1	0.5
61	0.5	1	0	1	0.5
62	1	1	0	1	0.5
63	0	0	0.5	1	0.5
64	0.5	0	0.5	1	0.5
65	1	0	0.5	1	0.5
66	0	0.5	0.5	1	0.5
67	0.5	0.5	0.5	1	0.5
68	1	0.5	0.5	1	0.5
69	0	1	0.5	1	0.5
70	0.5	1	0.5	1	0.5
71	1	1	0.5	1	0.5
72	0	0	1	1	0.5
73	0.5	0	1	1	0.5
74	1	0	1	1	0.5
75	0	0.5	1	1	0.5
76	0.5	0.5	1	1	0.5
77	1	0.5	1	1	0.5
78	0	1	1	1	0.5
79	0.5	1	1	1	0.5
80	1	1	1	1	0.5

Table 4-1 Amplitude modulation coding

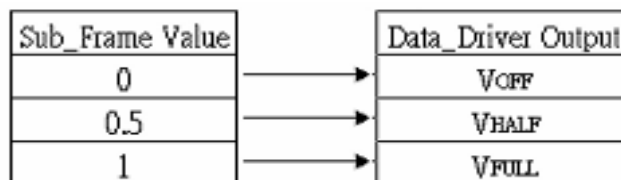


Table 4-2 Sub-frame value vs. physical output

This coding driving divides a picture frame into four sub-frames to implement 81 gray levels. From SF1 to SF4, length of each sub-frame is 2/80, 6/80, 18/80 and 54/80 of a picture frame time, respectively. Improved time ratio grayscale with double rate serial-in only use half addressing time compared to conventional time ratio scale, only there are four sub-frames in a picture frame by amplitude modulation coding. The composition of each frame is shown by Fig. 4-12. Each pixel structure is selected with four times per frame. Under the system clock (25MHz), 60frames/sec and QCIF, the first sub-frame of each picture frame, the data signal voltage kept by storage capacitor for lighting in SF1 is valid for 2/80 of a picture frame which is 345usec. Through the same lighting mechanism, the individual lighting time for other sub-frames are as follows: SF2 is valid for 6/80 of a picture frame which is 1035usec. SF3 is valid for 18/80 of a picture frame which is 3105usec. SF4 is valid for 54/80 of a picture frame which is 9315usec. This behavior is equivalent to conventional time ratio grayscale. According to the above result, the improved time-ratio grayscale indicates the following formula:

$$\text{Grayscale} = \sum_{i=1}^n S_i * S_v * [2 * 3^{i-1} / (3^n - 1)] * T_L \dots \dots \dots (4-2)$$

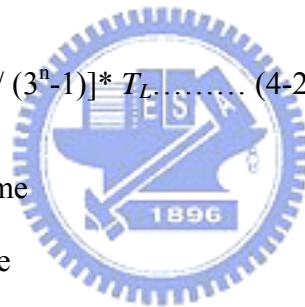
T_L : Total Lighting Time in Frame

S_i : Light factor for #i sub-frame

S_v : Amplitude value for #i sub-frame

n: n bits for gray choicde

i: #i sub-frame



The difference between conventional time ratio grayscale and improved time ratio grayscale is that half-luminance voltage and double rate serial-in are adopted in improved time ratio with amplitude. For example, there are three gray levels for SF1 in improved time ratio grayscale with amplitude, but only two gray levels for SF1 in conventional time ratio grayscale. In AMOLED display by analog driving, the number of data voltage value represents the number of gray levels. The method is described in section 3.1. The kind of driving circuits include expensive and complex DAC. Moreover, even though the output of the DAC is accurate, the step size is too small compared to the threshold voltage variations in pixel driving TFT. It will result in a huge variation for luminance. Only there data voltage

levels which are V_{off} -luminance, V_{half} -luminance and V_{full} -luminance are adopted in improved time ratio grayscale with amplitude modulation, and the voltage step is large compared to the analog driving. Therefore, the threshold voltage variation related luminance can be reduced, and the complex DAC is not necessary.

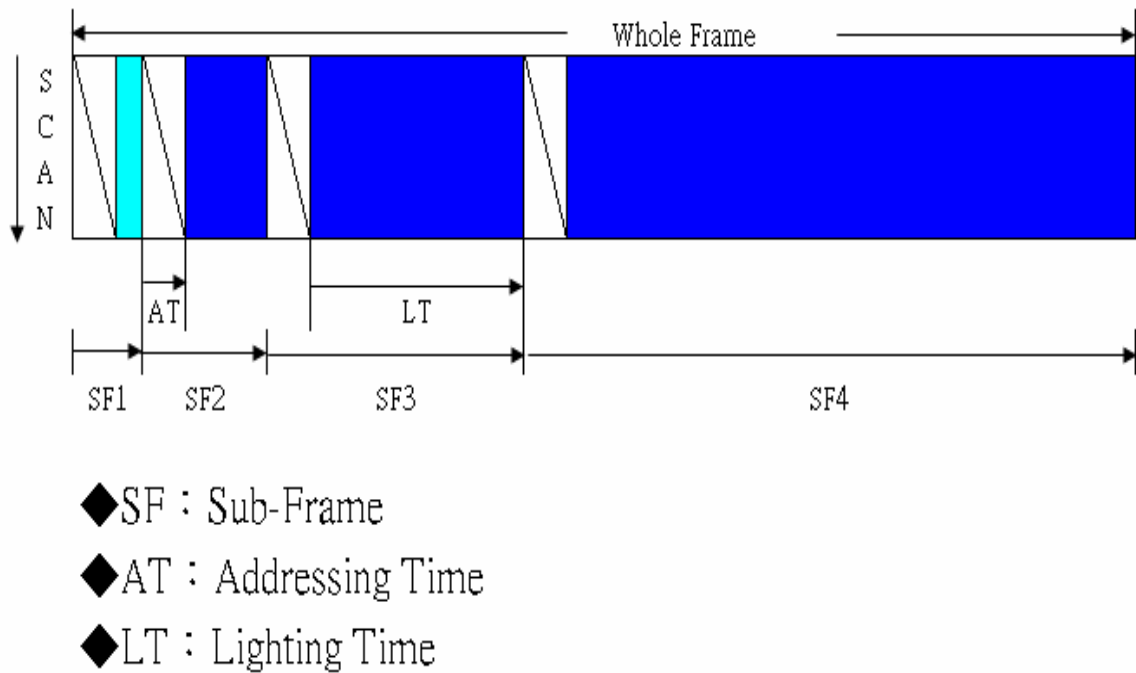


Fig. 4-12 Composition of each frame by proposition

4.3.4 Decoder and Analog Switch

In the previous section, improved time ratio grayscale with amplitude coding is described. According to the method, the output stage and related circuit will be implemented. In the driving skill, it don't need the complex DAC, and only use a simpler data driving circuit as shown in Fig. 4-6. Instead of using DAC in each channel of data driver, the method use two bits sampling path. The outputs of sampling latch are connected to register whose outputs are connected to the set of analog switch.

The part of Fig. 4-6 including holding latch, level shift and analog switch is equal to Fig. 4-13. As shown in Fig. 4-13, there are three TFT analog switches which send proper data line

voltage. The decoder decodes register A and register B, and select the only one in the analog switch group. For example, when the outputs of A and B registers are 0, and outputted after decoding, the analog switch that provides Voff_luminance would be selected and connected to data line. Similarly, when A and B registers output 1, the switch of Vfull_luminance would be selected and connected to data line. A complete decoding relationship is shown in Table 4-3.

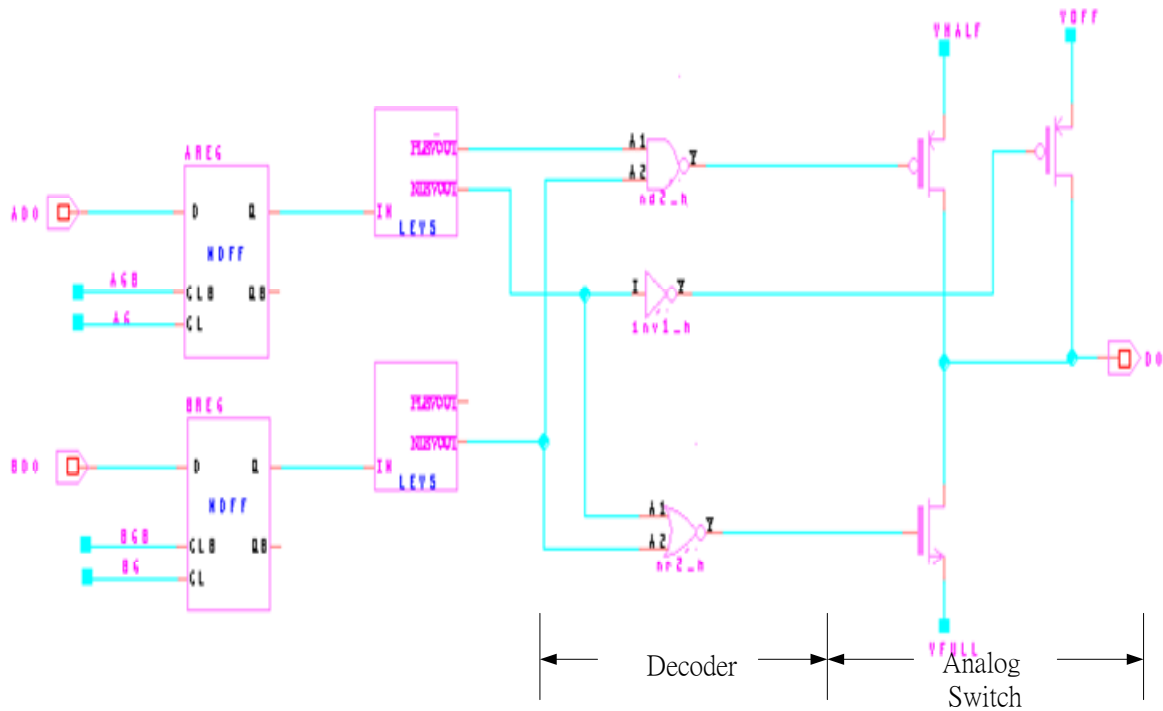


Fig. 4-13 Output stage for data driver

Sub_Frame Value	B-register	A-register	Data_Driver Output
0	0	0	VOFF
0.5	0	1	VHALF
1	1	1	VFULL

Table 4-3 Decoding relationship

4.3.5 Simulation Result and Summary

As seen from Fig. 4-14, the correct potentials of $V_{full_luminance}$, $V_{half_luminance}$ and $V_{off_luminance}$ could be outputted to data line according to the actual output by data driver and capacitive load $C_L=30pF$. Moreover, the voltage step is large compared to the analog driving, luminance fluctuation can be reduced [4-2].

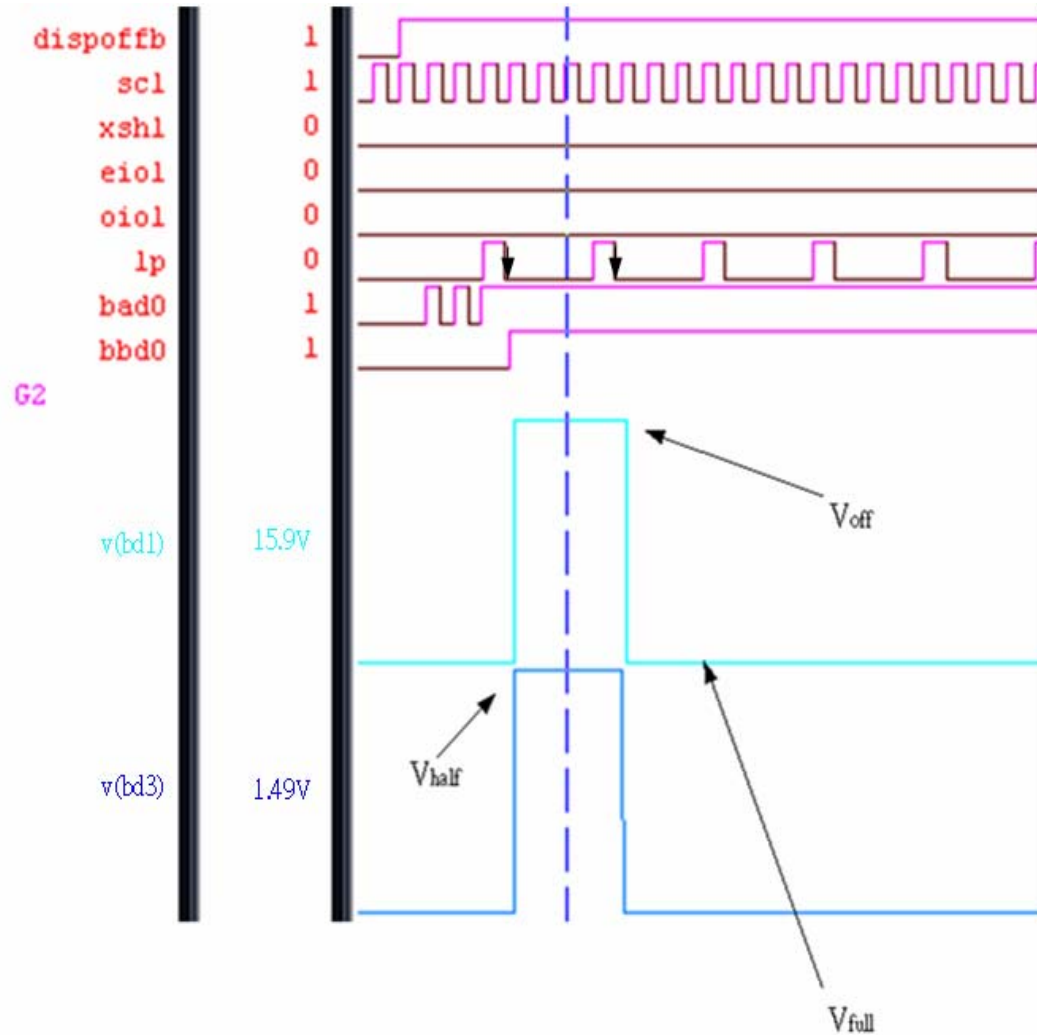
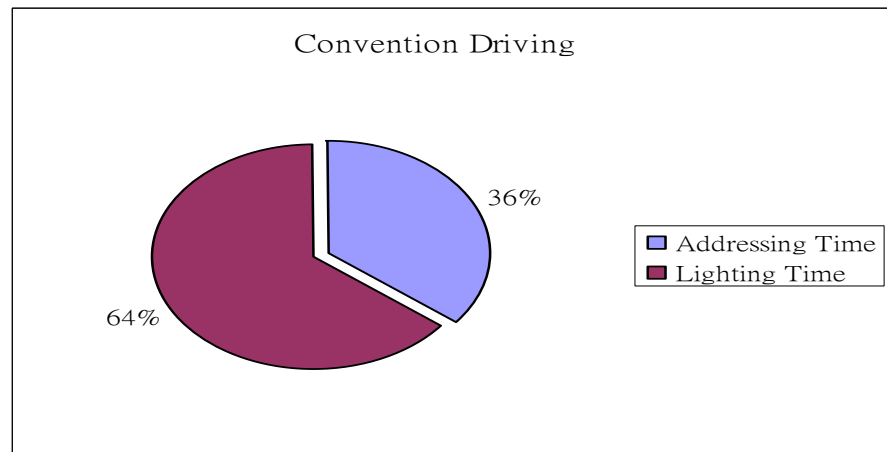


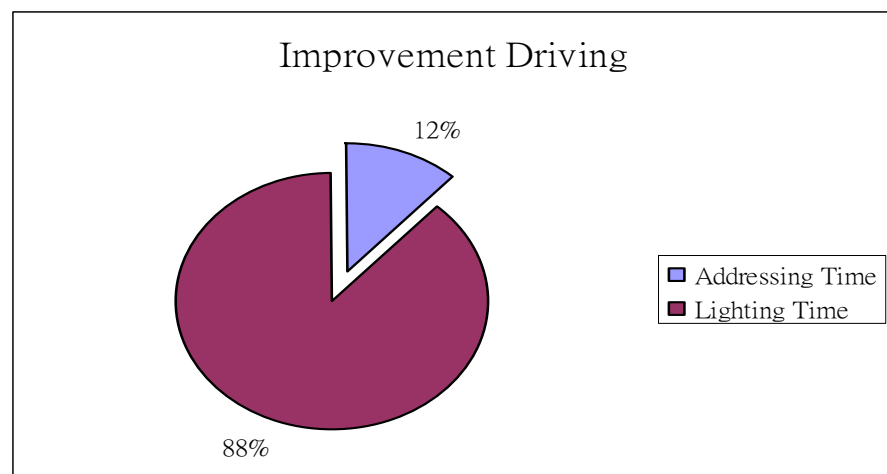
Fig. 4-14 Output of data driver

For improved time ratio grayscale, each sub-frame has a weighting ranging from 2 time unit to 54 time units; moreover, by double rate serial-in, the addressing time is shorted to half time compared with conventional time ratio grayscale. By amplitude modulation, three levels for OLED luminance levels which were controlled by driving TFT's gate voltages, V_{off} -luminance, V_{half} -luminance, V_{full} -luminance. 3^4 gray levels are obtained.

To compare with conventional time ratio grayscale, efficiency and gray levels will be improved by the method of improved time ratio grayscale. Conventional time ratio grayscale demanded n sub-frames to achieve 2^n gray levels. That is, 64 gray levels are required by 6 sub-frames. In the method, 81 gray levels only use 4 sub-frames. Using fewer sub-frames could actually obtain more grayscales. Also, less sub-frames mean less addressing time, the lighting time for the same frame would be enhanced. Under the following condition: system clock (25MHz), frame rate (60frames/sec), QCIF(Quarter Common Intermediate Format; 176×144), Fig. 4-15(a) shows the ratio of addressing time and lighting time for the conventional time ratio grayscale. Fig. 4-15(b) shows the ratio of addressing time and lighting time for the improved time ratio grayscale. As seen in comparison Fig. 4-15(a) and 4-15(b), the improvement driving could enhance 24% luminance.



(a) Convention driving



(b) Improvement driving

Fig. 4-15 Lighting percentage in frame

To compare with analog driving by amplitude modulation, there is no analog design in data driver by the method of improved time ratio grayscale. The variation of threshold voltage is a key issue for analog design. If we want to implement the improved driving circuit on panel, then it is possible that the driving circuit is fully implemented to SOP (System on Panel).

The display performance of improved time ratio grayscale is limited due to the serial to parallel driving scheme. When the panel dimension is increased, the addressing time is also enhanced. It will lead to a shorter lighting time. Multi-channel data driving shift register was used [4-5]. When four channels shift register is adopted, the addressing time is reduced to quarter time. Fig. 4-16 show those lighting times including QCIF, QVGA (Quarter Video Graphic Array; 320x240) and VGA (Video Graphic Array; 640x480). We find QVGA can be lighted by improved time ratio grayscale with serial in. If improved time ratio grayscale with multi-channel data driving shift register is also adopted by the higher resolution panel, then VGA or bigger dimension panel is also lighted.

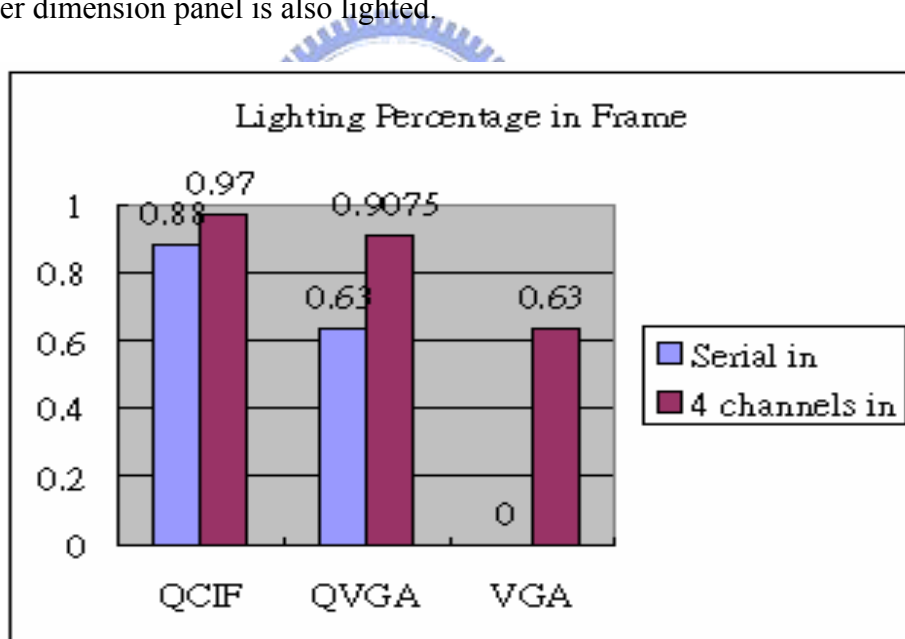


Fig. 4-16 Compared lighting percentage

4.4 Scan Driver

To complete the pixel programming, it requires the cooperation of the data driver and scan driver. Data driver adopt the improved time ratio grayscale with amplitude coding, and whole frame consist of four sub-frames and each sub-frame is divided into addressing time and lighting time. During a sub-frame, all pixels are addressed – lit pixels are addressed by a specific voltage and then the display voltage for 2T1C structure is applied to the entire screen lighting those during the lighting time. Each pixel is addressed meaning the scan driver needs to scan from the first scan line to the last. As discussed in section 4.2, the cycle for the scan driver to change scan line is the cycle for each latch pulse to pick up one entire scan line, as well as the time for the image data to fill the data driver.

At this addressing period, the high voltage is applied to the cathode and is equal to the high voltage applied to the voltage in the supply line. Every OLED pixel are not emitting because the method will prevent from I-R drop issue under addressing time. I-R drop will lead to the divergent presentation color for same required color. About I-R drop issue, we will discuss and implement it in the following. Another concern without error programming is also implemented in scan driver.



4.4.1 Architecture

Scan driver, based on the control signals transmitted by the sequence controller, choose the row of displayed data. Fig. 4-17 shows a architecture of scan driver with cathode electrical switch. The proposed driver including shift registers with scan signal gating, level shift and analog switch. Image handstand control with bi-directional shift register is also concern.

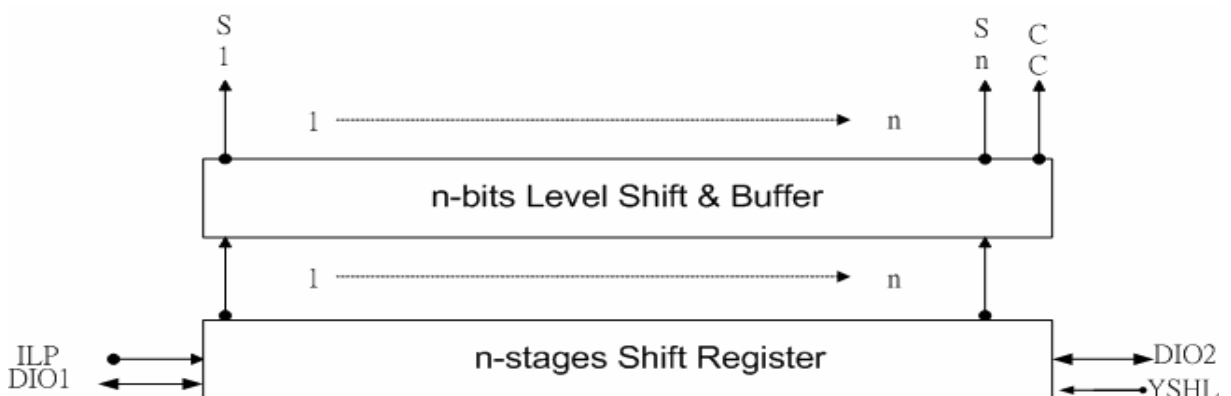


Fig. 4-17 Block diagram of scan driver

4.4.2 Sequential Scan with Image Handstand

As the scan line is activated as shown in Fig. 4-3, display signal on the data line is programmed into the pixel, when scan signal change from high to low. Base on Fig. 2-11, TFT M1 turned on and voltage on data signal is stored in the gate of TFT M2 and storage capacitor (Cs). Since each pixel needs to be addressed, the scan driver should scan from the first line to the last for the same sub-frame. The one-by-one scan could be done by using shift register. To achieve image handstand, directional shift register should be designed. Fig. 4-18 shows the four levels of bi-directional shift register, while all other parts remain the same.

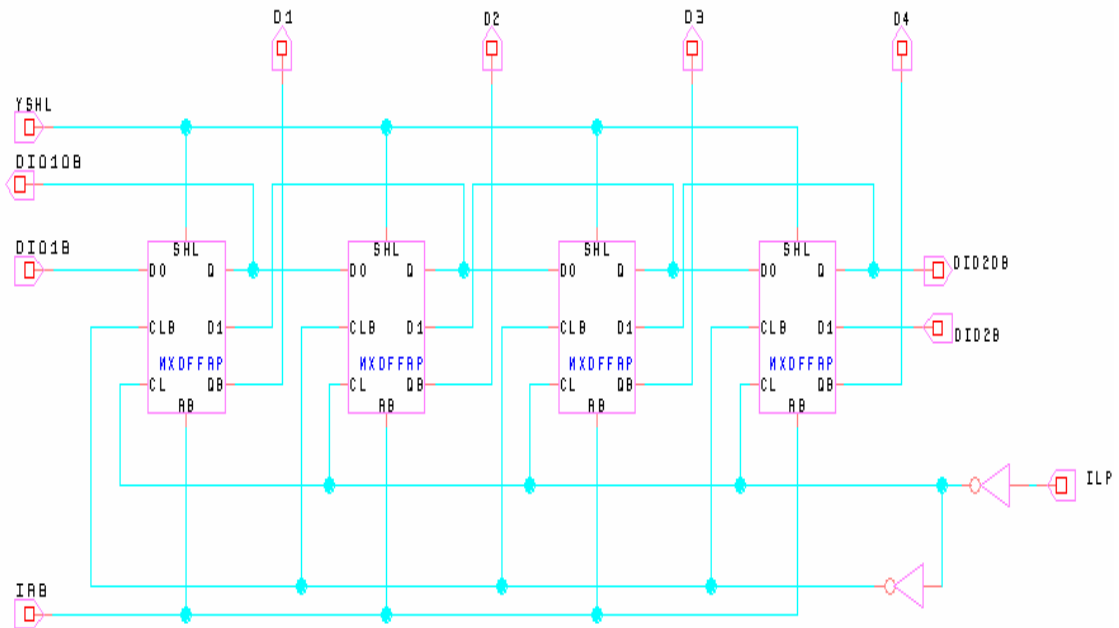
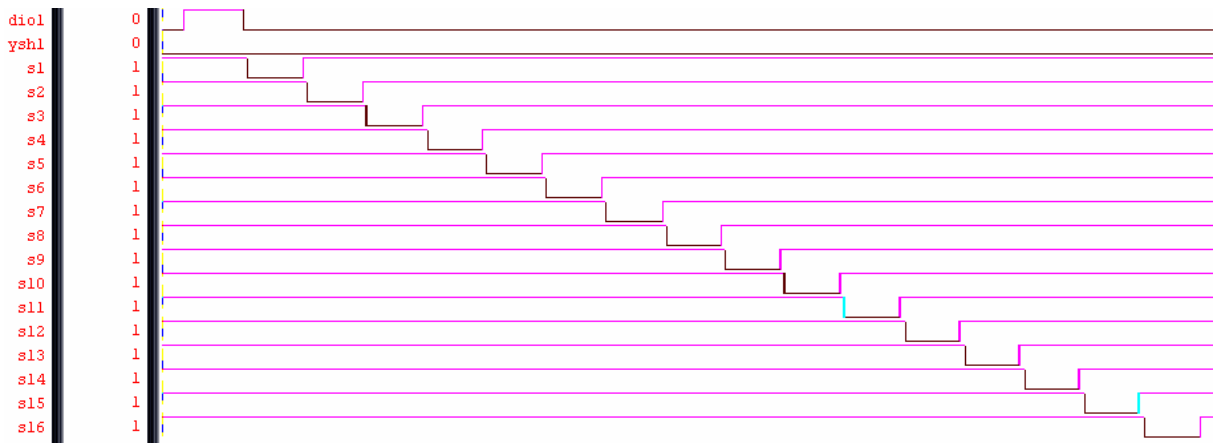
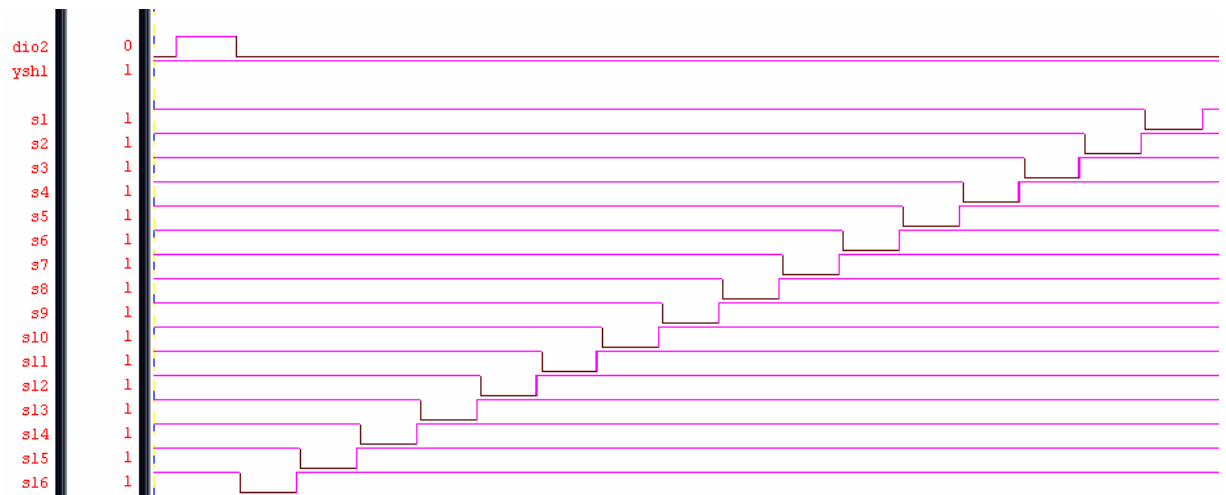


Fig. 4-18 Image handstand with shift register control

Fig. 4-19(a) shows the count for the following number, Fig. 4-19(b) shows the count for the previous number. Due to different counts are used, the sequence of saving horizontal signal into data driver may be opposite. The function for image handstand mirror is able to achieve.



(a) Up count

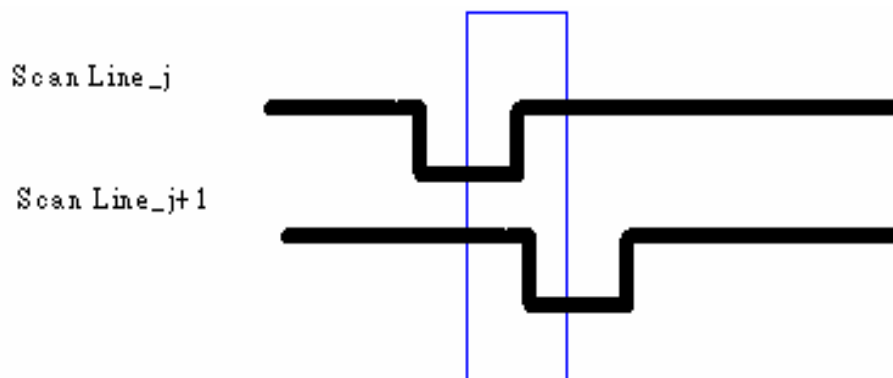


(b) Down count

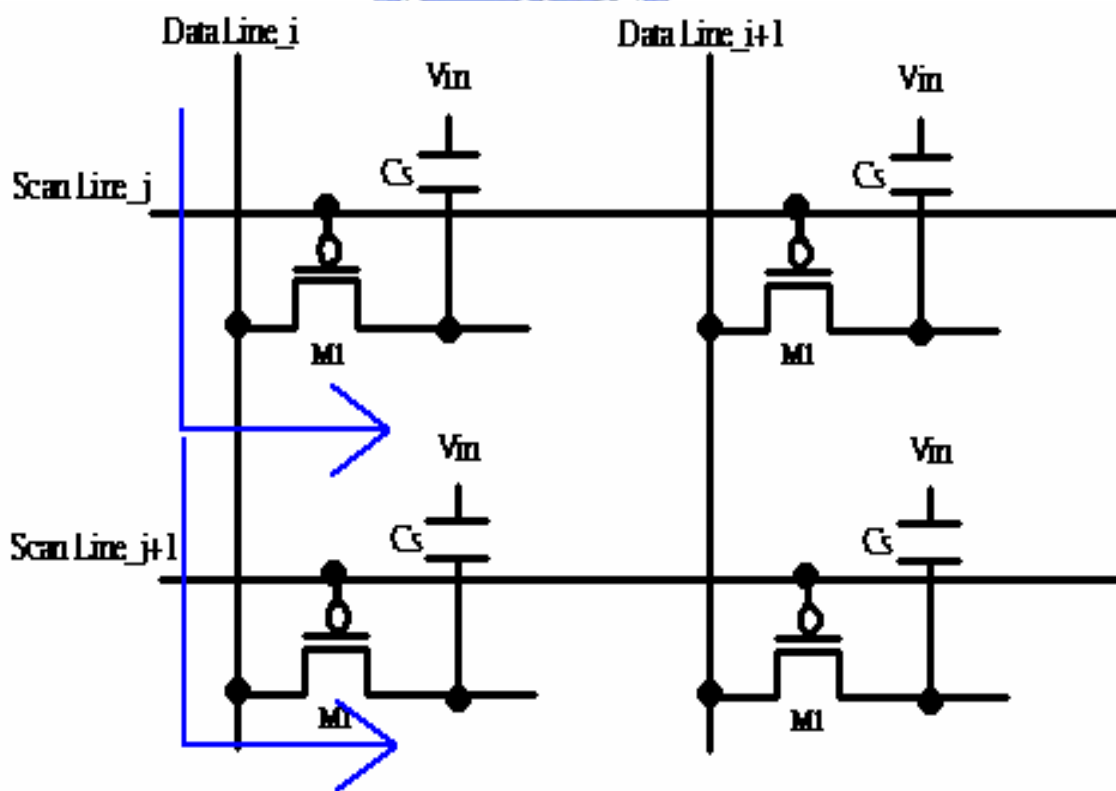
Fig. 4-19 Signal sequential for scan driver

4.4.2.1 Non-overlap with scan signal gating

Fig. 4-20 explains that when the scan driver scans from the first scan line to the last, if the j^{th} row of the scan line completes addressing and shifts to the $j+1^{\text{th}}$ row for addressing, and the scan line encounters overlap, the j^{th} row would receive error programming because the it is overwritten by the $j+1^{\text{th}}$ row. If the content of pixel is overwritten, error messages may appear.



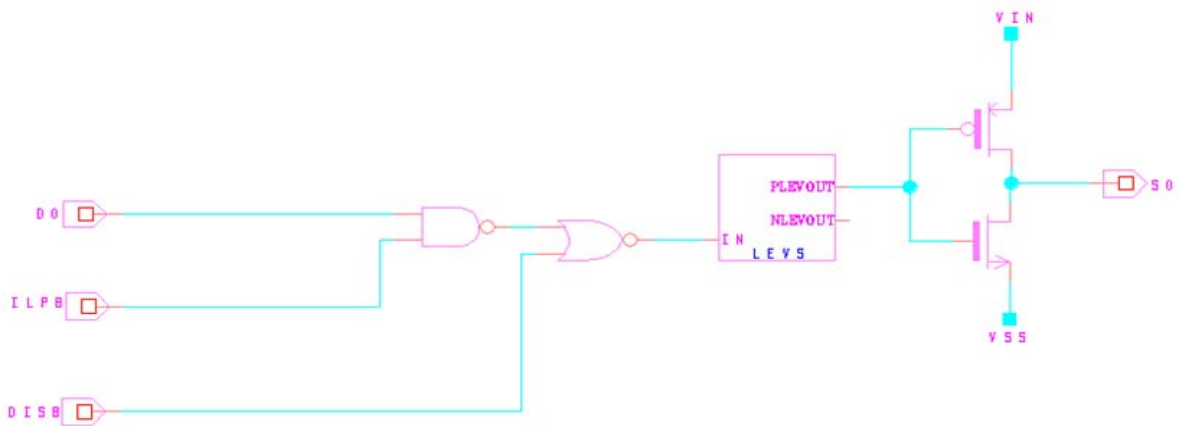
(a) Scan line overlap



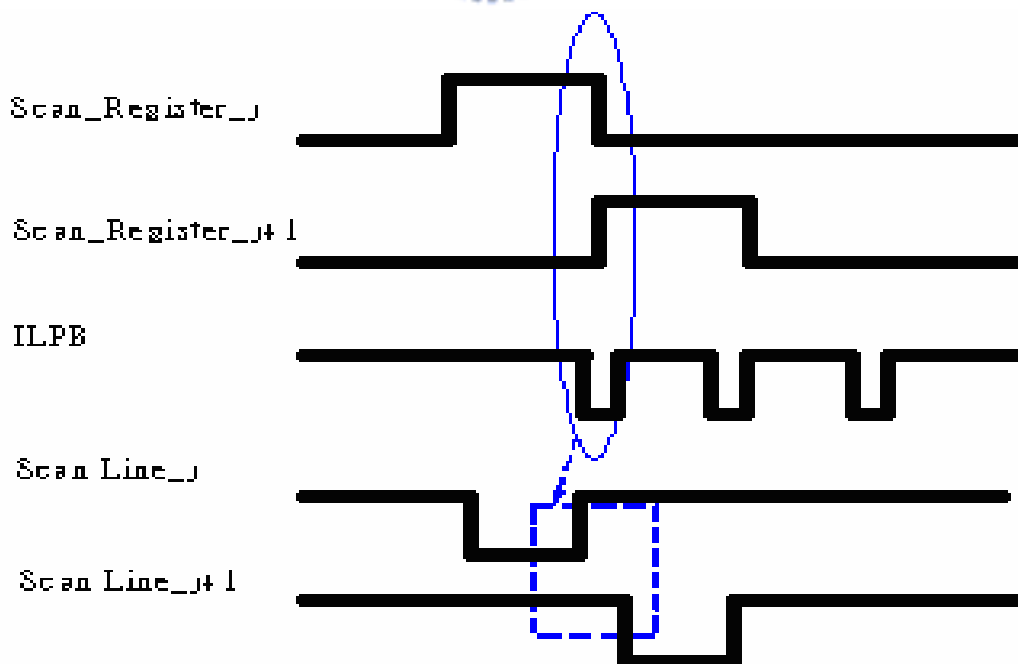
(b) Error-Programming

Fig. 4-20 Adjacent scan line overlapping

To prevent the problem of error programming caused by scan line overlap, the technique of non-overlap with scan signal gating is applied. As shown in Fig. 4-21, whenever ILPB which is a trigger source touches off the shift register, and ILPB creates a gating through NAND gate (NAND1), the neighboring scan signal would be staggered, thus, prevent the problem of error programming.



(a) Mechanism for scan signal gating



(b) Signal relation for scan signal gating

Fig. 4-21 Scan signal gating

4.4.3 Cathode Electrical Switch for IR Drop Issue

OLED makes a direct current pass and emit light from the organic compound of the fluorescence excited by supplying electric field. The current is proportion to the data voltage which is written onto the data storage capacitor C_s . The period for the written data voltage is called addressing time. Since OLED is a current driver element, there is an IR drop issue along scan line direction while a turned on OLED is during addressing time. A bad affect exist. That is, the pixel closed to supply line will be programmed an exact data voltage, but the far pixel will be programmed a wrong data voltage. The variation of gate-source leads to the divergent presentation color for same required color. To correct gate-source voltage store, an additional TFT isolate the OLED during addressing time. It leads to no voltage drop along scan line direction during addressing time. The drawback of this circuit is the aperture-ratio reduction because it results from the number of TFT. Therefore, another skill by voltage switching is used to solve the IR drop issue [4-6]. Fig. 4-22 shows the method by cathode electrical switch. The terminal voltage of cathode is switched to V_{supply} while the OLED is during addressing time. It is effective to prevent the voltage drop, moreover, it have not additional element.

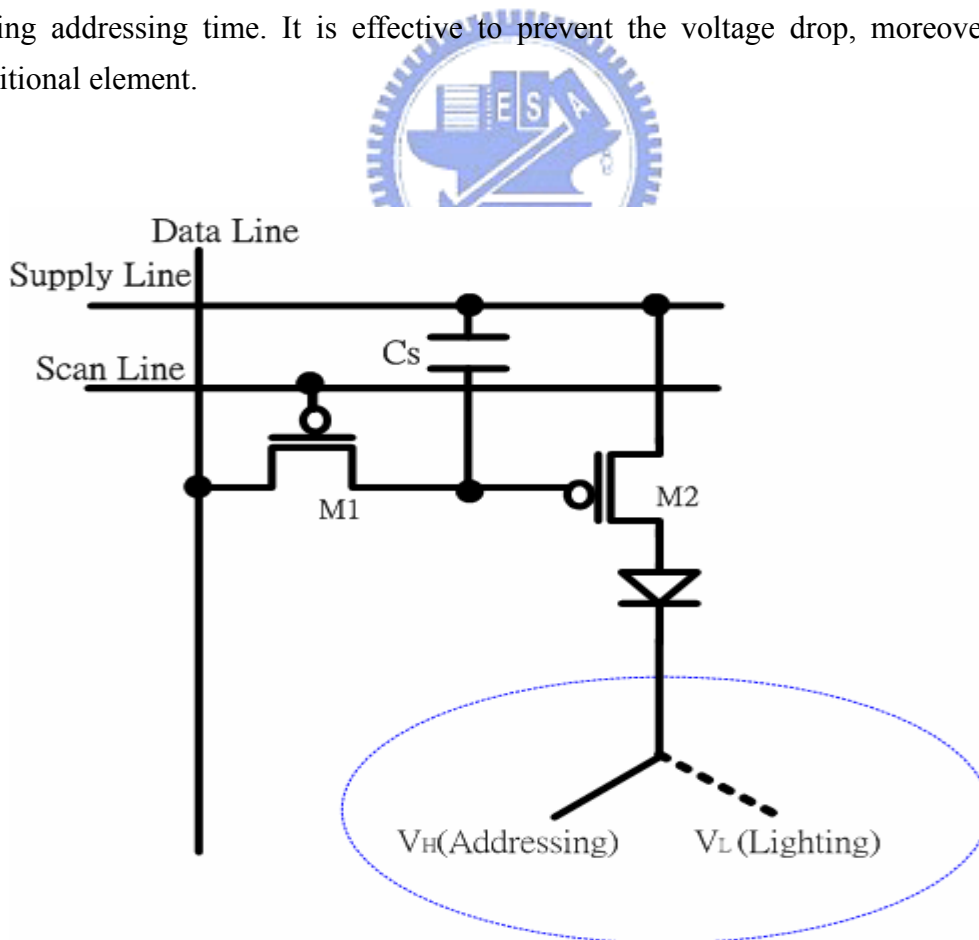
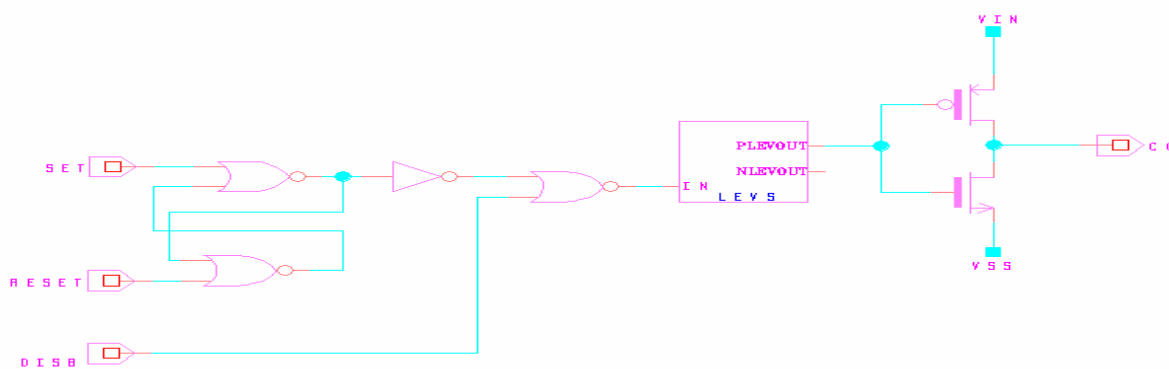
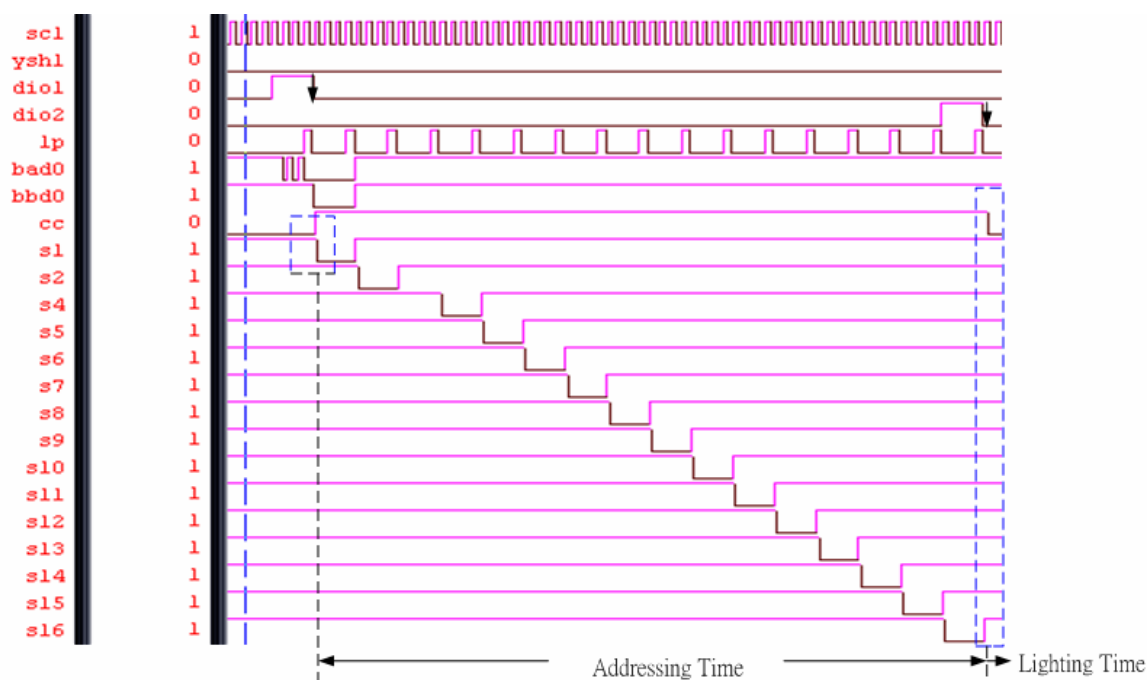


Fig. 4-22 Cathode electrical switch

In order to prevent the divergent presentation color for same required color, the skill of cathode electrical switch is adopted. As shown in Fig. 4-23(a), CC pin is connected to the cathode of panel. As shown in Fig. 4-23(b), If addressing time begins, then the mechanism of cathode electrical switch will be operated. In the addressing time, a signal was added and stored in the gate electrode of the driving TFT of each pixel by scanning entire pixel. At this addressing period, the high voltage is switch to the cathode and is equal to the voltage in the supply line, every OLED pixels are not emitting ,and there is no current pass through OLED pixel. I-R drop issue will be prevented by the method. Shifting to a lighting time, low voltage is switch to the cathode. Then all of the pixels in which low voltage was given to the gate electrode of the driving TFT become bright.



(a) Mechanism of cathode electrical switch



(b) Signal relation with sub-frame

Fig. 4-23 I-R drop prevention

4.4.4 Simulation Result and Summary

To get a good and correct image quality, cathode electrical switch and scan signal gating are adopted individually. As shown in Fig. 4-24, every scan signal non-overlap each other in addressing period, and CC pin go low in lighting period. Thus the all of the pixels are given to the correct voltage from the driving , and are lit without divergent presentation color for same required color.

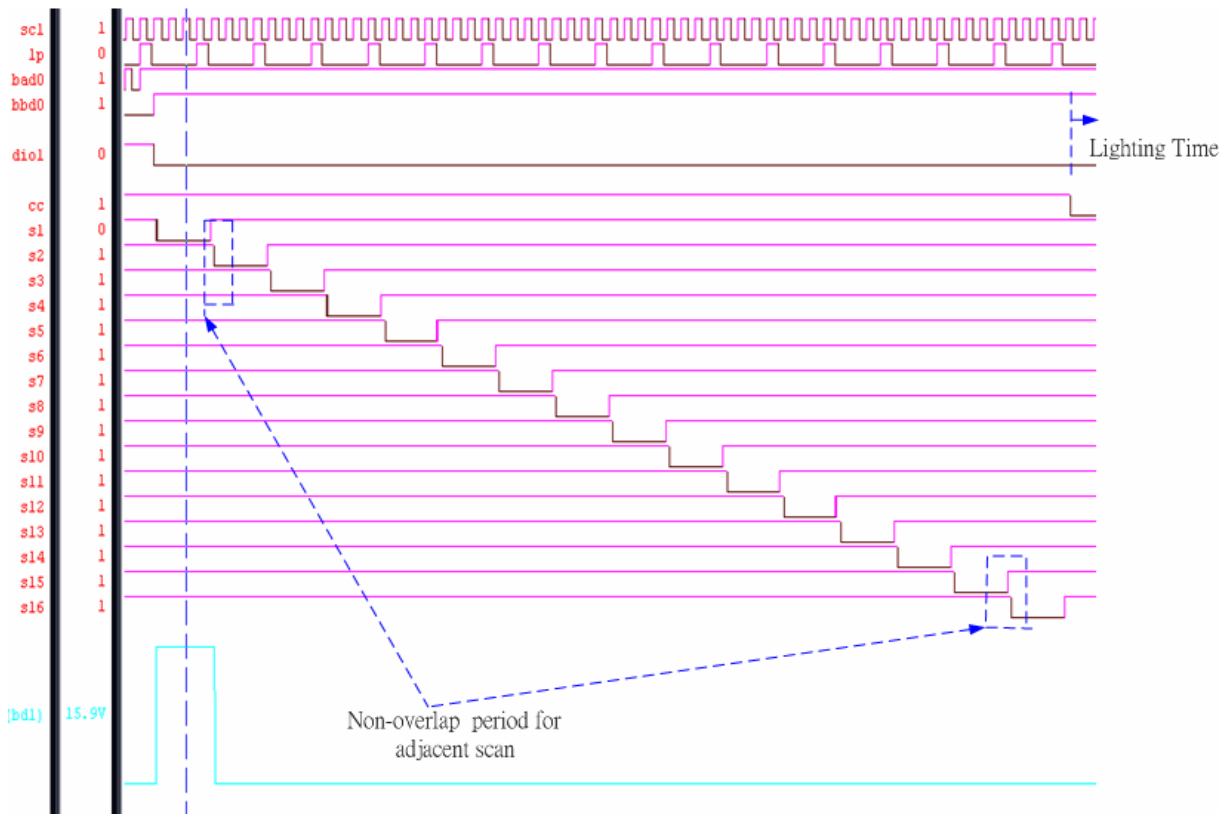


Fig. 4-24 Output of scan driver

4.5 Voltage Regulator

Voltage driving works by applying image signals to pixels as voltage data, which are converted to current data by pixel driving transistors. The current is proportion to the data voltage which is written onto the data storage capacitor C_s of 2T1C pixel. OLED emit light in proportion to current flow. As shown in Fig. 4-25, the voltage-current curve is for poly-silicon pixel. A 2T1C pixel made up of poly-silicon TFT is lit when V_{supply} is over than 12V. According to this chart, the potential including $V_{off-luminance}$, $V_{half-luminance}$, and $V_{full-luminance}$ will be discussed. In improved time ratio grayscale with amplitude, $V_{off-luminance}$, $V_{half-luminance}$ and $V_{full-luminance}$ are required for data driver. In general, $V_{off-luminance}$ is the highest voltage in system, and $V_{full-luminance}$ is the lowest voltage in sytem. $V_{off-luminance}$, $V_{off-luminance}$ and $V_{full-luminance}$ can be provided by power supply, and $V_{half-luminance}$ will be generated by voltage regulator. For example, $V_{off-luminance}$ and $V_{full-luminance}$ are 16V and 0V individually. As shown in Fig. 4-25, if $V_{supply-data}=16V$ for full-luminance and driver current $I=200mA/cm^2$ are pointed, then $V_{supply-data}=14.5V$ and driver current $I=100mA/cm^2$ are adopted for half-luminance. Thus minimum $V_{half-luminance}=1.5V$ is provided by voltage regulator under $V_{supply}=16V$.

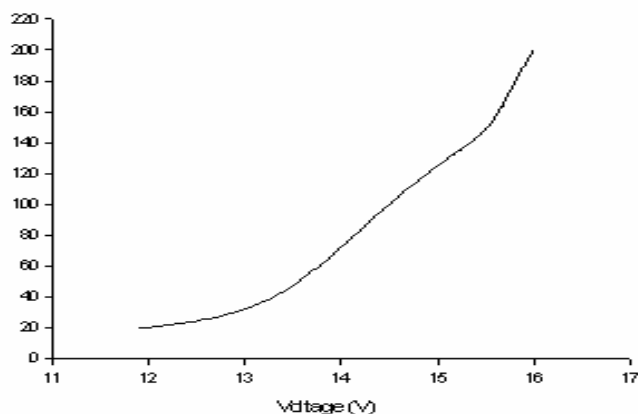
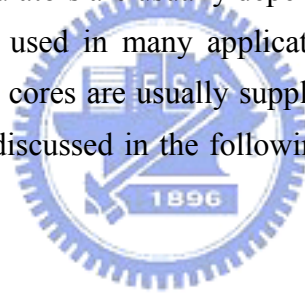


Fig. 4-25 Voltage-current curve for poly-silicon pixel

The common architectures of the voltage regulators [4-7] [4-8] are composed of switching regulators and linear regulators. Switching regulators also called switch-mode regulators. The most advantage of switching regulators over conventional linear regulators is their higher efficiency because the output pass transistor is operated as a switch. When the output pass transistor is operated in the cutoff region, it dissipates no power. When the output pass transistor is operated in the triode region, it is nearly a short circuit with little voltage

drop across it, and it dissipates little power. In this manner, almost all power from input node is transferred to load, so very high power efficiency can be achieved typically in the range between 70% and 90%, relatively independent of input-to-output voltage differences. Switching regulators also have some disadvantages. They are more complex and usually require external components such as large inductances, and capacitances. And they are slower than conventional series regulators. Another drawback of switching regulators is more output noise and ripples than that of series regulators. This is because the pass devices switch high current through an inductor, resulting in the generation of electromagnetic and radio-frequency interference.

Another different type of IC voltage regulator is linear regulator. The major advantages of linear regulators are that a better load transient response, smaller noise, smaller chip layout occupied than equivalent switching regulators. The major disadvantage of linear regulators is poor power efficiency, which is dependent on input-to-output voltage difference. The characteristics of the linear regulators are usually dependent on structures of output series pass devices. Linear regulators are used in many applications. One common application is the supply of digital cores. Digital cores are usually supplied at a lower voltage than the IO and the analog cores. Hence, it is discussed in the following. In this design, Digital core is a 5V system.



The option of architectures about the linear regulators is typically dependent on what process (bipolar, BiCMOS, or CMOS) is to be adopted, what application (automotive, portable equipments) is used in, what specifications is for the application. These specifications include dropout voltage, input voltage, output voltage, response time, power consumption, current rating etc. The detail terms and definition [4-9] are reviewed and the fundamental concepts [4-10] are described such that it will be easier to design or to evaluate a linear regulator.

Some conventional linear regulators, however, are implemented in non-CMOS processes and require large quiescent current for the regulator itself. The efficiency is poor at a low load current. Besides, most of these topologies are based on the pole splitting and pole-zero cancellation. The most common approach is the use of the Miller capacitor [4-11][4-12][4-13]. However, the large load range results in time-constants widely spaced, requiring very large compensation capacitors.

The block diagram of proposed linear regulator includes the error amplifier with OTA, output buffer for achieving fast response time, voltage reference. In the following sections, the design considerations and implementations of these circuits are discussed and presented. The regulator has been optimized to regulate a very wide load range with large current transients without internal compensation capacitors..

4.5.1 Block Diagram of Linear Regulator

A typical block diagram of linear regulators is shown in Fig. 4-26. The principle of operation of a linear regulator can be described in the following. The internal voltage reference provides a reference voltage V_{ref} , which is almost independent of unregulated supply input and temperature variations. The error amplifier compares V_{ref} with the feedback signal V_{fb} , and amplifies the voltage difference of two signals. The linear regulator can control output voltage by controlling the voltage drop across the output pass transistor, which is connected between the unregulated input and the load. The output voltage regulated is given by

$$V_{out} = V_{ref} \times \frac{R_{f1} + R_{f2}}{R_{f2}} \dots\dots\dots (4-3)$$

Where V_{ref} is reference voltage and R_{f1} and R_{f2} are the external adjustable resistors of the feedback network.

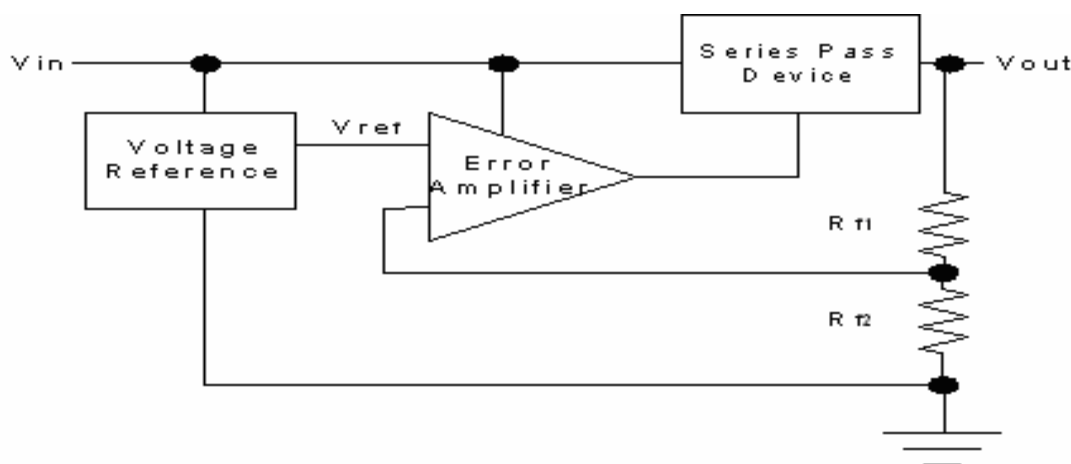


Fig. 4-26 Block diagram of linear regulators

As shown in Fig. 4-26, these structures of series pass transistors include NMOS, NMOS with charge pump control, and PMOS in CMOS technologies. The characteristics of these

linear regulators with different structures of serial pass devices will be discussed at section 4.5.3. In following section, we will adopt the linear regulator structures with PMOS as show in Fig. 4-27 to implement the voltage regulator.

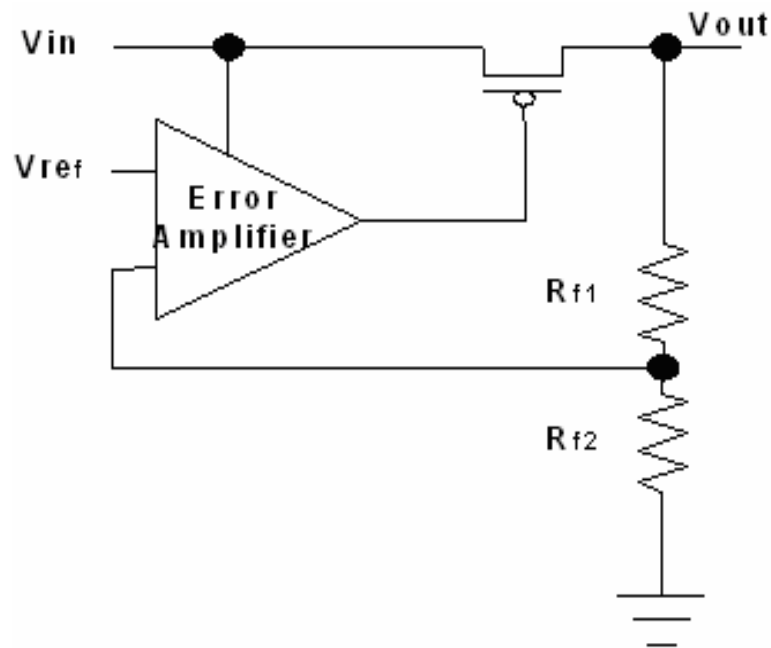


Fig. 4-27 Linear regulator structures with PMOS



4.5.2 Voltage Reference

In Fig. 4-26 requires a voltage reference, whose output voltage is independent of both supply voltage and operating temperature. Although several different types of circuit [4-14] have been developed to meet these requirements, the most popular technique remains the bandgap reference. The bandgap reference can achieve a low temperature coefficient by combining a forward-biased pn diode voltage with negative temperature coefficient with the voltage difference between two pn junctions with the positive temperature coefficient. The main advantages of bandgap reference involve low supply voltage required, low power consumption over equivalent zener diodes and easily implemented in CMOS technologies without the need of additional process step.

How do we generate a voltage that remains constant with temperature? That is how to get a voltage with zero temperature coefficients (TCs): for examples, $V_{ref} = \alpha_1 V_1 + \alpha_2 V_2$,

with zero TCs. For two voltages V_1 and V_2 vary in opposite direction with temperature.

$$\alpha_1 \text{ and } \alpha_2 \text{ are selected such that } \alpha_1 \frac{\partial V_1}{\partial T} + \alpha_2 \frac{\partial V_2}{\partial T} = 0. \dots\dots\dots (4-4)$$

Among various device parameters in semiconductor technologies, the characteristics of bipolar transistors have proven the most reproducible and well-defined quantities that can provide positive and negative TC. Fig. 4-28 [4-15] shows a conceptual block diagram of bandgap if α_1 is set to one. Since the bias sources referenced to $V_{BE(ON)}$ and V_T have opposite temperature coefficient, output voltage V_{ref} with almost zero TCs. In order to determine the required value α_2 , the temperature coefficient of negative-TC voltage and positive-TC voltage [4-16] are analyzed in the following.

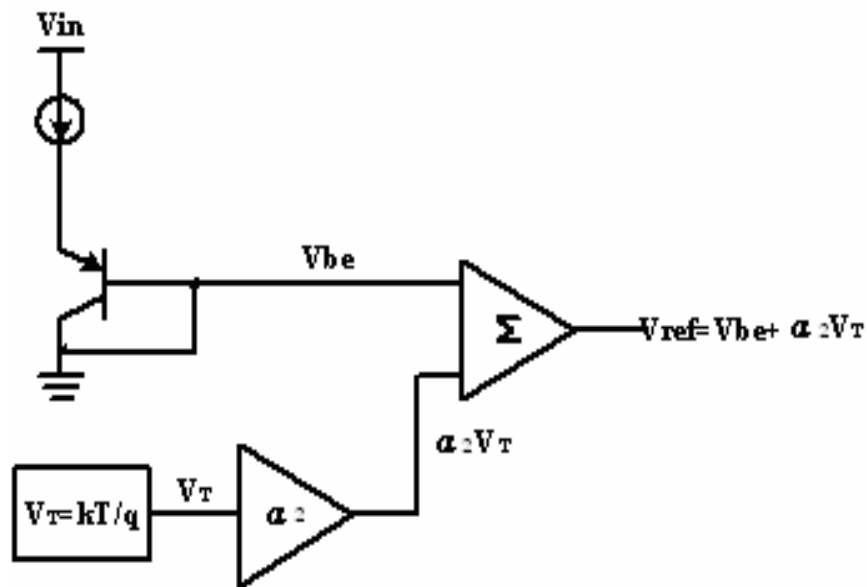


Fig. 4-28 Conceptual block diagram of bandgap

4.5.2.1 Zero Temperature Coefficient

Firstly, it was recognized that if two bipolar transistors have the different size, then the difference between their base-emitter voltages is directly proportional to the absolute temperature. For example as shown in Fig.4-29, where base currents are assumed negligible, transistor Q_2 consists of n unit transistors in parallel, and Q_1 is a unit transistor.

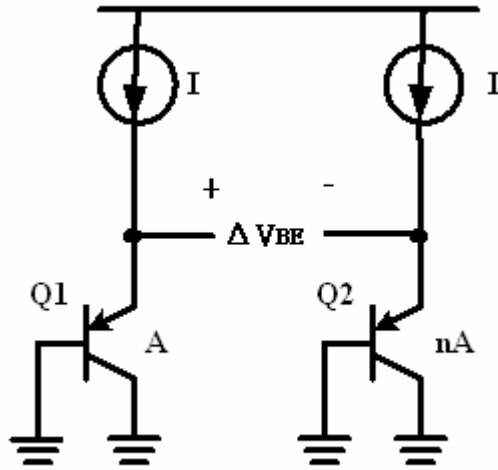
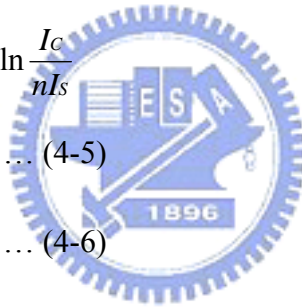


Fig. 4-29 Generation of PTAT voltage

$$\begin{aligned} \Delta V_{BE} &= V_{BE1} - V_{BE2} \\ &= V_T \ln \frac{I_C}{I_S} - V_T \ln \frac{I_C}{nI_S} \\ &= V_T \ln n \dots \dots \dots (4-5) \end{aligned}$$

$$\frac{\partial \Delta V_{BE}}{\partial T} = \frac{k}{q} \ln n \dots \dots \dots (4-6)$$



Thus, the V_{BE} difference exhibits a positive temperature coefficient

For a bipolar device, we can write $I_C = I_S \exp(V_{BE}/V_T)$, where $V_T = kT/q$. The saturation current I_S is proportional to $\mu k T n_i^2$, where μ denotes the mobility of minority carriers and n_i is the intrinsic minority carrier concentration of silicon. The temperature dependence of these quantities is represented as $\mu \propto \mu_0 T^m$, where $m \approx -3/2$, and $n_i^2 \propto T^3 \exp[-E_g/(kT)]$, where $E_g \approx 1.12\text{eV}$ is the bandgap energy of silicon. Thus,

$$I_S = b T^{4+m} \exp \frac{-E_g}{kT} \dots \dots \dots (4-7)$$

where b is a proportionality factor. Writing $V_{BE} = V_T \ln(I_C/I_S)$, we can now compute the TC of the base-emitter voltage. In taking the derivative of V_{BE} with respect to T , we must know the behavior of I_C is held constant. Thus,

$$\frac{\partial V_{BE}}{\partial T} = \frac{\partial V_T}{\partial T} \ln \frac{I_C}{I_S} - \frac{V_T}{I_S} \frac{\partial I_S}{\partial T} \dots \dots \dots (4-8)$$

From (4-7), we have

$$\frac{\partial I_S}{\partial T} = b(4+m)T^{3+m} \exp \frac{-E_g}{kT} + bT^{4+m} \left(\exp \frac{-E_g}{kT} \right) \left(\frac{E_g}{kT^2} \right) \dots \dots \dots (4-9)$$

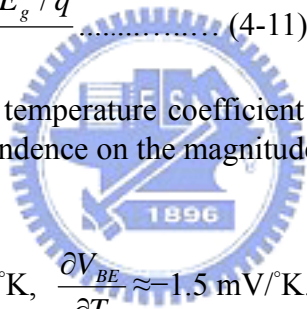
Therefore,

$$\frac{V_T}{I_S} \frac{\partial I_S}{\partial T} = (4+m) \frac{V_T}{T} + \frac{E_g}{kT^2} V_T \dots \dots \dots (4-10)$$

With the aid of (4-8) and (4-9), we can write

$$\begin{aligned} \frac{\partial V_{BE}}{\partial T} &= \frac{V_T}{T} \ln \frac{I_C}{I_S} - (4+m) \frac{V_T}{T} - \frac{E_g}{kT^2} V_T \\ &= \frac{V_{BE} - (4+m)V_T - E_g/q}{T} \dots \dots \dots (4-11) \end{aligned}$$

Equation (4-11) gives the temperature coefficient of the base-emitter voltage at a given temperature T , revealing dependence on the magnitude of V_{BE} itself.



with $V_{BE} \approx 750\text{mV}$ and $T = 300^\circ\text{K}$, $\frac{\partial V_{BE}}{\partial T} \approx -1.5 \text{ mV}/^\circ\text{K}$.

We obtain the base-emitter voltage of bipolar transistors exhibits a negative TC.

With the negative-and positive-TC voltages obtained above, we can now develop a reference having a nominally zero temperature coefficient. We rewrite $V_{ref} = \alpha_1 V_{BE} + \alpha_2 (V_T \ln n)$, Where $V_T \ln n$ is the difference between the base-emitter voltages of the two bipolar transistors operating at different current densities. How do we choose α_1 and α_2 ? Since at room temperature $\partial V_{BE} / \partial T \approx -1.5 \text{ mV}/^\circ\text{K}$ whereas $\partial V_T / \partial T \approx +0.087 \text{ mV}/^\circ\text{K}$, we may set $\alpha_1 = 1$ and choose $\alpha_2 \ln n$ such that $(\alpha_2 \ln n)(0.087 \text{ mV}/^\circ\text{K}) = 1.5 \text{ mV}/^\circ\text{K}$. That is, $\alpha_2 \ln n \approx 17.2$, indicating that for zero TC:

$$V_{ref} \approx V_{BE} + 17.2 V_T \approx 1.25V \dots \dots \dots (4-12)$$

As shown in Fig. 4-33 is a curve which is the actually variation of V_{ref} . The difference between actually value and ideal value result from process parameter is slightly different.

4.5.2.2 Architecture

Fig 4-30, shows a bandgap structure base on the configuration, using PMOS devices to isolate the amplifier. The gates and sources of M1 / M2 are at the same potential, so the same current is forced through each side. For the amplifier to be stable, the amount of signal fed back and subtracted from the input is larger than the amount of signal fed back and added to the input. Because M1 and M2 are inverting common-source amplifiers, we want the signal fed back to the +input of the amplifier to be larger than the signal fed back to the – input of the amplifier. Since the AC currents flowing in M1 and M2 are equal and the branch containing Q2 is a higher resistance than the branch containing Q1, the Q2 branch is always connected to the +amplifier input. In the following, Vref is analyzed.

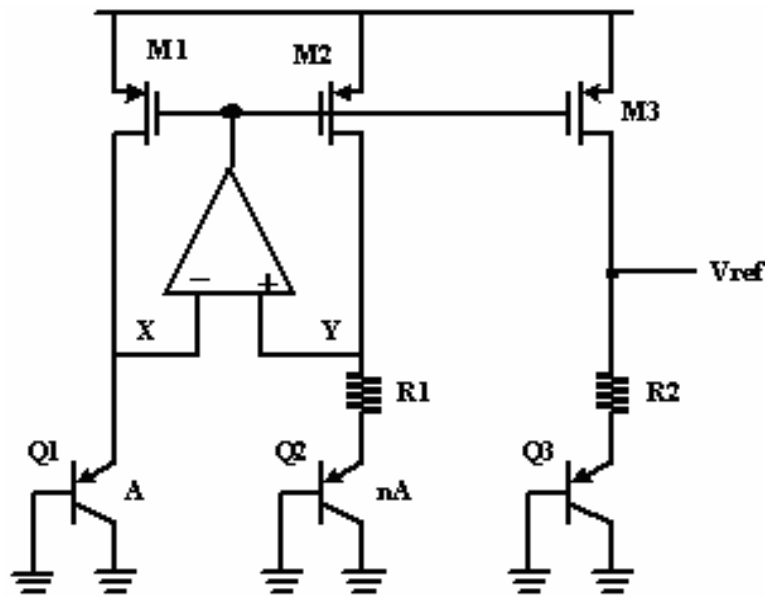


Fig. 4-30 Bandgap structure

According to Fig. 4-30 , we write down the below equations.

$$I_C = I_S \exp(V_{BE} / V_T),$$

$$I_{D1} = I_{D2} = I$$

$$V_X = V_Y, V_X = V_{BE1} = V_T \ln \frac{I}{I_S}$$

$$V_Y = V_{BE2} + I \cdot R_1 = V_T \ln \frac{I}{n \cdot I_S} + I \cdot R_1$$

$$I = \frac{1}{R_1} V_T \ln n$$

$$V_{ref} = V_{BE3} + I \cdot R_2 = V_{BE3} + \frac{R_2}{R_1} V_T \ln n \dots\dots(4 - 13)$$

From the above equation (4-13), we can set those value which include R_1 , R_2 and n to decide the V_{ref} . In general, n is set to eight for layout concern. The choice of ratio of R_1 to R_2 will result in V_{ref} with zero temperature coefficient.

Another important issue is the existence of degenerate bias points. As shown in Fig. 4-30, if the transistors carry zero current when the supply is turned on, they may remain off indefinitely. Called the “start-up” problem, the above issue is resolved by adding a mechanism that drives the circuit out of the degenerate bias point when the supply is turned on. Comparing Fig.4-30, a start-up circuit has added to Fig. 4-31, where the device M_9 provides a voltage path to ground upon start-up. Through M_6 and M_7 , M_9 is turned on and force M_1 ~ M_4 cannot remain off. When the start-up is finished, M_8 by I_{D5} force M_9 turned off. Thus, M_1 ~ M_4 is still turn on because the current for branch X and Y are built up. After start-up period, V_{ref} will output a voltage with zero temperature coefficient. The simulation result is shown Fig. 4-32.

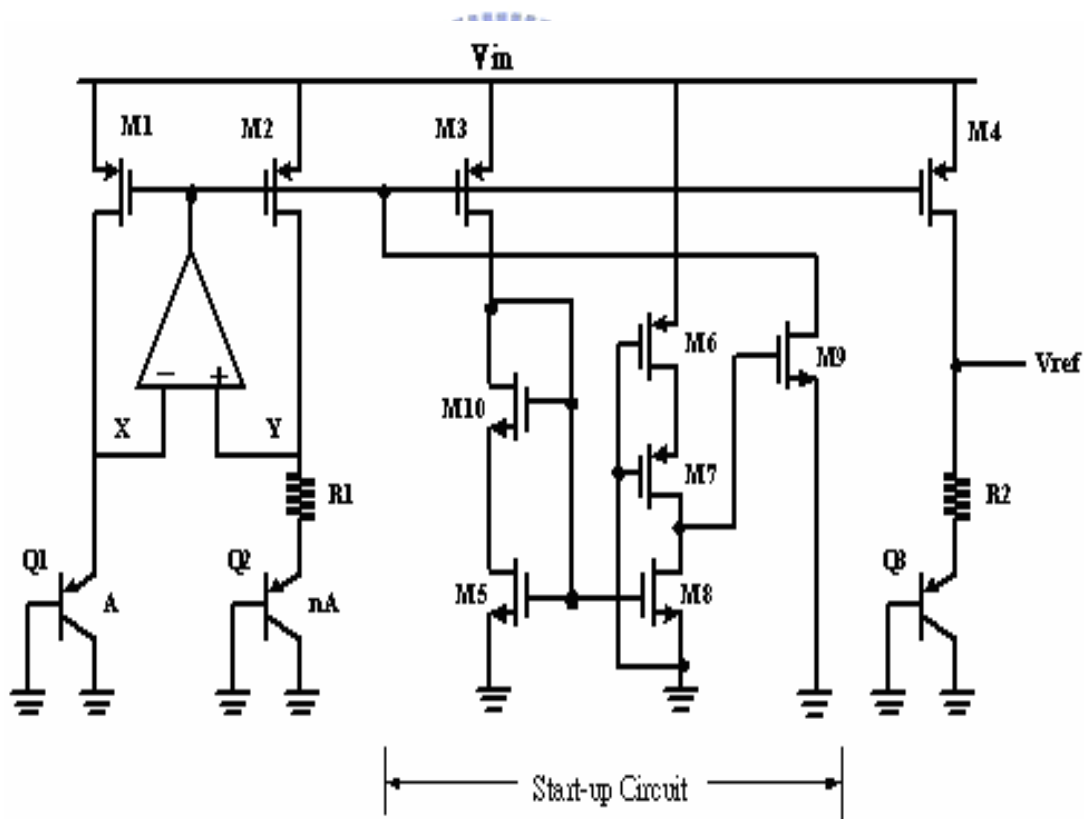
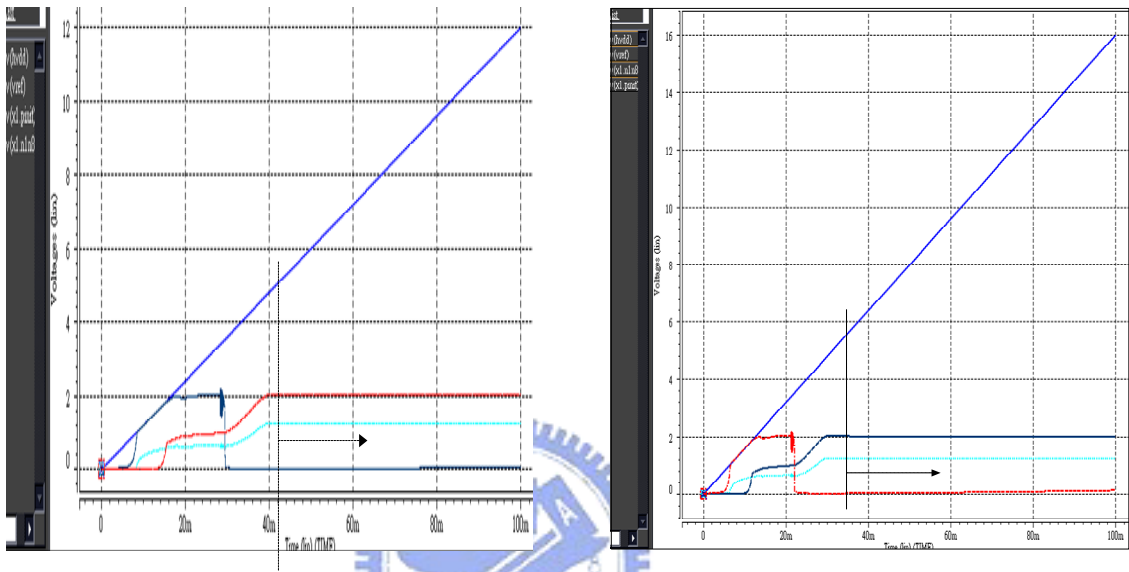


Fig. 4-31 Bandgap with start-up circuit

4.5.2.3 Simulation Result and Summary

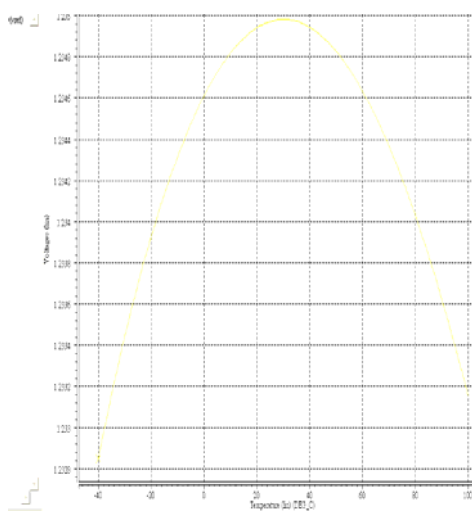
The problem of start-up generally requires careful analysis and simulation. The supply voltage is ramped from zero in a dc sweep simulation. As shown in Fig. 4-32, we sweep the supply voltage for bandgap circuit from zero to V_{in} , and the start-up circuit is able to auto-on and auto off. As shown in Fig. 4-33, the actually variation for bandgap output is from 1.23V to 1.235V.



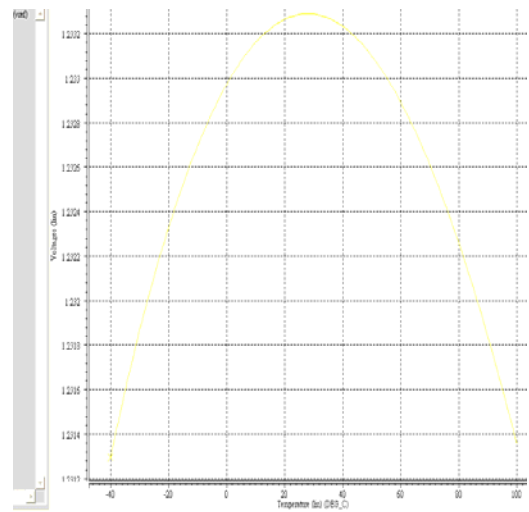
(a) $V_{in}=12V$

(b) $V_{in}=16V$

Fig. 4-32 Simulation for start-up circuit in bandgap



(a) $V_{in}=12V$



(b) $V_{in}=16V$

Fig. 4-33 Variation of the zero-TC

4.5.3 Pass Devices Concern

The option of pass devices of the linear regulators is typically dependent on what process (bipolar, BiCMOS, or CMOS) is to be adopted, what application is used. The specifications of the regulators in the application linear regulators can be classified based on pass device structures: NPN-Darlington, NPN, PNP, PMOS, and NMOS. Fig. 4-34 shows five topologies of serial pass devices. The primary distinctions in performances between these topologies of the pass devices are in the parameters of dropout voltage and quiescent current. Bipolar-based pass devices can typically deliver largest output currents for a given supply voltage, but require more quiescent current because they belong to current-driven devices. The driving performance of MOS-based pass devices is greatly influenced by aspect ratio and gate drive voltage. However, MOS transistors require little quiescent current because they are voltage-driven devices. The NPN Darlington pass transistor with a PNP buffer used in an NPN Darlington regulator typically requires at least 1.6 V of input-to-output voltage differential for proper work, but linear regulators usually work under the operational environment with less than 0.5 V of input-to-output voltage differential. The advantage of the NPN Darlington regulator is less drive current required compared to other BJT-based pass devices because of its high current gain. The dropout voltage of NPN Darlington regulators is described as follows:

$$V_{\text{drop}} = 2V_{\text{BE}} + V_{\text{CE(SAT)}} \cong 1.6 \sim 2.5\text{V} \dots\dots\dots (4-14)$$

The NPN pass device is made of a single NPN transistor driven by a PNP transistor. The dropout voltage of the NPN regulator is described as follows:

$$V_{\text{drop}} = V_{\text{BE}} + V_{\text{CE(SAT)}} \geq 0.9\text{V} \dots\dots\dots (4-15)$$

The PNP pass device is a single PNP transistor, and the major advantage of PNP regulator is that PNP pass transistor can maintain output regulation with very little voltage drop across it. The dropout voltage of the PNP regulator is described as follows:

$$V_{\text{drop}} = V_{\text{CE(SAT)}} \approx 0.1 \sim 0.4\text{V} \dots\dots\dots (4-16)$$

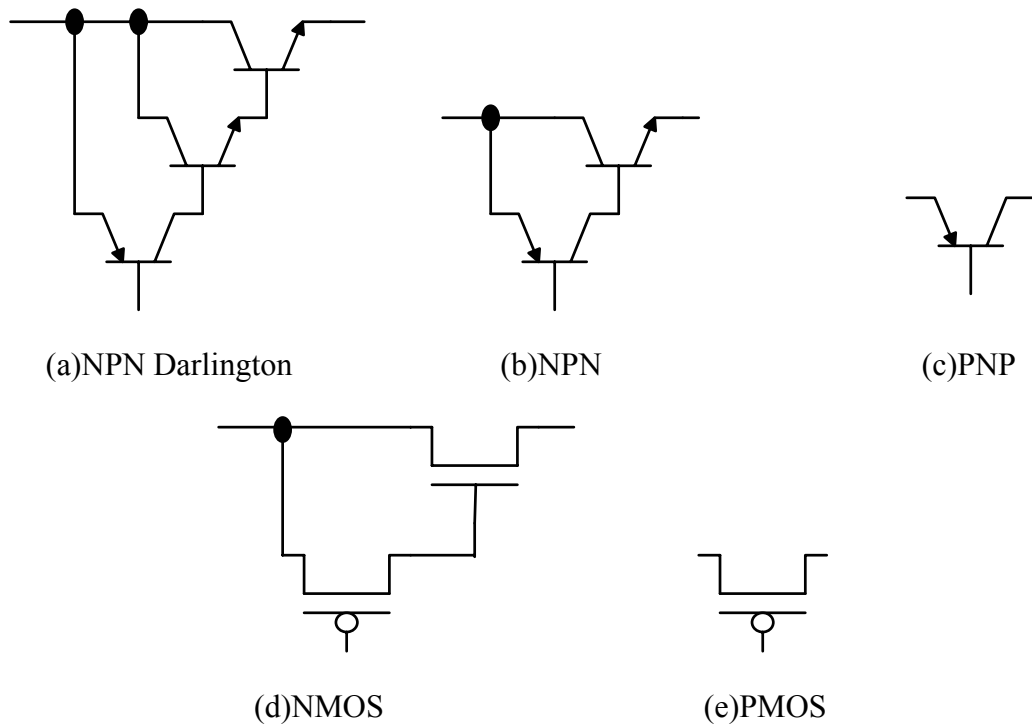


Fig. 4-34 Pass devices topologies

Fig. 4-34(d) and 4-34(e) show the MOS-based pass devices. The major advantage of NMOS regulators is its low output resistance, and hence variations of the output current will only slightly change the output voltage. The major drawback of NMOS regulators is the dropout voltage required at least larger than one gate-source voltage. The dropout voltage of NMOS regulators can be improved by using a charge pump circuit. The PMOS regulators exhibit low dropout voltages, depending on on-resistance of PMOS pass transistor and the current through the pass transistor, which is expressed as follows:

$$V_{\text{drop}} = I_{\text{out}} \cdot R_{\text{on}} \dots\dots\dots (4-17)$$

where R_{on} is the on-resistance of the PMOS pass transistor, I_{out} is the current through the pass transistor.

Table 4-4 [4-2] lists the comparison of these pass devices.

Parameter	DARLINTON	NPN	PNP	NMOS	PMOS
Output Current	High	High	High	Medium	Medium
Quiescent current	Medium	Medium	Large	Low	Low
Dropout	$V_{ce(sat)} + 2V_{be}$	$V_{ce(sat)} + V_{be}$	$V_{ce(sat)}$	$V_{ds(sat)} + V_{gs}$	$V_{SD(sat)}$
Speed	Fast	Fast	Slow	Medium	Medium

Table 4-4 Comparison of pass element devices

4.5.4 Frequency Response of Voltage Regulator

Fig. 4-35 shows a block diagram of linear regulators using conventional frequency compensation by inserting a large output capacitor with equivalent linear resistance. The error amplifier acts a gain stage in the feedback loop to provide a regulated output voltage. The buffer provides low output impedance at the gate of the output pass transistor. The output voltage of this circuit is sensed by feedback resistors R_{f1} and R_{f2} , and fed back into one of the inputs of the error amplifier. The error amplifier compares V_{ref} with the feedback signal V_{fb} and amplifies the voltage difference of two signals. This linear regulator can control output voltage by controlling the voltage drop across the output pass transistor, which is connected in linear between the unregulated input and the load. The output pass transistor is a common-source PMOS transistor to provide output current. There are three poles and one zero in the feedback loop, which are expressed as follows:

$$f_{p1} \approx \frac{1}{2\pi \cdot R_{op} \cdot C_{out}} \cong \frac{\lambda \cdot I_L}{2\pi \cdot C_{out}} \dots\dots\dots (4-18)$$

$$f_{p2} \approx \frac{1}{2\pi \cdot R_{O1} \cdot C_{p1}} \dots\dots\dots (4-19)$$

$$f_{p3} \approx \frac{1}{2\pi \cdot R_{O2} \cdot C_{p2}} \dots\dots\dots (4-20)$$

$$f_{z1} \approx \frac{1}{2\pi \cdot R_{e\ sr} \cdot C_{out}} \dots\dots\dots (4-21)$$

Where C_{out} is an output capacitor, C_{p1} and C_{p2} are the parasitic capacitances at output nodes of the error amplifier and buffer, R_{O1} and R_{O2} are the output resistances at output node of the error amplifier and buffer, R_{op} is the output resistance of the pass transistor, $R_{e\ sr}$ is the

equivalent linear resistance of the output capacitor, λ is the channel length modulation parameter, I_L is the current through output pass transistor M_{OP} . To achieve optimum stability, f_{z1} should be equal to f_{p2} for pole-zero cancellation, and f_{p3} should be placed after the unity-gain frequency of feedback loop.

From the above equations, we find the fact that the variations of the load current will change the position of f_{p1} . As depiction in Fig. 4-36, the first pole f_{p1} is shifted to a higher frequency f_{p1}' for a higher load current, but other poles are almost fixed. Therefore, phase margin of the linear regulators will decrease with load current increasing, and linear regulators will tend to be un-stable. Moreover, the matching of f_{p2} and f_{z1} is very important for the stability of the linear regulators. Unfortunately, ESR of nowadays is too small to compensate f_{p2} . The result makes the linear regulators tend to be unstable.

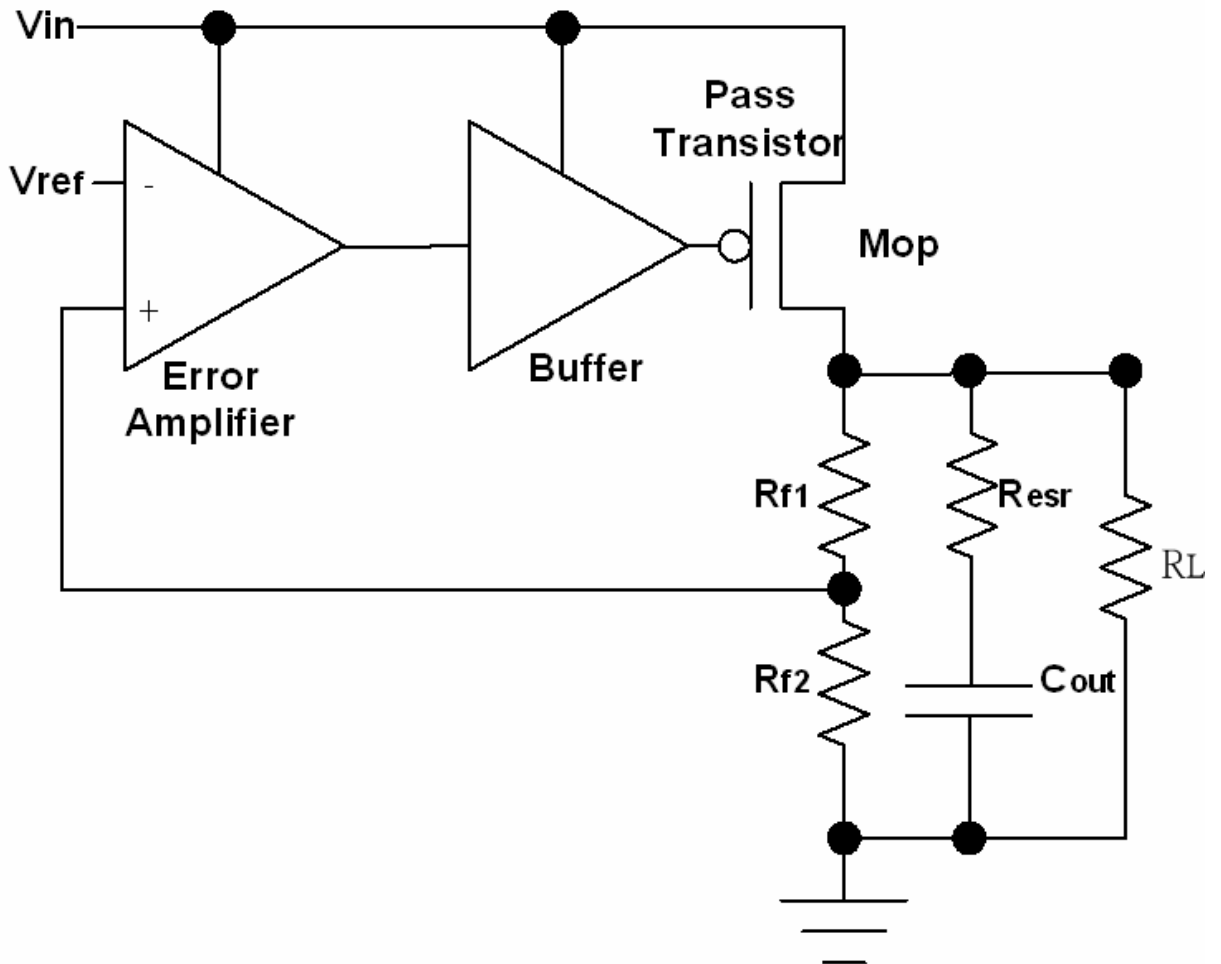


Fig. 4-35 Block diagram of linear regulator

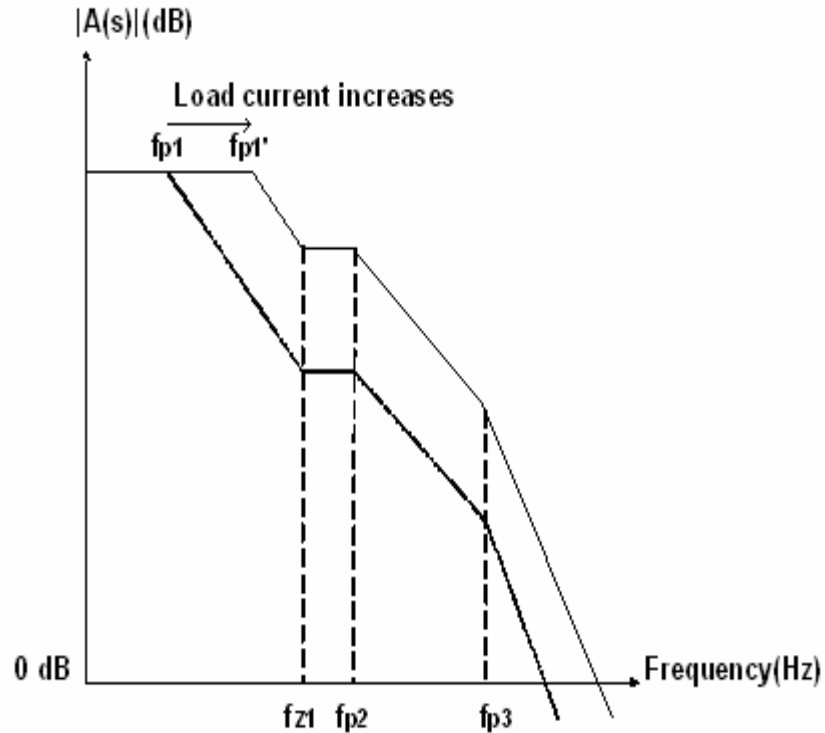


Fig. 4-36 Frequency response of linear regulator under two different loads

4.5.5 Voltage Regulator with OTA Structure

From the previous analysis, the main problems of conventional linear voltage regulators are that the position of the pole at the output node is pushed to high frequencies with the load current increasing, and ESR is too small. Therefore, many techniques are discussed whereby the compensating capacitor of internally compensated linear regulator. A technique for linear regulator without compensating capacitor is presented by operational transconductance amplifier (OTA) [4-14] and a buffer. Without compensating capacitor, the circuit allows to occupy less silicon area.

Fig. 4-37 shows the complete schematic of the control loop, including an error amplifier, buffer, PMOS pass transistors. Transistors included Mn1-Mn4, Mp2-Mp6 construct the error amplifier. The error amplifier with a OTA op amp is utilized to provide enough loop gain.

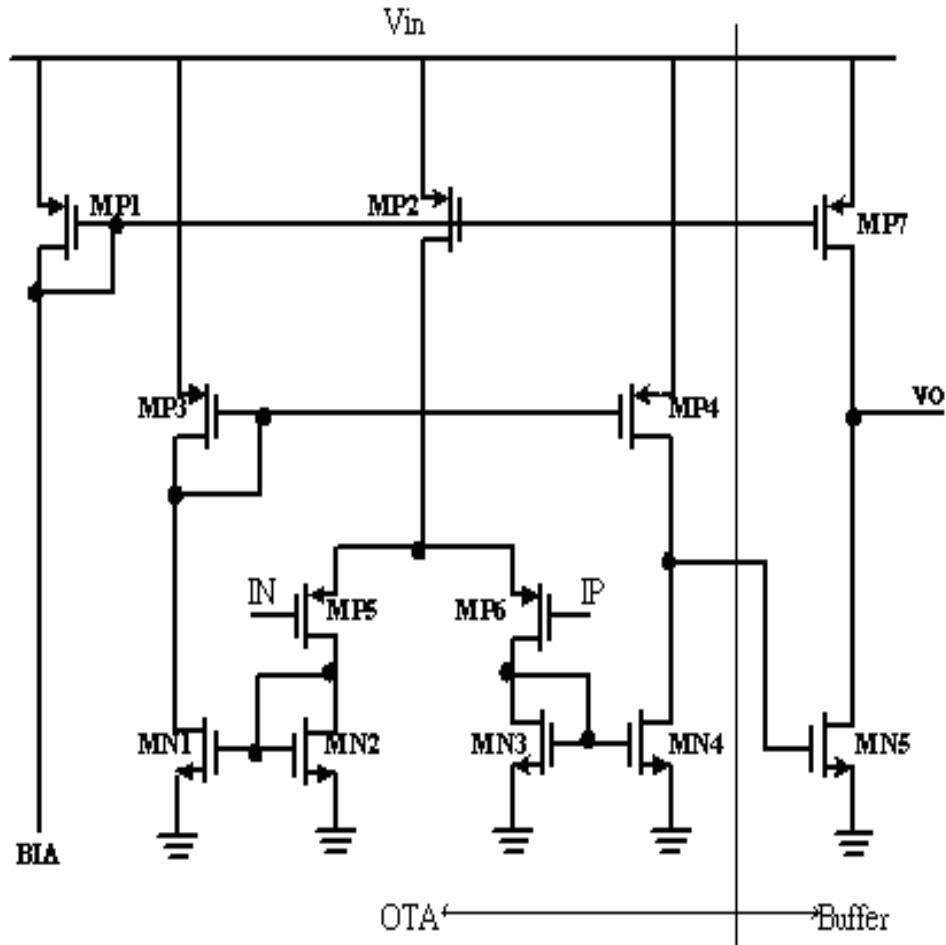
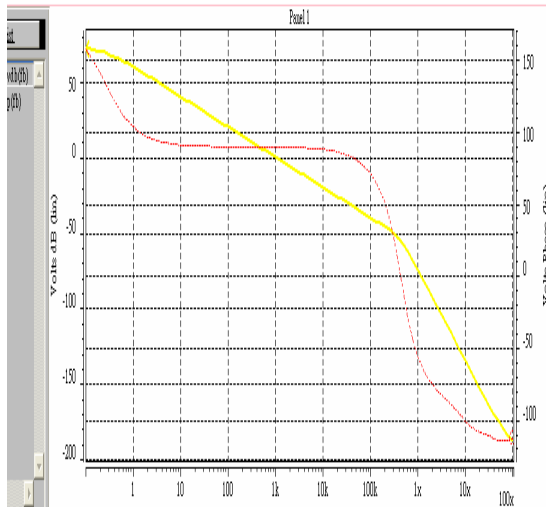


Fig. 4-37 Linear regulator with OTA structure

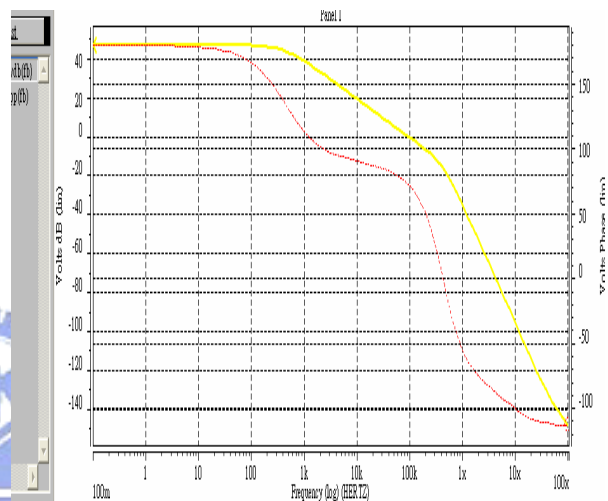
The OTA can be defined as an amplifier where all nodes are low impedance except the input and output nodes, and the design can stabilize this linear regulator under the variations of the load current. For an OTA without buffer can only drive capacitive loads. The buffer is normally presented only when resistive loads need to be driven. If the load is purely capacitive, then it is seldom included. From equation (4-18), (4-19) and (4-20) equation, we get a information which pole form. The buffer is added to acquire a fine frequency response. The buffer provides low output impedance at the gate of the output pass transistor. By this arrangement, dominator pole must be located in output node due to output capacitor is huger than internal parasitic capacitances.

4.5.6 Simulation Result and Summary

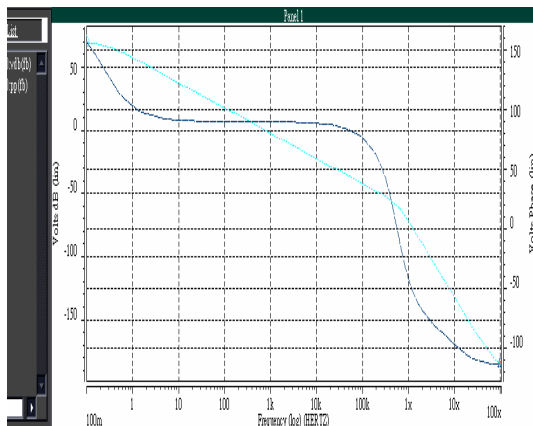
ESR is set to 0.005Ω , output capacitor is set to $4.7\mu\text{F}$. Output transient variation under the simulated conditions that supply voltage (V_{in}) changes from 12V to 16V. Fig. 4-38 shows the simulated bode plot of this linear regulator with the load current of $0\mu\text{A}$ and 100mA. From the simulation result, the phase margins are almost above 70° for min. and max. load current levels. As shown in Fig. 4-39, the result shows the maximum output variation under a full load current change is below 50 mV for target $V_{out} = 5\text{V}$ and 1.5V. According to these results, the regulator can provide the $V_{\text{half-luminance}}$ and $V_{\text{digital-core}}$.



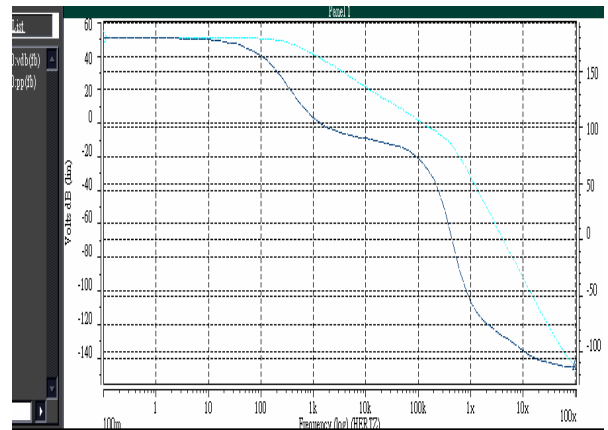
(a) $V_{in}=16\text{V}$ and min. load



(b) $V_{in}=16\text{V}$ and max. load

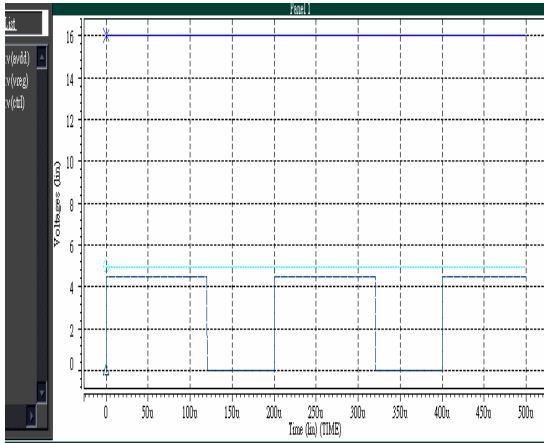


(c) $V_{in}=12\text{V}$ and min. load

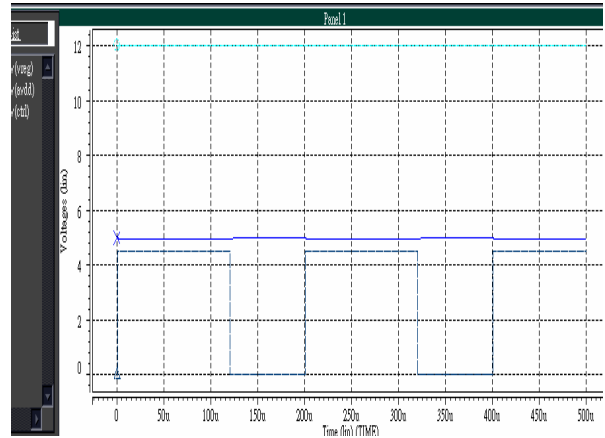


(d) $V_{in}=12\text{V}$ and max. load

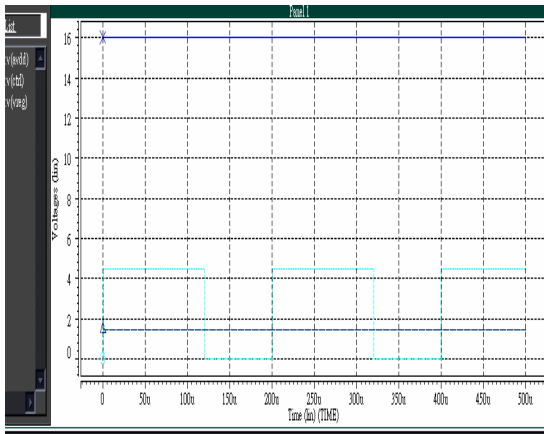
Fig. 4-38 Simulated bode plot for loop response



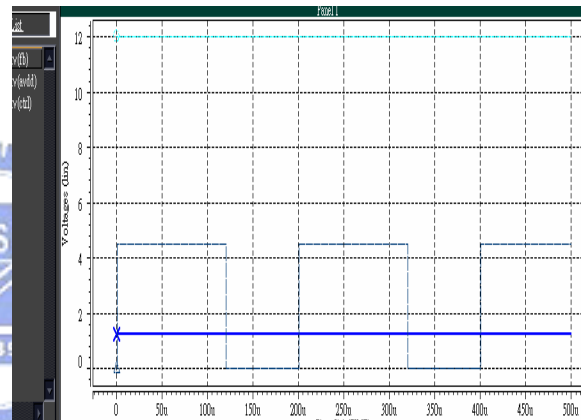
(a) $V_{in}=16V$ and $V_{out}=5V$



(b) $V_{in}=12V$ and $V_{out}=5V$



(c) $V_{in}=16V$ and $V_{out}=1.5V$



(d) $V_{in}=12V$ and $V_{out}=1.5V$

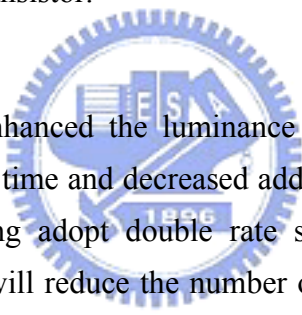
Fig. 4-39 Output variation under a full load current change

Chapter5

Conclusions and Future Work

5.1 Conclusions

The pixel of 2T1C owns the least number of TFT in all pixel structure, and has a max. aperture-ratio comparing other pixel structure. TFT is always made from both amorphous and poly-silicon. Poly-silicon has much higher mobility, reducing the size of the drive TFT. Poly-silicon is always required. For poly-silicon TFT, both mobility and threshold-voltage vary randomly across the plate. Unfortunately, this structure of pixel does not compensate the variation of V_t and mobility (μ_p), the former two variables would lead to variation in illumination strength. Thus the driving by time ratio grayscale is adopted. Since the large voltage step is forced to pixel, it results in the reduction influence of variation of the characteristics of the driving transistor.



In this thesis, we have enhanced the luminance efficiency of conventional time ratio grayscale by increased lighting time and decreased addressing time. For decreased addressing time, shift register of sampling adopt double rate serial-in. For increased lighting time, amplitude modulation coding will reduce the number of sub-frame, and increase the lighting time. The combined method could enhance 24% luminance. The higher luminance allows a small pixel. Small pixel will allow high resolution displays to be created. The method eliminates any unnecessary digital to analog conversions, making the OLED technology ideal for the all-digital age. Without analog circuits, driver circuits by poly-silicon TFT can be integrated to the display panel. For scan signal, the another proposed scan signal gating is developed. It also prevent from error programming issue when adjacent scan line are toggling.

5.2 Future Work

A prototype of this AMOLED driver is simulated by 0.6 um 18V CMOS technology. Because lighting time is limited, it is suitable for the QVGA (Quarter Video Graphic Array) or below the resolution. The future work is driving an AMOLED panel by the driver chip, and find out the image performance. From the engineering evaluation, we will get much more experience for the next generation driver development. The final goals are that driver structure are integrated on the display panel and drive a bigger dimension panel. There is no analog design in driver by this method. Thus it is possible that the driving circuit is fully implemented to SOP. Without extra-chip for driver, the panel price will be reduced. The price is a key factor for competition with many kinds of displays. Besides, multi-channel data driving shift register must be used for larger panel. VGA or bigger dimension panel is also lighting.



Reference

In Chapter1

[1-1] Lawrence E. Tannas, “The Ultimate Avionics Display”, SID '00 DIGEST, pp. 1145-1147, 2000.

[1-2] Sixto Ortiz Jr, “New monitor technologies are on display”, Computer, vol:36, pp. 13-16, 2003.

[1-3] Collins. L, “Roll-up displays: fact or fiction? “, IEE Review, Volume: 49, pp. 42–45, 2003.

[1-4] C. W. Tang, S.A. Van Slyke., “Organic electroluminescent diodes”, Appl. Phys. Lett. Vol. 51, pp. 913-915, 1987.

[1-5] J.H. Burroughes, D.D.C. Bradley, A.R. Brown, R.N. Marks, K. Mackay, R.H. Friend, P.L. Burn, A.B. Holmes, “ Light-emitting organic electroluminescent devices based on conjugated polymers”, Nature, vol. 347, pp. 539-541,1990.

[1-6] M.T.Johnson, I.M.Hunter, N.D.Young, I.G.J.Camps, “Active matrix polyLED displays”, IDW '00, pp. 235-238, 2000.

[1-7] Tatsuya Shimode, Mutsumi Kimura, Satoru Miyashita, “Current status and future of light emitting polymer display driven by poly-Si TFT”, SID '99 DIGEST, pp. 372-375, 1999.

[1-8] GRajeswaran, M. Itoh, M. Boroson, “Active matrix low temperature poly-Si TFT/OLED full color displays: development status”, SID '00 DIGEST, pp. 974-977, 2000.

[1-9] Y. Sakaguchi, H. Tada, T. Tanaka, E. Kitazume, K. Mori, S. Kawashima, J. Suzuki, “Color Passive-Matrix Organic LED Display using Three Emitters”, SID '02, pp. 1182-1185, 2002.

[1-10] S. Xiong, B. Guo, C. Wu, Y. Chen, Y. Hao, Z. Zhou, H. Yang, “A Novel Design of Sub-frame and Current Driving Method for PM-OLED”, SID '02, pp. 1174-1176, 2002.

[1-11] A. Hunze, M. Scheffel, J. Birnstock, J. Blässing, A. Kanitz, W. Rogler, G. Wittmann, A. Winnacker, S. Rajoelson, H. Hartmann, “Passive Matrix Displays Based on the New Red Emitting Dopant RedATDBstors”, SID '02, pp. 1186-1189, 2002.

[1-12] James L. Sanford, Frank R. Libsch, “TFT AMOLED Pixel Circuits and Driving Methods”, SID '03 DIGEST, pp. 10-13, 2003.

[1-13] Masuyuki Ohta, Hiroshi Tsutsu, Hiroshi Takahara, Ikunori Kobayashi, Tsuyoshi Uemura, Yoneharu Takubo, “A Novel Current Programmed Pixel for Active Matrix OLED Displays”, SID '03 DIGEST, pp. 108-111, 2003.



In Chapter2

[2-1] Byeong-Gyu Rohr, Tae-Joon Ahn, Jae-Young Cho, Hwan-Sool Oh, “The fabrication of green organic light-emitting-diode by evaporation process”, TENCON '99. Proceedings of the IEEE Region 10 Conference , vol. 2 , pp. 1103-1105,1999.

[2-2] Takahisa Shimizu, Akio Nakamura, Hatsumi Komaki, Takao Minato ,Hubert Spreitzer, Jonas Kroeber “Fabrication Technique of PELD by Printing Methods” SID '03 DIGEST, pp. 1290-1293, 2003.

[2-3] Tatsuya Shimoda , “Ink-jet Technology for Fabrication Processes of Flat Panel Displays”, SID '03 DIGEST, pp. 1178-1181, 2003.

[2-4] GRajeswaran, M. Itoh, M. Boroson, “Active matrix low temperature poly-Si TFT/OLED full color displays: development status”, SID '00 DIGEST, pp. 974-977, 2000.

[2-5] Shoustikov. A., Yujian You, Thompson, M.E. “Electroluminescence color tuning by dye doping in organic light-emitting diodes”, IEEE Journal -vol.4 , pp. 3 - 13, 1998.

[2-6] G. GU, Stephen R. Forrest, “Design of flat-panel displays based on organic light-emitting devices”, IEEE Journal of selected topics in quantum electronics, pp. 83-99, 1998.

[2-7] C. C. Wu, J. C .Sturm, R.A. Register, M. E. Thompson, “Integrated three-color organic light-emitting devices”, Appl. Phys. Lett., vol. 69, pp. 3117-3119, 1996.

[2-8] C. W. Tang, D. J. Williams, J. C. Chang, “Organic electroluminescent multicolor image display device”, U.S. Patent 5294870, 1994.

[2-9] J. Kido, M. Kimura, K. Nagai, “ Multilayer white light-emitting organic electroluminescent device”, Science, vol. 267, pp. 1332-1334, 1995.

[2-10] J. E. Littman and S. A. Vanslyke, “White light-emitting internal junction organic electroluminescent device”, U.S. Patent 5405709, 1995.

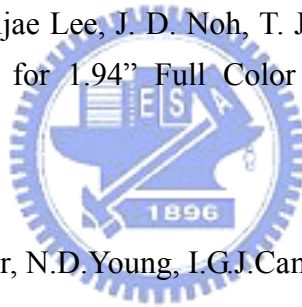
[2-11] J. Kalinowski, P.Di Marco, M. Cocchi, V. Fattori, N. Camaioni, J. Duff, “Voltage-tunable-color multilayer organic light emitting diode”, Appl. Phys. Lett., vol. 68, pp. 2317-2319, 1996.

[2-12] P.E. Bruuows, G. Gu, V. Bulovic, Z. Shen, S. R. Forrester, M.E. Thompson, “Achieving Full-Color Organic Light-Emitting Devices for Lightweight, Flat-Panel Displays”, IEEE TRANSACTIONS ON ELECTRON DEVICES, vol. 44, NO.8, pp. 1188-1202, 1997.

[2-13] J.R. Sheats, “Stacked Organic Light-Emitting Diodes in Full Color”, Science 1997 277, pp. 191-192, 1997.

[2-14] L E. Tannas, Jr., “ Flat Panel Displays and CRTs”, New York: Van Nostrand Reinhold, 1985.

[2-15] Jin Kim, J. H. Back, Giljae Lee, J. D. Noh, T. J. Kim, H. R. Ann, “A Development of Driving Chip-set and System for 1.94” Full Color PM OLED”, SID '03 DIGEST, pp. 1127-1129, 2003.



[2-16] M.T.Johnson, I.M.Hunter, N.D.Young, I.G.J.Camps, “Active matrix polyLED displays”, IDW '00, pp. 235-238, 2000.

[2-17] T. P. Brody et al, IEEE Trans Elec Dev, Vol ED-22, No 9, pp. 739-748, 1975.

[2-18] R.M.A Dawson, Z.Shen,D.A.Furst, S. Connor, J. Hsu, M.G. Kane, R.G. Stewart, A.Ipri,C.N.King, P.J. Green, R.T. Flegal, S.Pearson, W.A. Barrow, E. Dickey, K. Ping, C.W.Tang, S. Van Slyke, F. Chen, J. Shi, J.C. Sturm, M.H. Lu, “Design of an improved pixel for a polysilicon active-matrix organic LED display”, SID '98 DIGEST, pp. 11-14, 1998.

[2-19] M. J. Powell, “Bias-stress-induced creation and removal of dangling-bond states in amorphous silicon thin-film transistors”, Appl. Phy. Lett. 60,2, pp. 207-209, 1992.

[2-20] Reiji HATTORI, Tsutomu TSUKAMIZU, Ryusuke TSUCHIYA, Kazunori MIYAKE, Yi HE, Jerzy KANICKI, "Current-Writing Active-Matrix Circuit for Organic Light-Emitting Diode Display Using a-Si:H Thin-Film-Transistors", IEICE TRAN. ELECTRON., VOL.E83-C, NO.5, pp. 779-782, 2000.

[2-21] R.M.A.Dawson, Z. Shen, D.A. Furst, S. Connor, J. Hsu, M.G. Kane, R.G. Stewart, A. Ipri, C.N. King, P.J. Green, R.T. Flegal, S. Pearson, W.A. Barrow, E. Dickey, K. Ping, S. Robinson, C.W. Tang, S. Van Slyke, C.H. Chen, J. Shi, M.G. Lu, M. Moskewicz, J.C. Sturm, "A polysilicon active matrix organic light emitting diode display with integrated drivers", SID '99 DIGEST, pp. 438-441, 1999.

[2-22] R.M.A.Dawson, Z. Shen, D. A. Furst, S. Connor, J. Hsu, M. G. Kane, R. G. Stewart, A. Ipri, C. N. King, P. J. Green, R. T. Flegal, S. Pearson, W. A. Barrow, E. Dickey, K. Ping, S. Robinson, C. W. Tang, S. Van slyke, F. Chen, J. Shi, M. H. Lu, J. C. Sturm, "The impact of the transient response of organic light emitting diodes on the design of active matrix OLED displays", IEDM '98, pp. 875-878, 1998.

[2-23] Simon W.-B. Tam, Yojiro Matsueda, Mutsumi Kimura, "Improved polysilicon TFT drivers for light emitting polymer display", IDW '00, 00 243-246, 2000

[2-24] T.Sasaoka, M Shimoda, Piero Migliorato, " Poly-Si Driving Circuits for Organic EL Displays", Electronic.Sekiya, A.Yumoto, J.Yamada, T.Hirano, Y.Iwase, T.Yamada, T.Ishibashi, T.Mori, M.Asano, S.Tamura, T.Urabe, " A 13.0 inch AMOLED Display witho TOP Emitting Structure and Adaptive Current Mode Programmed Pixel Circuit,TAC", SID '01, pp. 384-387, 2001.

In Chapter3

[3-1] D. Pribhat, F. Palis, “Matrix addressing for organic electroluminescent displays”, *Thin Solid Films*, 383, pp. 25-30, 2001.

[3-2] Simon W.-B. Tam, Yojiro Matsueda, Mutsumi Kimura, Hiroshi Maeda, Tatsuya Shimoda , Piero Migliorato “ Poly-Si Driving Circuits for Organic EL Displays”, *Electronic Imageing* 2001, pp. 4920-4925, 2001.

[3-3] Reiji Hattori, Tsutomu Tsukamizu, “Current-writing active-matrix circuit for organic light-emitting diode display using a-Si:H thin-film-transistors”, *IEICE TRANS.Electron*, VOL-E83-C,NO.5, pp. 779-782, 2000.

[3-4] G. GU, Stephen R.Forrest, “Design of flat-panel displays based on organic light-emitting devices”, *IEEE Journal of selected topics in quantum electronics*, pp. 83-99, 1998.

[3-5] J.J.Lih, C.F.Sung, M.S.Weaver, M.Hack,J.J.Brown, “A phosphorescent Active-Matrix OLED Display driven by Amorphous Silicon Backplane”, *SID '03 DIGEST*, pp. 14-17, 2003.

[3-6] R.M.A.Dawson, M.G.Kane, “Pursuit of active matrix organic light emitting diode displays”, *SID '01 DIGEST*, pp. 372-375, 2001.

[3-7] M.T.Johnson, I.M.Hunter,N.D.Young, I.G.J.Camps, “Active matrix polyLED displays”, *IDW '00*, pp.235-238, 2000.

[3-8] Yi He, Reiji Hattori, Jerzy Kanicki, “Current-source a-Si:H thin-film-transistor circuit for active-matrix organic light-emitting displays”, *IEEE ELECTRON DEVICE LETTER '00*, pp. 590-592, 2000.

[3-9] Takashi Chuman, Satoru Ohta, Satoshi Miyaguchi, Hideo Satoh, Takahisa Tanabe, Yoshiyuki Okuda, Masami Tsuchida, “Active Matrix Organic Light Emitting Diode Panel using Organic Thin-Film Transistors”, *SID '04 DIGEST*, pp. 45-47, 2004.

[3-10] R.M.A.Dawson, Z. Shen, D.A. Furst, S. Connor, J. Hsu, M.G. Kane, R.G. Stewart, A. Ipri, C.N. King, P.J. Green, R.T. Flegal, S. Pearson, W.A. Barrow, E. Dickey, K. Ping, S. Robinson, C.W. Tang, S. Van Slyke, C.H. Chen, J. Shi, M.G. Lu, M. Moskewicz, J.C. Sturm, "A polysilicon active matrix organic light emitting diode display with integrated drivers", SID '99 DIGEST, pp. 438-441, 1999.

[3-11] R.M.A Dawson, Z.Shen,D.A.Furst, S. Connor, J. Hsu, M.G. Kane, R.G. Stewart, A.Ipri,C.N.King, P.J. Green, R.T. Flegal, S.Pearson, W.A. Barrow, E. Dickey, K. Ping, C.W.Tang, S. Van Slyke, F. Chen, J. Shi, J.C. Sturm, M.H. Lu, "Design of an improved pixel for a polysilicon active-matrix organic LED display", SID '98 DIGEST, pp. 11-14, 1998.

[3-12] Sang-Moo Choi, Oh-Kyong Kwon, Ho-Kyun Chung, "An improved voltage programmed pixel structure for large size and high resolution AM-OLED displays", SID '04 DIGEST, pp. 260-263, 2004.

[3-13] Yang-Wan Kim, Oh-Kyong Kwon, Keum-nam Kim, Dong- Young Shin, Byung-Hee Kim, Ho-Kyoon Chung, "A New Current Programmable Pixel Structure for Large-Size and High-Resolution AMOLEDs", IDW, international Symp. Proc., pp. 367-369, 2002.

[3-14] Masuyuki Ohta, Hiroshi Tsutsu, Hiroshi Takahara, Ikunori Kobayashi, Tsuyoshi Uemura, Yoneharu Takubo, "A novel current programmed pixel for active matrix OLEDs", SID '03 DIGEST, pp. 108-111, 2003.

[3-15] James L. Sanford, Frank R. Libsch, "TFT AMOLED Pixel Circuits and Driving Methods", SID '03 DIGEST, pp. 10-13, 2003.

[3-16] T. Sasaoka, M. Sekiya, A. Yamagata, J. Yamada, T. Hirano, Y.Iwase, T. Yamada, T. Mori, M. Asano, S. Tamura, T. Urabe, "A 13.0-inch AM-OLED display with top emitting structure and adaptive current mode programmed pixel circuit", SID '01 DIGEST, pp. 384-387, 2001.

[3-17] K Inukai, H Kimura, M Mizukami, J. Maruyama, S.Murakami, J. Koyama, T, Konuma, S. Yamazaki, "4.0-in. TFT-OLED displays and a novel digital driving method", SID '00, pp. 924-927, 2000.

[3-18] M Mizukami, K Inukai, H Yamagata, T. Konuma, T.Nishi, J. Koyama, S. Yamazaki , ‘T. Tsutsui , “6-Bit digital VGA OLED”, SID ’00, pp. 912-915, 2000.



In Chapter4

[4-1] James L. Sanford, Frank R. Libsch "TFT AMOLED Pixel Circuits and Driving Methods", SID '03 DIGEST, pp.10-13, 2003.

[4-2] R.M.A. Dawson et al., U.S. Pat. 6307322, 2001.

[4-3] Childs M, Nisato G, Fish D, Giraldo A, Jenkins A, Johnson M, "Advance Poly-LED Displays", Philips Research Laboratories Redhill, to be published., 2003.

[4-4] K Inukai, H Kimura, M Mizukami, J. Maruyama, S.Murakami, J. Koyama, T, Konuma , S. Yamazaki, "4.0-in. TFT-OLED displays and a novel digital driving method", SID '00, pp. 924-927, 2000.

[4-5] Ju Young Jeong, Jaegeun Kim, " Dual Modulation Driving for Poly-Si TFT Active Matrix OLED Displays", IDW '03, pp. 551-554, 2003.

[4-6] M Mizukami, K Inukai, H Yamagata, T. Konuma, T.Nishi, J. Koyama, S. Yamazaki , 'T. Tsutsui , "6-Bit digital VGA OLED", SID '00, pp. 912-915, 2000.

[4-7] Yen-Shyung Shyu, "Low Operating Current Analog Integrated Circuits", NCTU, Phd. Thesis, Jun. 2002.

[4-8] Zi-Long Hung, "A Precision 2.5V to 1.8V Low Dropout Voltage Drgulator", NCKU, Master Thesis, Jun. 2003.

[4-9] Band S. Lee, "Understanding the Terms and Definitions of LDO Voltage Regulator", Texas Instruments Inc., Application Report, to be published.

[4-10] Band S. Lee, "Technical Review of Low Dropout Voltage Regulator Operation and Performance" , Texas Instruments Inc., Application Report, to be published.

[4-11] Gabriel A. Rincon-Mora, "Active Capacitor Multiplier in Miller-Compensated Circuits", IEEE TRANSACTIONS ON SOLID-STATE CIRCUITS, vol. 35, No.1, pp. 26-32, 2000.

[4-12] Ka Namg Leung, K.T. Mok, Wing Hung Ki, "A Novel Frequency Compensation Technique for Low-Voltage Low Dropout Regulator", IEEE ISCAS 1999, pp.102-105, 1999.

[4-13] Ka Chun Kwok, K.T. Mok, “Pole-Zero Tracking Frequency Compensation for Low Dropout Regulator”, ISCAS 2002, pp.735-738, 2002.

[4-14] R. Jacob Baker, “CMOS Circuit Design, Layout and Simulation”, John Wiley & Sons Inc., 2005.

[4-15] PAUL R. GRAY et al., “Analysis and Design of Analog Integrated Circuits”, John Wiley & Sons Inc., 2001.

[4-16] Behzad Razavi, “Design of Analog CMOS Integrated Circuits”, McGRAW-HILL Inc., 2001.



Vita

PERSONAL INFORMATION

Chinese Name: 曾銘松

English Name: Min-Sung Tseng

Birth Date: August 6, 1969

Birth Place: Taipei, Taiwan, R.O.C.

Address: Department of Electronics Engineering
National Chiao Tung University
1001 Ta-Hsueh Road
Hsin-chu, Taiwan 30050, R.O.C.

E-Mail Address: mstseng.eic91g@nctu.edu.tw



EDUCATION

B.S. [1996] Department of Electrical Engineering, National Taipei University of Technology.

M.A. [2005] Degree Program of Electrical Engineering and Computer Science, National Chiao-Tung University.